NUREG/CR-0765
TREE-1271
for the U.S. Nuclear Regulatory Commission

EXPERIMENT DATA REPORT FOR TEST RIA 1-2 (REACTIVITY INITIATED ACCIDENT TEST SERIES)

CAROLYN L. ZIMMERMANN CHRISTINE E. WHITE
ROBERT P. EVANS

7908140116

June 1979

EG&G Idaho, Inc.
IDAHO NATIONAL ENGINEERING LABORATORY
DEPARTMENT OF ENERGY
IDAHO OPERATIONS OFFICE UNDER CONTRACT DE-AC07-76ID01570

831 055

Available from
National Technical Information Service
Springfield, Virginia 22161
Price: Printed Copy A05; Microfiche $3.00

The price of this document for requesters outside the North American continent can be obtained from the National Technical Information Service.

631 056

NUREG/CR-0765
TREE-1271
R3

EXPERIMENT DATA REPORT FOR TEST RIA 1-2 (REACTIVITY INITIATED ACCIDENT TEST SERIES)

Carolyn L. Zimmermann
Christine E. White
Robert P. Evans

EG&G Idaho, Inc.
Idaho Falls, Idaho 83401

Published June 1979

PREPARED FOR THE
U.S. NUCLEAR REGULATORY COMMISSION
AND THE U.S. DEPARTMENT OF ENERGY
IDAHO OPERATIONS OFFICE
UNDER CONTRACT NO. DE-AC07-76IDO1570
NRC FIN NO. A6041

631 057

ABSTRACT

Recorded test data are presented for the second of six planned tests in the Reactivity Initiated Accident (RIA) Test Series I, Test RIA 1-2. This test, conducted at the Power Burst Facility, had the following objectives:

(1) Characterize the response of preirradiated fuel rods during an RIA event conducted at boiling water reactor hot-startup conditions

(2) Evaluate the effect of rod internal pressure on preirradiated fuel rod response during an RIA event.

The data from Test RIA 1-2 are graphed in engineering units and have been appraised for quality and validity. These uninterpreted data are presented for use in the nuclear fuel behavior research field before detailed analysis and interpretation have been completed.

631 058

SUMMARY

The Reactivity Initiated Accident (RIA) Test Series I is part of the Thermal Fuels Behavior Program which is conducted by EG&G Idaho, Inc., for the U.S. Nuclear Regulatory Commission. Test RIA 1-2, completed November 22, 1978, was the second of six planned tests in the RIA Test Series I. The primary objectives of Test RIA 1-2 were to:

(1) Characterize the response of preirradiated fuel rods during an RIA event conducted at boiling water reactor (BWR) hot-startup conditions

(2) Evaluate the effect of rod internal pressure on preirradiated fuel rod response during an RIA event.

The Power Burst Facility (PBF) provided a neutron and coolant environment for simulating the postulated reactivity insertion accident for a BWR at hot-startup conditions. The test facility components used to meet the test requirements included: (a) a reactor vessel and driver core region to provide the neutron environment, (b) control rods and transient rods to dynamically control reactivity, (c) a water-filled in-pile tube (IPT) in the center of the driver core to contain the test rods, and (d) a pressurized water flow loop to provide the coolant environment in the IPT. Four individually shrouded, preirradiated test rods were installed in a test train and positioned in the IPT at the driver core level.

The test procedure included:

(1) Two nonnuclear heatups to establish the coolant conditions for the power calibration and preconditioning phase and the power burst

(2) A power calibration and preconditioning phase to condition the fuel and to determine the relationship between fuel rod power and core power

(3) A power burst to produce the experimentally required energy deposition in the four individually shrouded, preirradiated test rods.

The PBF data acquisition and reduction system (DARS) recorded measurements to characterize test rod behavior, test rod shroud coolant conditions, system pressure, neutron flux, PBF reactor power, and test rod failure. After the testing was completed, the recorded data were reviewed and verified to be qualified, restrained, trend, or failed data. The power burst data are presented in the main body of this report and data from the power calibration and preconditioning phase are included on microfi[illegible] attached to the back cover of this report.

CONTENTS

FIGURES

631 060

631 061

631 062

631 063

MICROFICHE ADDRESSES FOR TEST RIA 1-2

631 065

L1 Absolute pressure in upper test train (SYS PRES 17KA UTT), trend.

M1 Absolute pressure in upper test train (SYS PRES SCHAVUTT), trend.

N1 Absolute pressure in Rod 802-1 shroud (SHRDPRES 17KA 01), trend.

O1 Absolute pressure in Rod 802-2 shroud (SHRDPRES 17KA 02), trend.

P1 Absolute pressure in Rod 802-4 shroud (SHRDPRES 17KA 04), trend.

B2 Coolant temperature at Rod 802-1 shroud inlet (INLT TMP 01), qualified.

C2 Coolant temperature at Rod 802-2 shroud inlet (INLT TMP 02), qualified.

D2 Coolant temperature at Rod 802-3 shroud inlet (INLT TMP 03), qualified.

E2 Coolant temperature at Rod 802-4 shroud inlet (INLT TMP 04), qualified.

F2 Coolant temperature at Rod 802-1 shroud outlet (OUT TEMP 01), qualified.

G2 Coolant temperature at Rod 802-2 shroud outlet (OUT TEMP 02), qualified.

H2 Coolant temperature at Rod 802-3 shroud outlet (OUT TEMP 03), qualified.

I2 Coolant temperature at Rod 802-4 shroud outlet (OUT TEMP 04), qualified.

J2 Coolant temperature increase across Rod 802-1 shroud (DEL TEMP 01), qualified.

K2 Coolant temperature increase across Rod 802-2 shroud (DEL TEMP 02), qualified.

L2 Coolant temperature increase across Rod 802-3 shroud (DEL TEMP 03), qualified.

M2 Coolant temperature increase across Rod 802-4 shroud (DEL TEMP 04), qualified.

N2 Cladding elongation of Rod 802-1 (CLAD DSP 01), qualified.

O2 Cladding elongation of Rod 802-2 (CLAD DSP 02), qualified.

P2 Cladding elongation of Rod 802-3 (CLAD DSP 03), trend.

B3 Cladding elongation of Rod 802-4 (CLAD DSP 04), trend.

C3 Neutron flux in Quadrant 1, 0.09 m above fuel stack bottom (NEUT FLX 9-Q1 TT), restrained.

D3 Neutron flux in Quadrant 1, 0.27 m above fuel stack bottom (NEUT FLX 27-Q1 TT), qualified.

E3 Neutron flux in Quadrant 1, 0.46 m above fuel stack bottom (NEUT FLX 46-Q1 TT), qualified.

F3 Neutron flux in Quadrant 1, 0.64 m above fuel stack bottom (NEUT FLX 64-Q1 TT), qualified.

G3 Neutron flux in Quadrant 1, 0.82 m above fuel stack bottom (NEUT FLX 82-Q1 TT), qualified.

H3 Neutron flux in Quadrant 3, 0.09 m above fuel stack bottom (NEUT FLX 9-Q3 TT), qualified.

I3 Neutron flux in Quadrant 3, 0.27 m above fuel stack bottom (NEUT FLUX 27-Q3 TT), qualified.

631 060

TABLES

631 067

EXPERIMENT DATA REPORT FOR TEST RIA 1-2 (REACTIVITY INITIATED ACCIDENT TEST SERIES)

I. INTRODUCTION

The Thermal Fuels Behavior Program (TFBP) is one of several programs being conducted by the Water Reactor Research Directorate of EG&G Idaho, Inc., for the U.S. Nuclear Regulatory Commission. The TFBP performs an integrated analytical and experimental study of the behavior of nuclear fuel rods under normal, off-normal, and accident conditions in light water reactors. Data from the TFBP experimental effort are used to determine the completeness and accuracy of the analytical models developed to predict fuel rod behavior for a wide range of postulated reactor operating conditions.

The objectives of the TFBP Reactivity Initiated Accident (RIA) Test Series are to determine fuel failure thresholds, modes, and consequences as functions of energy depositions, irradiation history, and fuel rod design. For the RIA Test Series 1, the pressure, temperature, and flow rate of the coolant will be typical of the hot-startup conditions in commercial boiling water reactors (BWRs). These conditions were selected in order to simulate the coolant conditions of the most severe RIA postulated - the BWR control rod drop accident during hot-startup conditions.

Test RIA 1-2, completed November 22, 1978, was the second of six planned tests in the RIA Test Series 1. The main objectives of Test RIA 1-2 were to:

(1) Characterize the response of preirradiated fuel rods during an RIA event conducted at BWR hot-startup conditions

(2) Evaluate the effect of rod internal pressure on preirradiated fuel rod response during an RIA event.

During Test RIA 1-2, four individually shrouded, preirradiated test rods were subjected to steady state operation to condition the fuel and to determine the relationship between test fuel rod power and core power. Then the test rods were subjected to a single power burst of about a 4.3-ms period and a peak power of about 13 000 MW.

This report presents the data from Test RIA 1-2 in a form readily usable before detailed analysis and interpretation have been completed. These data were reviewed and verified to be qualified, restrained, trend, or failed data.

Section II of this report describes the experimental reactor system used to conduct Test RIA 1-2; Section III gives the test procedures and initial test conditions; Section IV specifies the test instrumentation; and Section V presents the data graphs and provides comments and supporting information necessary for data interpretation. Appendix A describes the methods used to apply the posttest corrective adjustments to the data and the subsequent qualification; and Appendix B is a guide to the uncertainty associated with the data.

II. SYSTEM CONFIGURATION

The Power Burst Facility (PBF) is located at the Idaho National Engineering Laboratory. The PBF reactor, shown in Figure 1, is contained in an open tank reactor vessel and consists of a driver core and a flux trap. A pressurized water coolant flow loop provides a wide range of coolant conditions in the flux trap test space.

The PBF core is a right-circular annulus 1.3 m in diameter and 0.91 m in length, enclosing a centrally located vertical flux trap 0.21 m in diameter. This core has been designed for steady state and power burst operation. The core contains eight control rods for reactivity control during steady state operation. During power burst operation, the control rods and four additional transient rods dynamically control reactivity. Each of the control and transient rods consists of a stainless steel canister which contains a cylindrical annulus of boron carbide and is operated in an air-filled shroud. A cutaway view of the PBF core is shown in Figure 2.

An in-pile tube (IPT) fits in the central flux trap region and contains the test train assembly. The IPT is a thick-walled, Inconel 718, high strength pressure tube designed to contain the steady-state operating pressure and any pressure surges from test fuel rod failures. Test fuel failures (such as cladding failure, gross fuel melting, fuel-coolant interactions, fuel failure propagation, fission product release, and metal-water reactions), can be safely contained in the IPT without damage to the driver core.

A flow tube is positioned inside the IPT to direct the coolant flow. Coolant enters the top of the IPT above the reactor core and flows down the annulus between the IPT wall and the flow tube. The flow reverses at the bottom, passes up through the test train, and exits above the reactor core at the IPT outlet. The flow tube consists of an upper stainless steel section, a center zircaloy-2 section for neutron economy in the test fuel, and a lower catch basket section for a heat sink and collection of fuel fragments. An axial cross section of the in-pile tube is given in Figure 3.

The loop coolant system provides cooling water for the IPT at controllable pressures, temperatures, and flow rates. For Test RIA 1-2, this system simulated the hot-startup coolant conditions of a BWR. The system includes a pressurizer, a pump, heat exchangers for removing the energy transferred to the coolant by the test fuel, a flow control valve, acoustic filters and thermal swell accumulators to attenuate any pressure surges from fuel failure, and electrical heaters to control the inlet temperature.

Four MAPI[a] fuel rods, Rods 802-1, 802-2, 802-3, and 802-4, were used during Test RIA 1-2. These rods had been previously irradiated to a burnup of about 4800 MWd/t in the Saxton reactor[1]. The original Westinghouse Electric Corporation test rod number and the burnup of each test rod are given in Table I. The nominal design characteristics of the test rods are listed in Table II.

Rod 802-1 was instrumented and then backfilled with 77.7% helium and 22.3% argon to a pressure of 0.103 MPa. This gas mixture simulates the thermal conductivity of fill gases, including fission gases, in the MAPI test rods. Rods 802-2 and 802-4 were instrumented and then backfilled with the 77.7% and 22.3% mixture of helium and argon to a pressure of 2.41 MPa. Rod 802-3 was not opened before Test RIA 1-2.

An individual zircaloy-4 flow shroud with a nominal inner diameter of 16.30 mm and an outer diameter of 22.6 mm surrounded each test rod and created a coolant flow area of 130.3 mm^2. An orifice plate with a 6.95 $\pm$ 0.025-mm-diameter hole was located below each shroud.

---

a. The MAPI rods were built by the Westinghouse Electric Corporation, and were irradiated in the Saxton reactor for the Mitsubishi Atomic Power Industries, Inc., Tokyo, Japan.

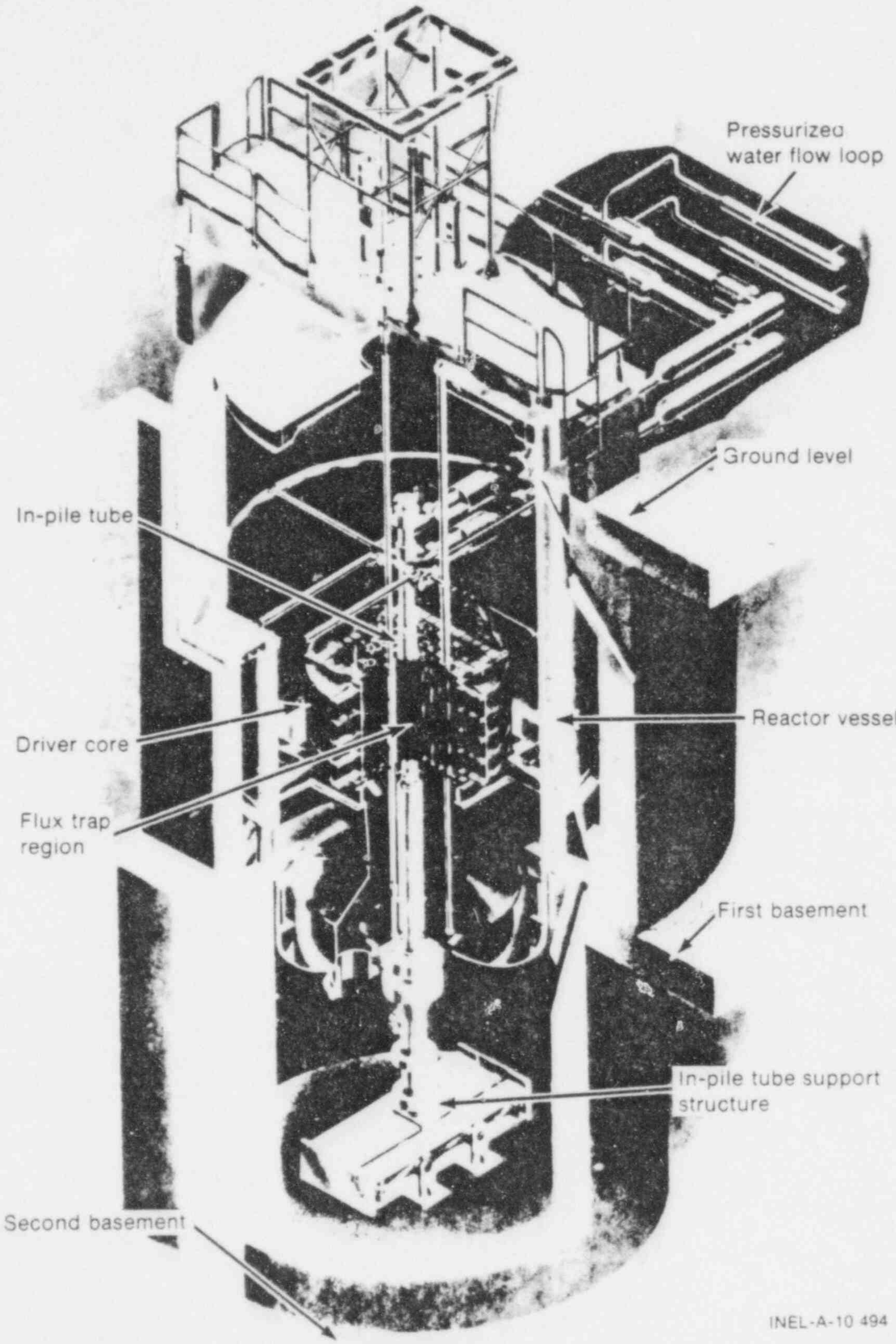

Fig. 1 Power Burst Facility reactor — cutaway view.

631 070

The test rods were installed in a four-rod test train fabricated by Battelle-Pacific Northwest Laboratories. In this test train, each fuel rod was rigidly secured at the top, but was free to expand axially downward. The location of each test rod is shown in Figure 3.

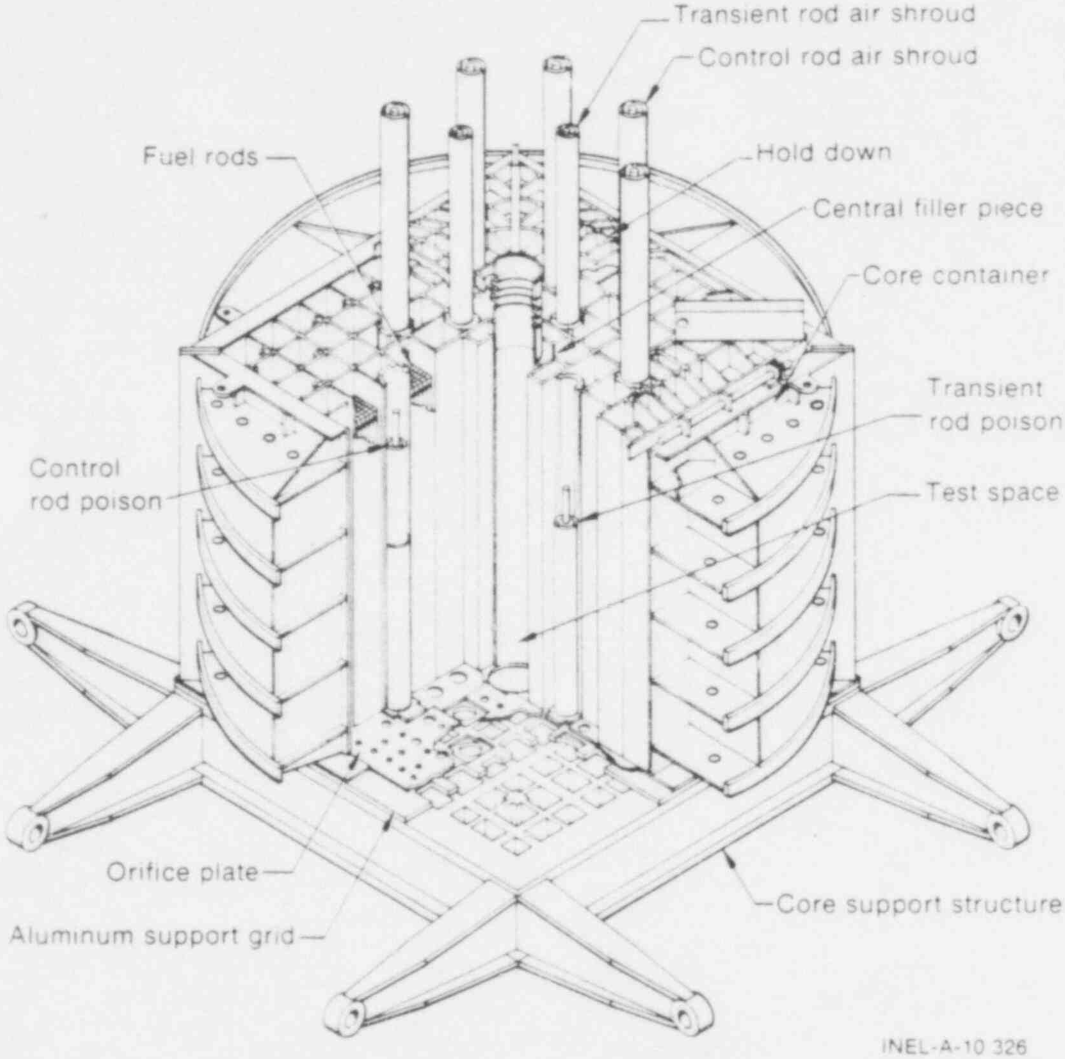

Fig. 2 Power Burst Facility core — cutaway view.

631 071

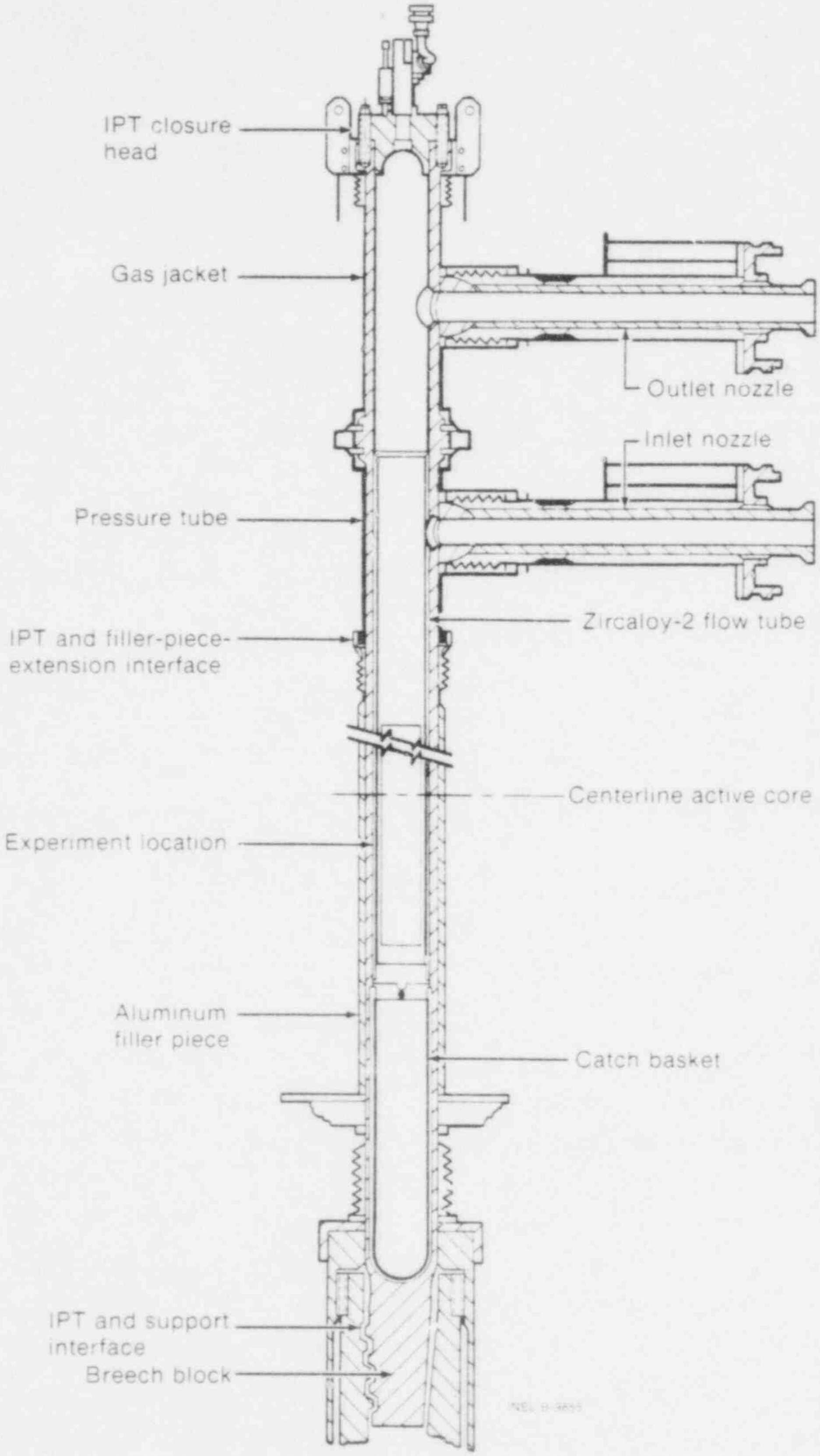

Fig. 3 Axial cross section of in-pile tube.

631 072

TABLE I

TEST RIA 1-2 ROD DESIGNATIONS AND BURNUP

Test RIA 1-2 Rod Identification	Westinghouse Electric Corp. Corresponding Rod Identification	Average Burnup (MWd/t)
802-1	MAPI M-2	5220
802-2	MAPI M-13	5110
802-3	MAPI M-59	4430
802-4	MAPI M-8	4530

TABLE II

TEST RIA 1-2 FUEL ROD DESIGN CHARACTERISTICS

Characteristics	Rods 802-1, -2, -3, and -4[a]
Fuel	
Material	UO_2
Pellet outside diameter (mm)	8.59
Pellet length (mm)	15.2
Pellet enrichment (wt%)	5.7
Density (% theoretical density)	94
Fuel stack length (m)	0.914
End configuration	Dished
Cladding	
Material	Zircaloy 4
Tube outside diameter (mm)	9.99
Tube wall thickness (mm minimum)	0.572
Yield strength (MPa)	570
Ultimate strength (MPa)	700
Fuel Rod	
Gas plenum length (mm)	45.7
Insulator pellets	None

a. Data are preirradiation values of the MAPI fuel rods.

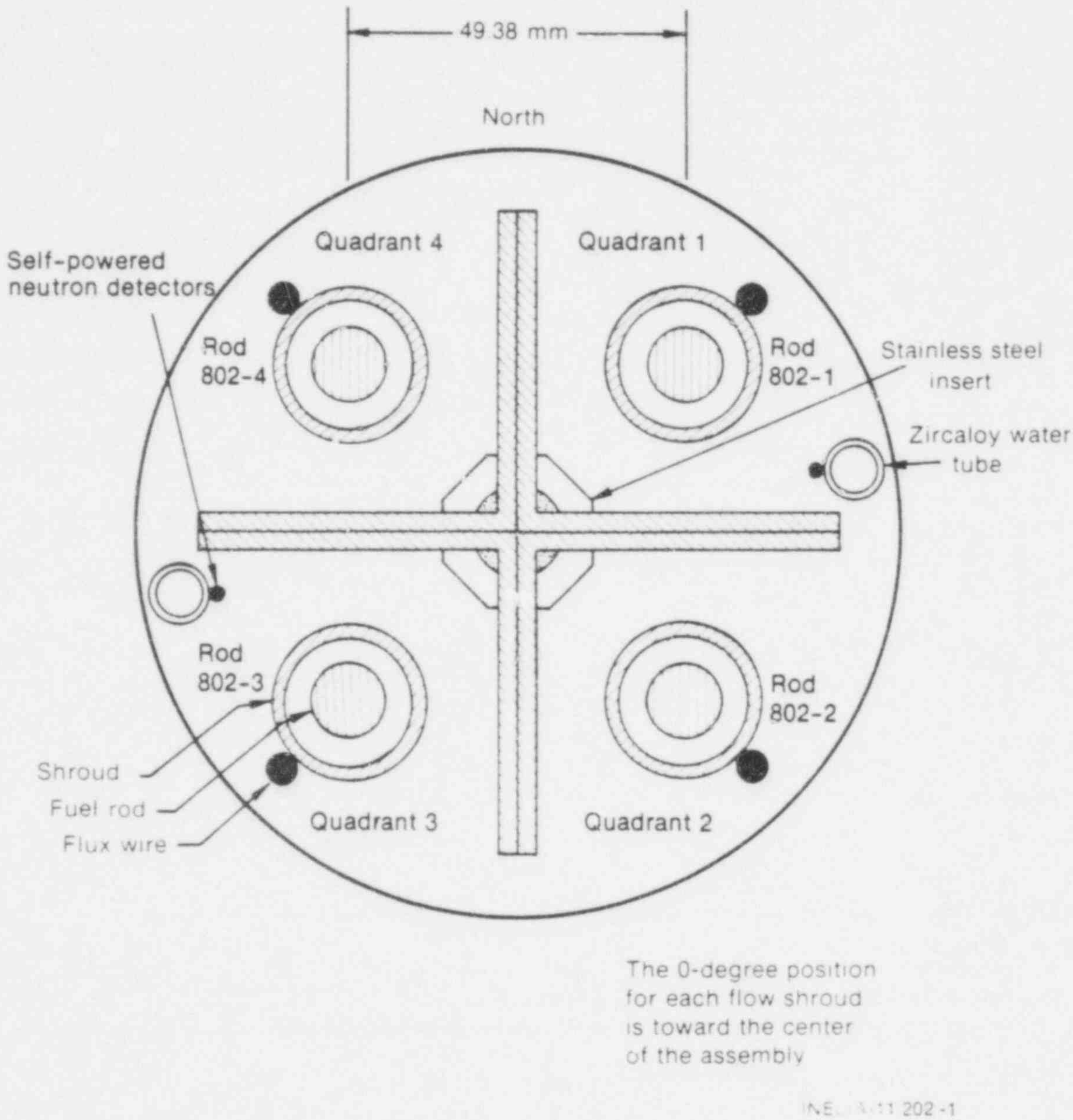

Fig. 4 Test rod arrangement of the four-rod hardware for Test RIA 1-2.

631 074

III. EXPERIMENT CONDUCT

Test RIA 1-2 included two nonnuclear heatups, a power calibration and a preconditioning phase, and a power burst. Before each test phase and during the coolant loop heatups, instrument status checks were made at several loop temperatures to initialize instrument readings and to ensure that critical instrumentation was operable.

1. HEATUP PHASE

A prepower calibration heatup established the loop coolant conditions specified for the power calibration and preconditioning phase - 538 K for the inlet temperature, 6.45 MPa for the pressure, and 0.760 l/s for the flow rate in each shroud. Before the power burst, another heatup was performed to establish loop conditions at 538 K for the inlet temperature, 6.45 MPa for the pressure, and 0.085 l/s for the flow rate in each shroud.

During each heatup, the chemistry requirements for the coolant were adjusted within the following limits:

pH range	5.7 to 10.2
Specific conductivity	1.4 to 48 μS/cm
Dissolved oxygen	Less than 0.1 ppm
Chlorides	Less than 0.15 ppm
Total suspended solids	Less than 1.0 ppm

Instrument status checks were performed at ambient conditions before each heatup. During heatup, several more status checks were performed on the instrumentation at several loop temperatures to confirm operability of the instrumentation.

2. POWER CALIBRATION AND PRECONDITIONING PHASE

For Test RIA 1-2, the power calibrations and the preconditioning were performed concurrently. The power calibrations were conducted to calibrate the thermal-hydraulically determined test rod power with the reactor neutron detecting chambers and the self-powered neutron detectors (SPNDs) mounted on the test train. The preconditioning was performed to promote cracking and relocation of the fuel and to build up the fission product inventory of the test rods for cladding failure indication by the Fission Product Detection System during the power burst. The reactor core power history during the power calibration and preconditioning phase is summarized in Table III. In addition, the reactor was operated for a total of about 125 minutes during several aborted reactor startups for the power calibration.

After completion of the power calibration and preconditioning phase, the coolant loop was cooled to ambient conditions and depressurized. The test train was removed from the IPT and the four flux wires mounted on the outer surface of each test rod shroud were replaced with 100% cobalt flux wires.

3. POWER BURST TESTING

After a heatup to establish the loop coolant conditions at 538 K, 6.45 MPa, and 0.085 l/s, a single power burst with a reactor period of about 4.3 ms and a peak power of about 13 000 MW was performed. A reactivity balance method was used to initiate the power burst. This method provides assurance that the control and transient rods have not been grossly mispositioned and no potentially dangerous reactivity addition can be made. The reactivity balance method is depicted in Figure 5 and included the following sequence of events:

(1) The control rods were withdrawn from their scram positions (Figure 5a) until criticality was achieved at about 100 W and the low power critical position of the control rods was determined (Figure 5b).

TABLE III

CORE POWER HISTORY DURING THE TEST RIA 1-2
POWER CALIBRATION AND PRECONDITIONING PHASE

Elapsed Operating Time (minutes)	Duration (minutes)	Reactor Power (MW)	Operation
--	--	0	Power Calibration
23	23	0 to 7.6	
27	4	7.6	
38	11	7.6 to 12.6	
45	7	12.6	
53	6	12.6 to 16.2	
58	5	16.2	
65	7	16.2 to 21.3	
70	5	21.3	
78	8	21.3 to 25.2	
91	13	25.2	
95	4	25.2 to 26.8	
215	120	26.8	Preconditioning
255	40	26.8 to 1.8	
259	4	1.8	
283	24	1.8 to 26.8	
366	83	26.8	
---	Scram occurred		
371	5	0 to 1.8	
376	5	1.8	
396	20	1.8 to 25.8	
516	120	25.8	
519	3	25.8 to 25.3	
522	3	25.3	
525	3	25.3 to 21.3	
528	3	21.3	
532	4	21.3 to 16.2	
534	2	16.2	
542	8	16.2 to 7.6	
546	4	7.6	
552	6	7.6 to 0	

631 076

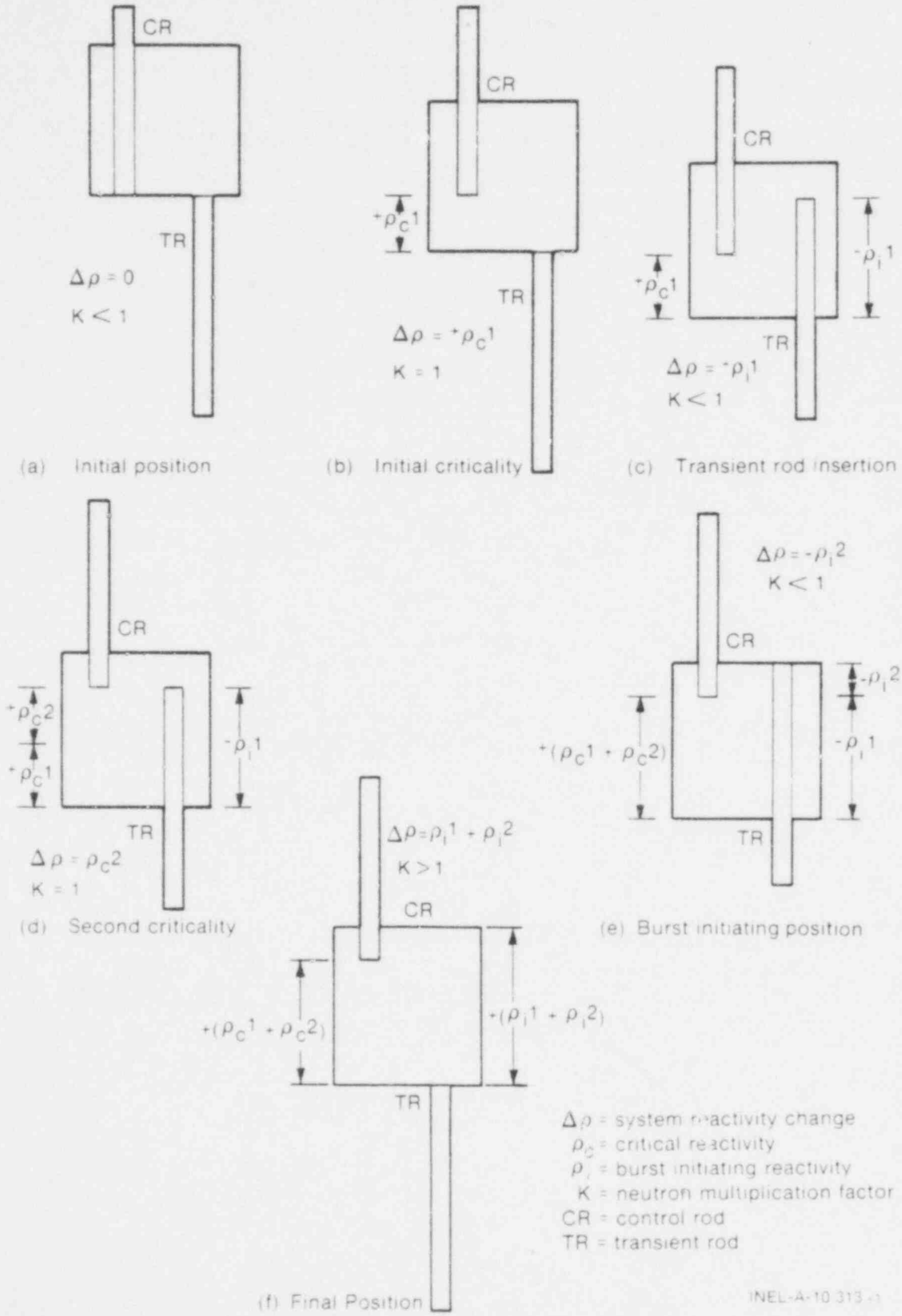

Fig. 5 Power burst testing sequence.

(2) From that position the control rods were further withdrawn until a reactor transient period of about 10 s was achieved. Then the reactor power was increased until the plant protection system was determined to be operating correctly. The control rods were then inserted until the reactor was subcritical.

(3) The transient rods were inserted into the core to a postion calculated for the reactivity insertion required for the power burst (Figure 5c).

(4) The control rods were then withdrawn again to reestablish criticality at a low power level (Figure 5d). The reactivity inserted by the withrawal of the control rods and the worth of the transient rods were compared for assurance that the increment of control rod withdrawal determined for the power burst was not grossly in error.

(5) The control rods were adjusted to the withdrawal position for the desired reactivity insertion.

(6) The transient rods were then fully inserted into the core (Figure 5e).

(7) To initiate the power burst, all four transient rods were ejected at a velocity of about 953 cm/s (Figure 5f). The power burst was self-terminating by the Doppler reactivity feedback which is capable of terminating the burst without primary dependence on mechanical systems. All eight control rods were then completely inserted into the driver core to provide mechanical shut down of the reactor.

IV. INSTRUMENTATION AND MEASUREMENTS

Instrumentation for Test RIA 1-2 was selected to aid in determining test rod response characteristics and failure mechanisms during the RIA event. Fuel rod instrumentation monitored test rod behavior. Test train instrumentation measured the temperature, pressure, and volumetric flow rate of the coolant, the local neutron flux, and the test rod cladding elongation. Plant instrumentation was used to provide reactor power information and indication of test rod failure.

1. FUEL ROD INSTRUMENTATION

Rod 802-1 was instrumented to measure the internal gas pressure, cladding surface temperature, and cladding elongation. Rod 802-2 was instrumented to measure the internal gas pressure, cladding surface temperature, plenum temperature, and cladding elongation. Rod 802-3 was instrumented for cladding elongation, and Rod 802-4 was instrumented to measure the internal gas pressure and cladding elongation.

The fuel rod instrumentation is specified in the following description. The measurement identifiers used for data reduction purposes are given in parentheses. The first eight characters indicated the type of measurement. Duplicate measurements were uniquely identified by the next six characters which specified the range, manufacturer, or axial, azimuthal, or quadrant location of the instrument. The last two characters for fuel rod measurement identifiers indicated the test rod number.

(1) Two EG&G Idaho, Inc., platinum/10% rhodium-platinum, Type S thermocouples with spaded junctions, titanium sheathings, and magnesia insulation were resistance welded to the cladding outer surface of each of Rods 802-1 and 802-2. One thermocouple (CLAD TMP 46-18001 and CLAD TMP 46-18002) was located 0.46 m from the bottom of each fuel stack and 180-degrees from the center of the test train assembly. The other thermocouple (CLAD TMP 79-0 01 and CLAD TMP 79-0 02) was located 0.79 m from the bottom of each fuel stack and 0-degrees from the center of the test train assembly.

(2) A 6.9-MPa Kaman Sciences Corp. pressure transducer was mounted on Rod 802-1 (ROD PRES 6.9KA 01), and a 17.2-MPa Kaman Sciences Corp. pressure transducer was mounted on each of Rods 802-2 (ROD PRES 17KA 02) and 802-4 (ROD PRES 17KA 04) to measure rod internal pressure in the upper plenum.

(3) An EG&G Idaho, Inc., Chromel-Alumel, Type K thermocouple with stainless steel sheathing and magnesia insulation (PLNM TMP 02) was located at the centerline of the spring in the plenum region of Rod 802-2 to measure the plenum gas temperature.

2. TEST TRAIN INSTRUMENTATION

The test train consisted of a four-quadrant experiment section with support hardware located above and below the quadrants. Each quadrant contained a shrouded test rod and instrumentation to characterize the neutron flux, the elongation of the test rod cladding, and the coolant conditions inside the test rod shroud. The test train instrumentation is shown in Figure 6 and specified in the following description. The measurement identifiers used for data reduction purposes are included in parentheses. An X is used for the last character of the measurement identifiers for quadrant measurements characterizing the test rod shroud coolant conditions and the elongation of the test rod cladding. The X indicates each of the four quadrants. The last two characters of the other measurement identifiers indicated a test train measurement with the characters TT.

(1) A Flow Technology, Inc., turbine flowmeter (FLOWRATE INLET 0X) was mounted at the inlet of each test rod shroud to measure the coolant flow rate in each shroud.

631 079

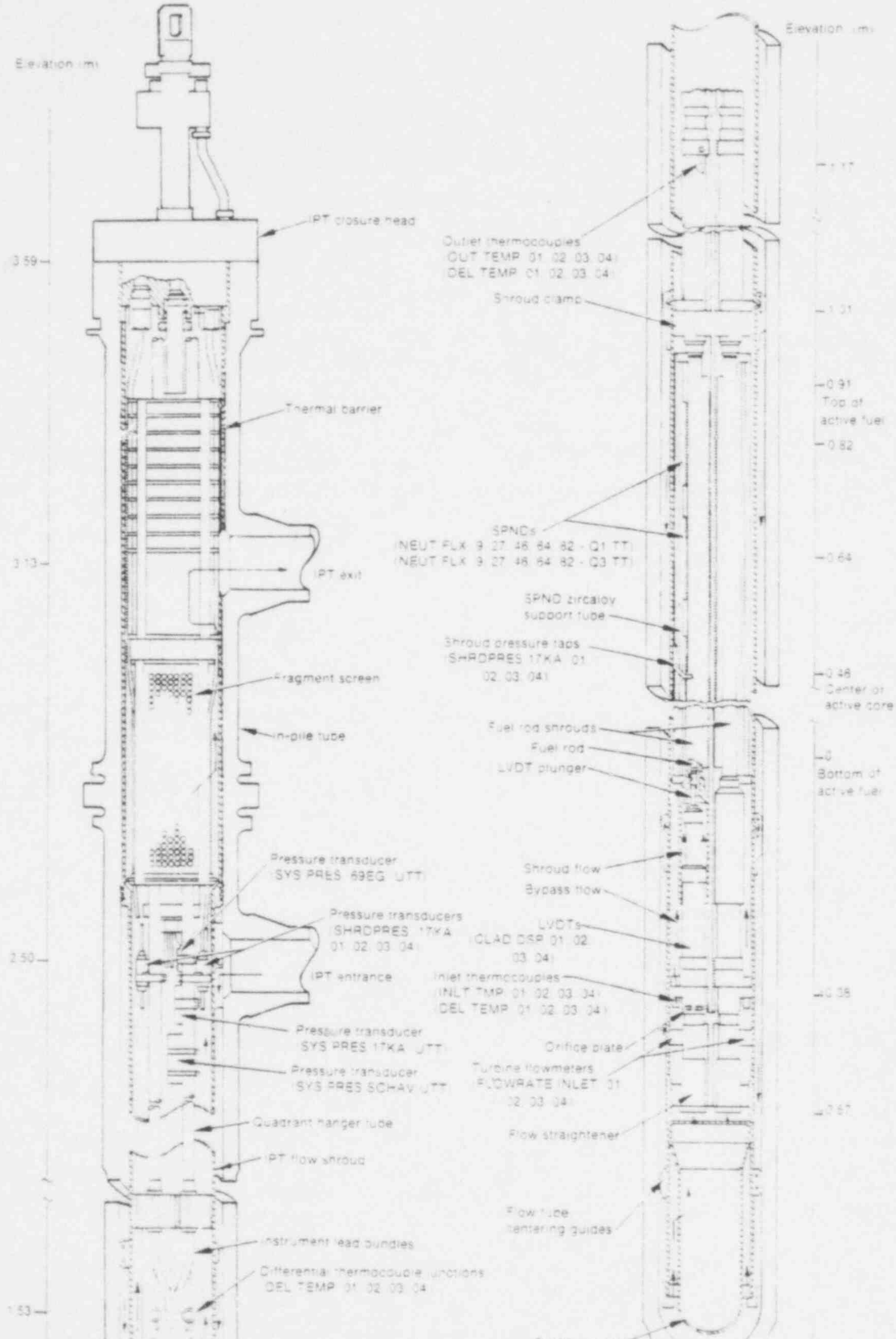

Elevation (m)
3.59
3.13
2.50
1.53
IPT closure head
Thermal barrier
IPT exit
Fragment screen
In-pile tube
Pressure transducer
(SYS PRES 69EG UTT)
Pressure transducers
(SHRDPRES 17KA
01 02 03 04)
IPT entrance
Pressure transducer
(SYS PRES 17KA UTT)
Pressure transducer
(SYS PRES SCHAV UTT)
Quadrant hanger tube
IPT flow shroud
Instrument lead bundles
Differential thermocouple junctions
DEL TEMP 01 02 03 04
Elevation (m)
1.01
0.91
Top of
active fuel
0.82
0.64
0.46
Center of
active core
0
Bottom of
active fuel
Outlet thermocouples
(OUT TEMP 01 02 03 04)
(DEL TEMP 01 02 03 04)
Shroud clamp
SPNDs
(NEUT FLX 9 27 46 64 82 - Q1 TT)
(NEUT FLX 9 27 46 64 82 - Q3 TT)
SPND zircaloy
support tube
Shroud pressure taps
(SHRDPRES 17KA 01
02 03 04)
Fuel rod shrouds
Fuel rod
LVDT plunger
Shroud flow
Bypass flow
LVDTs
(CLAD DSP 01 02
03 04)
Inlet thermocouples
(INLT TMP 01 02 03 04)
(DEL TEMP 01 02 03 04)
Orifice plate
Turbine flowmeters
(FLOWRATE INLET 01
02 03 04)
Flow straightener
Flow tube
centering guides
Catch basket

631 080

(2) A 69-MPa EG&G Idaho, Inc., pressure transducer (SYS PRES 69EG UTT), a 17.2-MPa Kaman Sciences Corp. pressure transducer (SYS PRES 17KA UTT), and a 17.2-MPa Schaevitz Engineering pressure transducer (SYS PRES SCHAVUTT) were located above the test rod shroud outlets in the upper test train to measure normal system pressure and pressure pulses.

(3) A 17.2-MPa Kaman Sciences Corp. pressure transducer (SHRDPRES 17KA OX) was connected with tubing to the interior of each test rod shroud at the axial peak power location to measure pressure pulses generated by test rod failure.

(4) A Control Products Corp., Chromel-Alumel, Type K thermocouple with stainless steel sheathing and magnesia insulation (INLT TMP OX) was mounted at the inlet of each test rod shroud to measure the coolant inlet temperature.

(5) A Control Products Corp., Chromel-Alumel, Type K thermocouple with stainless steel sheathing and magnesia insulation (OUT TEMP OX) was installed at the outlet of each test rod shroud to measure the coolant outlet temperature.

(6) A pair of Control Products Corp., Chromel-Alumel, Type K thermocouples with stainless steel sheathing and magnesia insulation (DEL TEMP OX) measured the temperature rise in the coolant from the test rod shroud inlet to the test rod shroud outlet.

(7) An EG&G Idaho, Inc., linear variable differential transformer, LVDT, (CLAD DSP OX) was mounted below the lower end of each test rod to measure the cladding axial elongation.

(8) Ten ARI Industries cobalt self-powered neutron detectors, (SPNDs) were installed in two vertical columns, 180-degrees apart in Quadrants 1 and 3, to measure the relative neutron flux. The detector midpoints in each quadrant were located at an elevation of 0.09 (NEUT FLX 9-Q1 TT and NEUT FLX 9-Q3 TT), 0.27 (NEUT FLX 27-Q1 TT and NEUT FLX 27-Q3 TT), 0.46 (NEUT FLX 46-Q1 TT and NEUT FLX 46-Q3 TT), 0.64 (NEUT FLX 64-Q1 TT and NEUT FLX 64-Q3 TT), and 0.82 m (NEUT FLX 82-Q1 TT and NEUT FLX 82-Q3 TT) above the bottom of the fuel stacks.

(9) A flux wire was placed 180 degrees from the center of the test train on the outer surface of each test rod shroud to measure the integrated neutron flux. During power calibration and fuel rod conditioning, flux wires with material compositions of 0.51% cobalt and 99.49% aluminum were used. Before the power burst, those wires were removed and replaced with 100% cobalt flux wires.

3. PLANT INSTRUMENTATION

The Fission Product Detection System (FPDS) was designed to withdraw a continuous sample stream from the coolant loop near the IPT outlet and monitor the sample stream for fission products that would indicate test rod failure. Prior to Test RIA 1-2, the 7.6- by 7.6-cm NaI crystal gamma ray detector used to measure the effectiveness of the shielding for the 2.5- by 3.8-cm NaI crystal gamma ray detector was removed and a new NaI detector was installed over the exit spool piece in the reactor piping tunnel. The FPDS includes some housekeeping measurements such as temperatures and flow rates, but only the fission product detectors are described. The measurement identifiers are given in parentheses. The last two characters of the measurement identifiers indicated an FPDS measurement with the characters FP.

(1) One 2.5- by 3.8-cm NaI crystal gamma ray detector was placed in a shielded housing and installed in the second basement of the reactor building to determine the background gamma count rate before fission product release and gamma count rate during and after fission product release. The ouput from this detector was fed into two single channel

analyzers. One analyzer (FP GAMMA NO.1 FP) measured the gamma-ray intensity in the 150- to 3400- keV energy range and the other (FP GAMMA NO.3 FP) measured the gamma-ray intensity in the 3400- to 6300-keV energy range.

(2) One 2.5- by 3.8-cm NaI crystal gamma ray detector (FP GAMMA NO.2 FP) was placed in a shielded housing and installed over the exit spool piece in the reactor piping tunnel located between the ground level and the first basement of the reactor building. This detector determined the background gamma count rate before fission product release and the gamma count rate during and after fission product release. It measured the gamma-ray intensity in the 150- to 6300-keV energy range.

(3) One BF_3 delayed neutron detector (FP NEUT FP) was installed in the second basement of the reactor building to detect delayed neutrons in the sample stream.

Four ionization chambers provided driver core power information during the power burst. Figure 7 shows the reactor core location of the ionization chambers. These ionization chambers are sensitive to

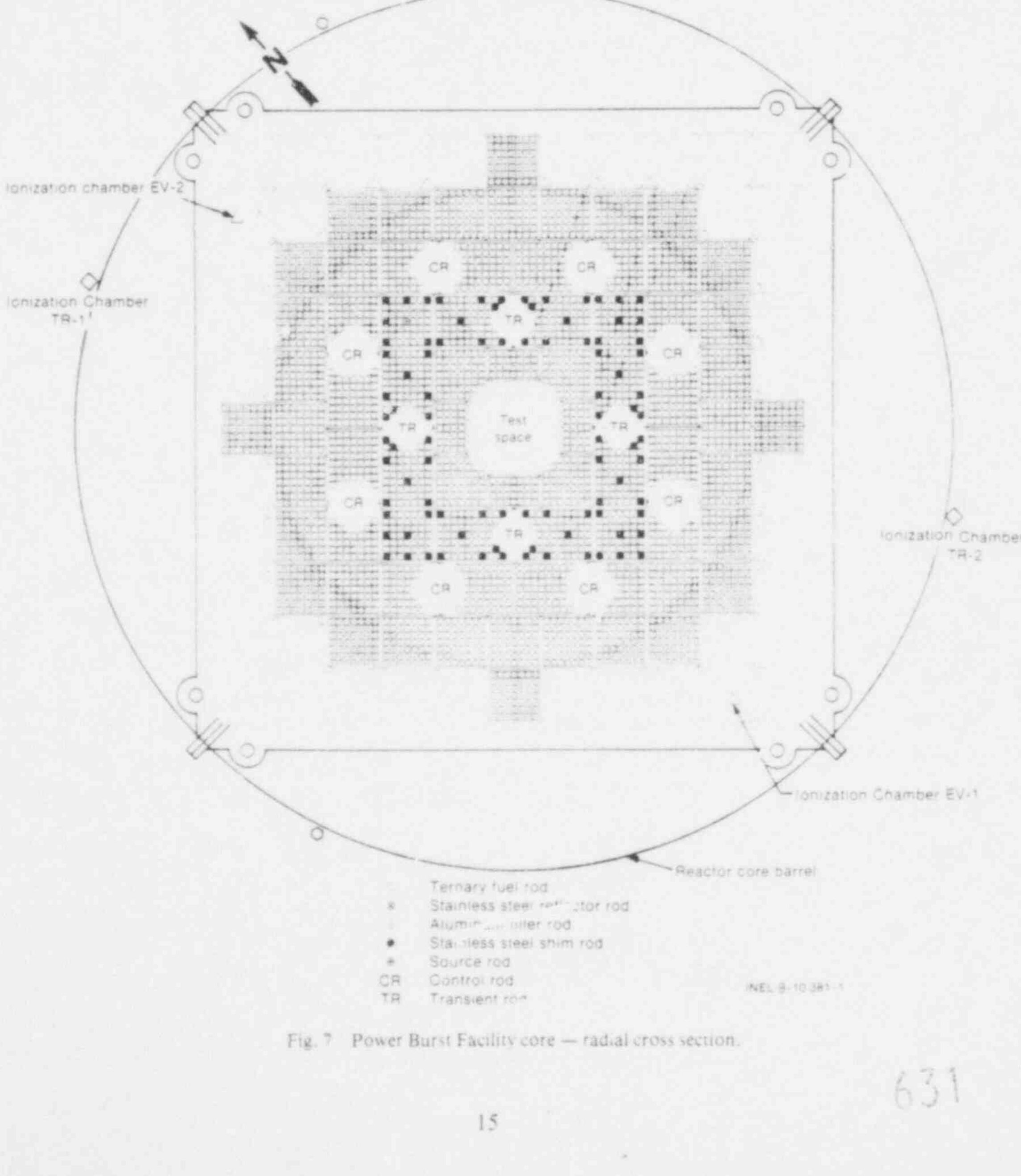

Fig. 7 Power Burst Facility core — radial cross section.

631 082

gamma and neutron radiation and produce current outputs proportional to the number of neutrons or gammas per second which ionize the gas inside the chambers. The measurement identifiers for these instruments are included in parentheses. The last two characters of the measurement identifiers indicated a plant instrumentation measurement with the characters PT.

(1) Two Westinghouse Electric Corp., WX-31994, nitrogen filled, ionization chambers, TR-1 (REAC POW 50TR1PT and REAC POW 50KTR1PT) and TR-2 (REAC POW 50TR2PT and REAC POW 50KTR2PT), designed to measure power bursts to 32 GW, are located outside the reactor core barrel.

(2) Two Westinghouse Electric Corp., WX-31845, evacuated ionization chambers EV-1 (REAC POW 50EV1PT and REAC POW 50KEV1PT) and EV-2 (REAC POW 50EV2PT and REAC POW 50KEV2PT), designed to measure high power bursts to 200 GW, are located in the south and north corners of the reactor core support structure.

631 083

V. DATA PRESENTATION

The data from Test RIA 1-2 are presented with brief comment. All the data in this report were reviewed and verified for consistency and validity. To determine the quality of the data, the output from each instrument was compared with initial conditions and the output from any instrument making a duplicate measurement. Processing analysis was done to obtain the appropriate engineering units and to determine data offsets from the calibration data. Appendix A describes the methods used to determine the adjustments that have been applied to the presented data and provides the basis for categorizing the data as follows:

(1) Qualified engineering unit data (Qualified) - have been verified to represent the variable being measured within specified uncertainty limits

(2) Restrained data - appear reasonable but are not within certainty limits, or data from an independent measurement are not available for comparison

(3) Trend data - are suitable for illustrative purposes but probably not for numerical analyses

(4) Failed data - are irretrievable due to a transducer, signal conditioning, or data channel failure or inadequate rejection of extraneous noise, transients, or frequencies.

All detector analog output was digitized and recorded by the PBF data acquisition and reduction system (PBF/DARS). The PBF/DARS tape recording system was configured to record at four different bandwidths:

dc to 10 Hz
dc to 100 Hz
dc to 5 kHz
dc to 20 kHz.

Table IV lists all the measurements included in this report and specifies the type, range, and location of the recording instrument, the PBF/DARS recording bandwidths, the frequency response of the recording instrument and the PBF/DARS, the figure numbers for the data plots, and the qualification category of the data.

The power burst data are presented in the subsequent pages of this report. The power calibration and preconditioning data are included on the microfiche attached to the back cover of this report.

Appendix B presents an analysis of selected data for use as a guide to the uncertainty associated with data measurements in the PBF system.

631 084

TABLE IV

DATA PRESENTATION FOR TEST RIA 1-2

Measurement	Instrument	Instrument Location	Range: Instrument	Range: Data Acquisition System	Frequency Response: Instrument (Hz)	Frequency Response: Data Acquisition System (Hz)	Steady State Operation: Figure	Steady State Operation: Comments	Test RIA 1-2: Figure	Test RIA 1-2: Comments
FUEL ROD										
CLAD TMP 46-180001	Type S thermocouple with titanium sheathing and magnesia insulation	Cladding surface of Rod 802-1 at an elevation of 0.46 m from bottom of fuel stack and 180-degrees from center of test train	478 to 1811 K	300 to 2100 K	350	100	B1	Qualified[a]	8 9	Qualified from -0.5 to 2 s[a] Qualified from -5 to 25 s[a]
CLAD TMP 79-0 01	Type S thermocouple with titanium sheathing and magnesia insulation	Cladding surface of Rod 802-1 at an elevation of 0.79 m from bottom of fuel stack and 0-degrees from center of test train	478 to 1811 K	300 to 2100 K	350	100	C1	Qualified[a]	10 11	Qualified from -0.5 to 2 s[a] Qualified from -5 to 25 s[a]
CLAD TMP 46-18002	Type S thermocouple with titanium sheathing and magnesia insulation	Cladding surface of Rod 802-2 at an elevation of 0.46 m from bottom of fuel stack and 180-degrees from center of test train	478 to 1811 K	300 to 2100 K	350	100	D1	Qualified[a]	12 13	Qualified from -0.5 to 2 s[a] Qualified from -5 to 25 s[a]
CLAD TMP 79-0 02	Type S thermocouple with titanium sheathing and magnesia insulation	Cladding surface of Rod 802-2 at an elevation of 0.79 m from bottom of fuel stack and 0-degrees from center of test train	478 to 1811 K	300 to 2100 K	350	100	E1	Qualified[a]	14 15	Qualified from -0.5 to 2 s[a] Qualified from -5 to 25 s[a]
ROD PRES 6.9KA 01	Kaman Sciences Corp. eddy current pressure transducer	Upper plenum of Rod 802-1	0 to 6.9 MPa	0 to 6.9 MPa	5.8×10^4	$10, 5 \times 10^3$		Failed[b]		Failed[b]
ROD PRES 17KA 02	Kaman Sciences Corp. eddy current pressure transducer	Upper plenum of Rod 802-2	0 to 17.24 MPa	0 to 17 MPa	5.8×10^4	$10, 5 \times 10^3$		Failed[c]	16	Trend
ROD PRES 17KA 04	Kaman Sciences Corp. eddy current pressure transducer	Upper plenum of Rod 802-4	0 to 17.24 MPa	0 to 17 MPa	5.8×10^4	$10, 5 \times 10^3$	F1	Trend	17	Trend
PLNM TMP 02	Type K thermocouple with stainless steel sheathing and magnesia insulation	Centerline of spring in upper plenum of Rod 802-2	273 to 1309 K	300 to 1100 K	350	100		Failed[e]		Failed[e]

631 085

TABLE IV (continued)

Measurement	Instrument	Instrument Location	Range: Instrument	Range: Data Acquisition System	Frequency Response: Instrument (Hz)	Frequency Response: Data Acquisition System (Hz)	Steady State Operation: Figure	Steady State Operation: Comments	Test RIA 1-2: Figure	Test RIA 1-2: Comments
TEST TRAIN										
FLOWRATE INLET 01	Flow Technology, Inc. turbine flowmeter	Rod 802-1 shroud inlet	0.06 to 0.82 l/s	0 to 0.82 l/s	120	100	G1	Qualified	18	Qualified, except for failed segment from 0.0 to 1.3 s[f]
FLOWRATE INLET 02	Flow Technology, Inc. turbine flowmeter	Rod 802-2 shroud inlet	0.06 to 0.82 l/s	0 to 0.82 l/s	120	100	H1	Qualified	19	Qualified, except for failed segment from 0.0 to 1.3 s[f]
FLOWRATE INLET 03	Flow Technology, Inc. turbine flowmeter	Rod 802-3 shroud inlet	0.06 to 0.82 l/s	0 to 0.82 l/s	120	100	I1	Qualified	20	Qualified, except for failed segment from 0.0 to 1.3 s[f]
FLOWRATE INLET 04	Flow Technology, Inc. turbine flowmeter	Rod 802-4 shroud inlet	0.06 to 0.82 l/s	0 to 0.82 l/s	120	100	J1	Qualified	21	Qualified, except for failed segment from 0.0 to 1.3 s[f]
SYS PRES 69EG UTT	EG&G Idaho, Inc. bellows-strain post pressure transducer	Above test rod shroud outlets	0 to 69 MPa	0 to 69 MPa	3.5×10^6	10, 2×10^4	K1	Trend[d]	22 23	Trend from -0.1 to 0.3 s[d] Trend from -1 to 5 s[d]
SYS PRES 17KA UTT	Kaman Sciences Corp. eddy current pressure transducer	Above test rod shroud outlets	0 to 17.24 MPa	0 to 17 MPa	5.8×10^4	10, 5×10^3	L1	Trend[d]	24 25	Trend from -0.1 to 0.3 s[d] Trend from -1 to 5 s[d]
SYS PRES SCHAVUTT	Schaevitz Engineering LVDT-bellows pressure transducer	Above test rod shroud outlets	0 to 17.24 MPa	0 to 17 MPa	350	10, 5×10^3	M1	Trend[d]	26 27	Trend from -0.1 to 0.3 s[d] Trend from -1 to 5 s[d]
SHRDPRES 17KA 01	Kaman Sciences Corp. eddy current pressure transducer	Near Rod 802-1 shroud outlet	0 to 17.24 MPa	0 to 17 MPa	5.8×10^4	10, 2×10^4	N1	Trend[d]	28 29	Trend from -0.1 to 0.3 s[d] Trend from -1 to 5 s[d]
SHRDPRES 17KA 02	Kaman Sciences Corp. eddy current pressure transducer	Near Rod 802-2 shroud outlet	0 to 17.24 MPa	0 to 17 MPa	5.8×10^4	10, 2×10^4	O1	Trend[d]	30 31	Trend from -0.1 to 0.3 s[d] Trend from -1 to 5 s[d]
SHRDPRES 17KA 03	Kaman Sciences Corp. eddy current pressure transducer	Near Rod 802-3 shroud outlet	0 to 17.24 MPa	0 to 17 MPa	5.8×10^4	10, 2×10^4		Failed[g]	32 33	Trend from -0.1 to 0.3 s[d] Trend from -1 to 5 s[d]
SHRDPRES 17KA 04	Kaman Sciences Corp. eddy current pressure transducer	Near Rod 802-4 shroud outlet	0 to 17.24 MPa	0 to 17 MPa	5.8×10^4	10, 2×10^4	P1	Trend[d]	34 35	Trend from -0.1 to 0.3 s[d] Trend from -1 to 5 s[d]
INLT TMP 01	Type K thermocouple with stainless steel sheathing and magnesia insulation	Rod 802-1 shroud inlet	273 to 1309 K	300 to 1000 K	350	10	B2	Qualified[a]	36	Qualified[a]
INLT TMP 02	Type K thermocouple with stainless steel sheathing and magnesia insulation	Rod 802-2 shroud inlet	273 to 1309 K	300 to 1000 K	350	10	C2	Qualified[a]	37	Qualified[a]
INLT TMP 03	Type K thermocouple with stainless steel sheathing and magnesia insulation	Rod 802-3 shroud inlet	273 to 1309 K	300 to 1000 K	350	10	D2	Qualified[a]	38	Qualified[a]

631 086

TABLE IV (continued)

Measurement		Instrument	Instrument Location	Range: Instrument	Range: Data Acquisition System	Frequency Response: Instrument (Hz)	Frequency Response: Data Acquisition System (Hz)	Steady State Operation: Figure	Steady State Operation: Comments	Test RIA 1-2: Figure	Test RIA 1-2: Comments
TEST TRAIN (continued)											
INLT TMP	04	Type K thermocouple with stainless steel sheathing and magnesia insulation	Rod 802-4 shroud inlet	273 to 1309 K	300 to 1000 K	350	10	E2	Qualified*	39	Qualified*
OUT TEMP	01	Type K thermocouple with stainless steel sheathing and magnesia insulation	Rod 802-1 shroud outlet	273 to 1309 K	300 to 1000 K	350	10	F2	Qualified*	40	Qualified*
OUT TEMP	02	Type K thermocouple with stainless steel sheathing and magnesia insulation	Rod 802-2 shroud outlet	273 to 1309 K	300 to 1000 K	350	10	G2	Qualified*	41	Qualified*
OUT TEMP	03	Type K thermocouple with stainless steel sheathing and magnesia insulation	Rod 802-3 shroud outlet	273 to 1309 K	300 to 1000 K	350	10	H2	Qualified*	42	Qualified*
OUT TEMP	04	Type K thermocouple with stainless steel sheathing and magnesia insulation	Rod 802-4 shroud outlet	273 to 1309 K	300 to 1000 K	350	10	I2	Qualified*	43	Qualified*
DEL TEMP	01	Pair of Type K thermocouples with stainless steel sheathing and magnesia insulation	Rod 802-1 shroud inlet and outlet	0 to 23 K	0 to 20 K	350	10	J2	Qualified	44	Trend[b]
DEL TEMP	02	Pair of Type K thermocouples with stainless steel sheathing and magnesia insulation	Rod 802-2 shroud inlet and outlet	0 to 23 K	0 to 20 K	350	10	K2	Qualified	45	Qualified
DEL TEMP	03	Pair of Type K thermocouples with stainless steel sheathing and magnesia insulation	Rod 802-3 shroud inlet and outlet	0 to 23 K	0 to 20 K	350	10	L2	Qualified	46	Qualified
DEL TEMP	04	Pair of Type K thermocouples with stainless steel sheathing and magnesia insulation	Rod 802-4 shroud inlet and outlet	0 to 23 K	0 to 20 K	350	10	M2	Qualified	47	Qualified
CLAD DSP	01	EG&G Idaho, Inc. linear variable differential transformer	Lower end of Rod 802-1	± 12.7 mm	-5 to 25 mm	3500	10, 5 x 10^3	N2	Qualified	48 49	Qualified from -0.1 to 0.3 s Qualified from -5 to 40 s

631 087

TABLE IV (continued)

Measurement	Instrument	Instrument Location	Range: Instrument	Range: Data Acquisition System	Frequency Response: Instrument (Hz)	Frequency Response: Data Acquisition System (Hz)	Steady State Operation: Figure	Steady State Operation: Comments	Test RIA 1-2: Figure	Test RIA 1-2: Comments
TEST TRAIN (continued)										
CLAD DSP 02	EG&G Idaho, Inc. linear variable differential transformer	Lower end of Rod 802-2	± 12.7 mm	-5 to 25 mm	3500	10, 5 x 10^3	O2	Qualified	50 51	Qualified from -0.1 to 0.3 s Qualified from -5 to 40 s
CLAD DSP 03	EG&G Idaho, Inc. linear variable differential transformer	Lower end of Rod 802-3	± 12.7 mm	-5 to 25 mm	3500	10, 5 x 10^3	P2	Trend[i]	52 53	Qualified from -0.1 to 0.3 s Restrained from -5 to 40 s[i]
CLAD DSP 04	EG&G Idaho, Inc. linear variable differential transformer	Lower end of Rod 802-4	± 12.7 mm	-5 to 25 mm	3500	10, 5 x 10^3	B3	Trend[j]	54 55	Restrained from -0.1 to 0.3 s[j] Restrained from -5 to 40 s[j]
NEUT FLX 9-Q1 TT	Cobalt SPND	Test train Quadrant 1 at an elevation of 0.091 m above fuel stack bottom	0 to 10^{-3} A	10^{-11} to 10^{-3} A	350	10, 5 x 10^3	C3	Restrained[l]	56	Restrained[k]
N . FLX 27-Q1 TT	Cobalt SPND	Test train Quadrant 1 at an elevation of 0.274 m above fuel stack bottom	0 to 10^{-3} A	10^{-11} to 10^{-3} A	350	10, 5 x 10^3	D3	Qualified	57	Restrained[k]
NEUT FLX 46-Q1 TT	Cobalt SPND	Test train Quadrant 1 at an elevation of 0.457 m above fuel stack bottom	0 to 10^{-3} A	10^{-11} to 10^{-3} A	350	10, 5 x 10^3	E3	Qualified	58	Restrained[k]
NEUT FLX 64-Q1 TT	Cobalt SPND	Test train Quadrant 1 at an elevation of 0.640 m above fuel stack bottom	0 to 10^{-3} A	10^{-11} to 10^{-3} A	350	10, 5 x 10^3	F3	Qualified	59	Restrained[k]
NEUT FLX 82-Q1 TT	Cobalt SPND	Test train Quadrant 1 at an elevation of 0.823 m above fuel stack bottom	0 to 10^{-3} A	10^{-11} to 10^{-3} A	350	10, 5 x 10^3	G3	Qualified	60	Restrained[k]
NEUT FLX 9-Q3 TT	Cobalt SPND	Test train Quadrant 3 at an elevation of 0.091 m above fuel stack bottom	0 to 10^{-3} A	10^{-11} to 10^{-3} A	350	10, 5 x 10^3	H3	Qualified	61	Trend, except for restrained segment from -0.03 to 0.03 s[k,m]
NEUT FLX 27-Q3 TT	Cobalt SPND	Test train Quadrant 3 at an elevation of 0.274 m above fuel stack bottom	0 to 10^{-3} A	10^{-11} to 10^{-3} A	350	10, 5 x 10^3	I3	Qualified	62	Restrained[k]
NEUT FLX 46-Q3 TT	Cobalt SPND	Test train Quadrant 3 at an elevation of 0.457 m above fuel stack bottom	0 to 10^{-3} A	10^{-11} to 10^{-3} A	350	10, 5 x 10^3	J3	Qualified	63	Restrained[k]

631 088

TABLE IV (continued)

Measurement	Instrument	Instrument Location	Range: Instrument	Range: Data Acquisition System	Frequency Response: Instrument (Hz)	Frequency Response: Data Acquisition System (Hz)	Steady State Operation: Figure	Steady State Operation: Comments	Test RIA 1-2: Figure	Test RIA 1-2: Comments
TEST TRAIN (continued)										
NEUT FLX 64-Q3 TT	Cobalt SPND	Test train Quadrant 3 at an elevation of 0.640 m above fuel stack bottom	0 to 10^{-3} A	10^{-11} to 10^{-3} A	350	10, 5×10^3	K3	Qualified	64	Restrained[b]
NEUT FLX 82-Q3 TT	Cobalt SPND	Test train Quadrant 3 at an elevation of 0.823 m above fuel stack bottom	0 to 10^{-3} A	10^{-11} to 10^{-3} A	350	10, 5×10^3	L3	Qualified	65	Restrained[b]
PLANT										
FP GAMMA NO.1 FP	NaI crystal gamma ray detector	Second basement of reactor building	10 to 10^6 counts/s	1 to 10^6 counts/s	Not available	10				Failed[a]
FP GAMMA NO.2 FP	NaI crystal gamma ray detector	Reactor piping tunnel located between ground floor and first basement of reactor building	10 to 10^6 counts/s	1 to 10^6 counts/s	Not available	10			66	Trend[a]
FP GAMMA NO.3 FP	NaI crystal gamma ray detector	Second basement of reactor building	10 to 10^6 counts/s	1 to 10^6 counts/s	Not available	10				Failed[a]
FP NEUT FP	BF_3 neutron detector	Second basement of reactor building	10 to 10^6 counts/s	1 to 10^6 counts/s	Not available	10				Failed[a]
REAC POW 50TR1PT	Westinghouse Electric Corp. nitrogen-filled ionization chamber	Outside reactor core barrel	0 to 32 MW	0 to 50 MW	> 5×10^3	10	M3	Qualified		
REAC POW 50KTR1PT	Westinghouse Electric Corp. nitrogen-filled ionization chamber	Outside reactor core barrel	0 to 32 GW	0 to 50 GW	> 5×10^3	5×10^3			67	Qualified
REAC POW 50TR2PT	Westinghouse Electric Corp. nitrogen-filled ionization chamber	Outside reactor core barrel	0 to 32 MW	0 to 50 MW	> 5×10^3	10	N3	Qualified		
REAC POW 50KTR2PT	Westinghouse Electric Corp. nitrogen-filled ionization chamber	Outside reactor core barrel	0 to 32 GW	0 to 50 G.	> 5×10^3	5×10^3			68	Qualified
REAC POW 50EV1PT	Westinghouse Electric Corp. evacuated ionization chamber	Near north corner of reactor core support structure	0 to 200 MW	0 to 50 MW	> 5×10^3	10	O3	Qualified		
REAC POW 50KEV1PT	Westinghouse Electric Corp. evacuated ionization chamber	Near north corner of reactor core support structure	0 to 200 GW	0 to 50 GW	> 5×10^3	5×10^3			69	Qualified
REAC POW 50EV2PT	Westinghouse Electric Corp. evacuated ionization chamber	Near south corner of reactor core support structure	0 to 200 MW	0 to 50 MW	> 5×10^3	10	P3	Qualified		

631 089

TABLE IV (continued)

Measurement	Instrument	Instrument Location	Range: Instrument	Range: Data Acquisition System	Frequency Response: Instrument (Hz)	Frequency Response: Data Acquisition System (Hz)	Steady State Operation: Figure	Steady State Operation: Comments	Test RIA 1-2: Figure	Test RIA 1-2: Comments
PLANT (continued)										
REAC POW 50KEV2PT	Westinghouse Electric Corp. evacuated ionization chamber	Near south corner of reactor core support structure	0 to 200 GW	0 to 50 GW	$> 5 \times 10^3$	5×10^3			70	Qualified

a. A superimposed square wave of unknown origin and a ±10 K magnitude (+% of range) was observed in the data.

b. The pressure transducer leads were open.

c. The data were inverted.

d. The data were normalized to the calibrated loop pressure gage. Hysteresis effects were evident in the data.

e. Major inconsistencies existed in the data.

f. Since the turbine flowmeter was not designed to indicate the direction of flow, it could not indicate flow reversal during the power burst.

g. The data values were erratic.

h. An unexplainable inconsistency exists in the shape of the data curve. No offset was applied to the data.

i. Hysteresis effects were evident in the data.

j. No exact calibration was available because the LVDT electronics were changed during the Test RIA 1-2.

k. The SPND measurements were inconsistent with other measurements used to calculate fuel rod energy values.

l. The zero level and the shape of the data curve did not correspond to the other SPND data curves.

m. The zero level of the data curve was questionable.

n. The FPDS sample line was clogged or a sample line valve was not opened and no sample coolant flow reached the FPDS detectors located in the second basement of the reactor building.

o. The FPDS was not set up for qualification of the detectors.

631 090

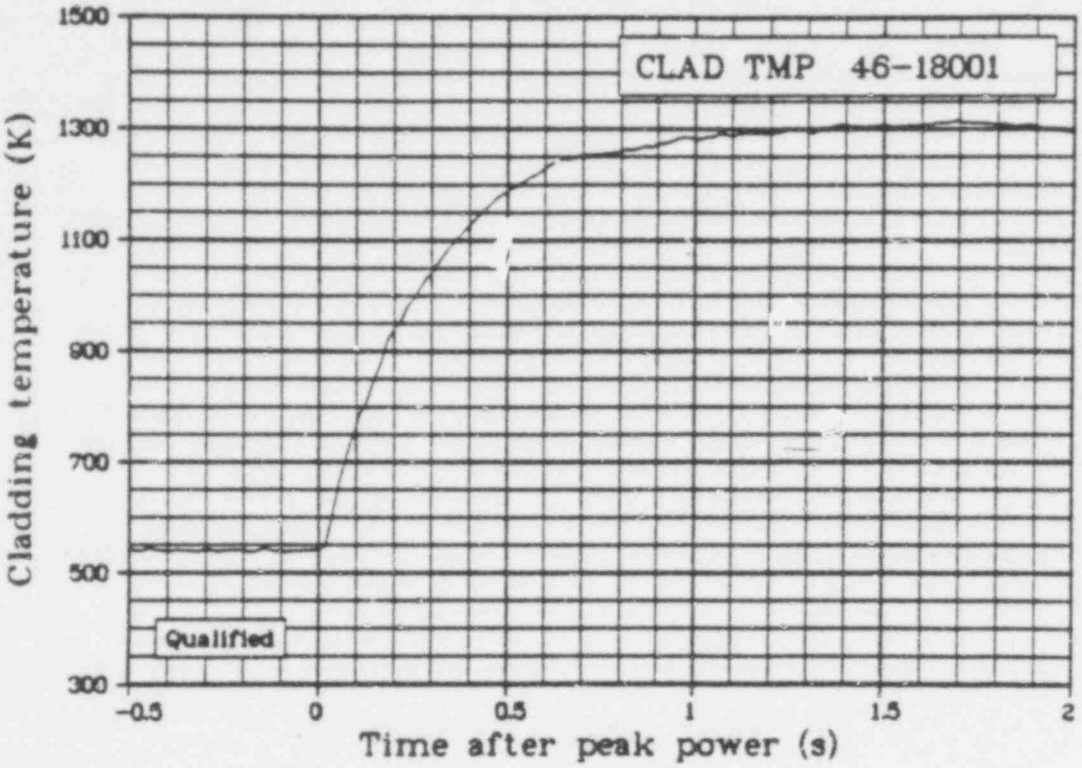

Fig. 8 Rod 802-1 cladding surface temperature at an elevation of 0.46 m above fuel stack bottom (CLAD TMP 46-18001), from -0.5 to 2 s, qualified.

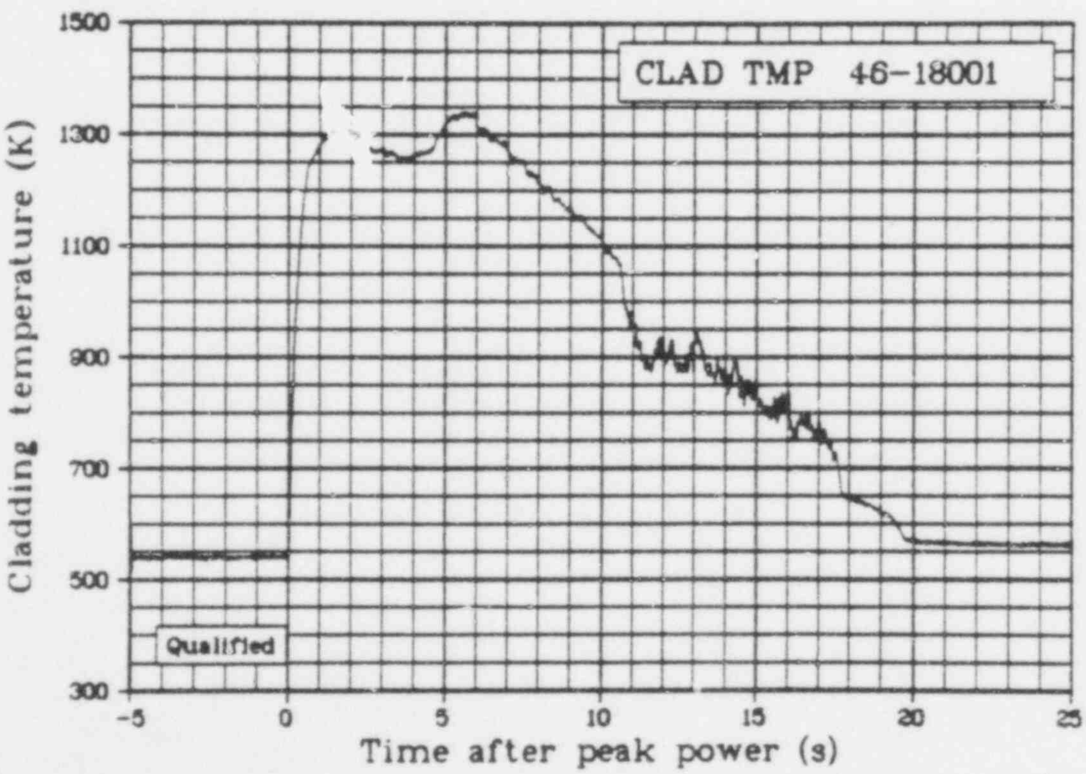

Fig. 9 Rod 802-1 cladding surface temperature at an elevation of 0.46 m above fuel stack bottom (CLAD TMP 46-18001), from -5 to 25 s, qualified.

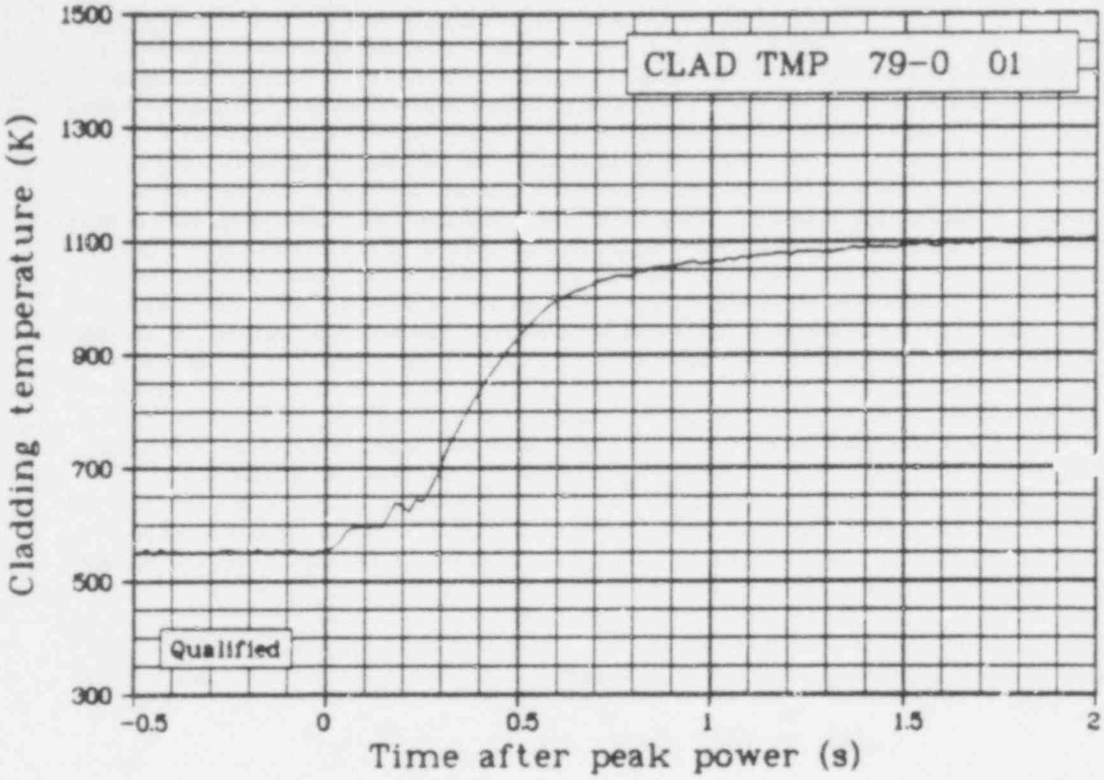

Fig. 10 Rod 802-1 cladding surface temperature at an elevation of 0.79 m above fuel stack bottom (CLAD TMP 79-0 01), from -0.5 to 2 s, qualified.

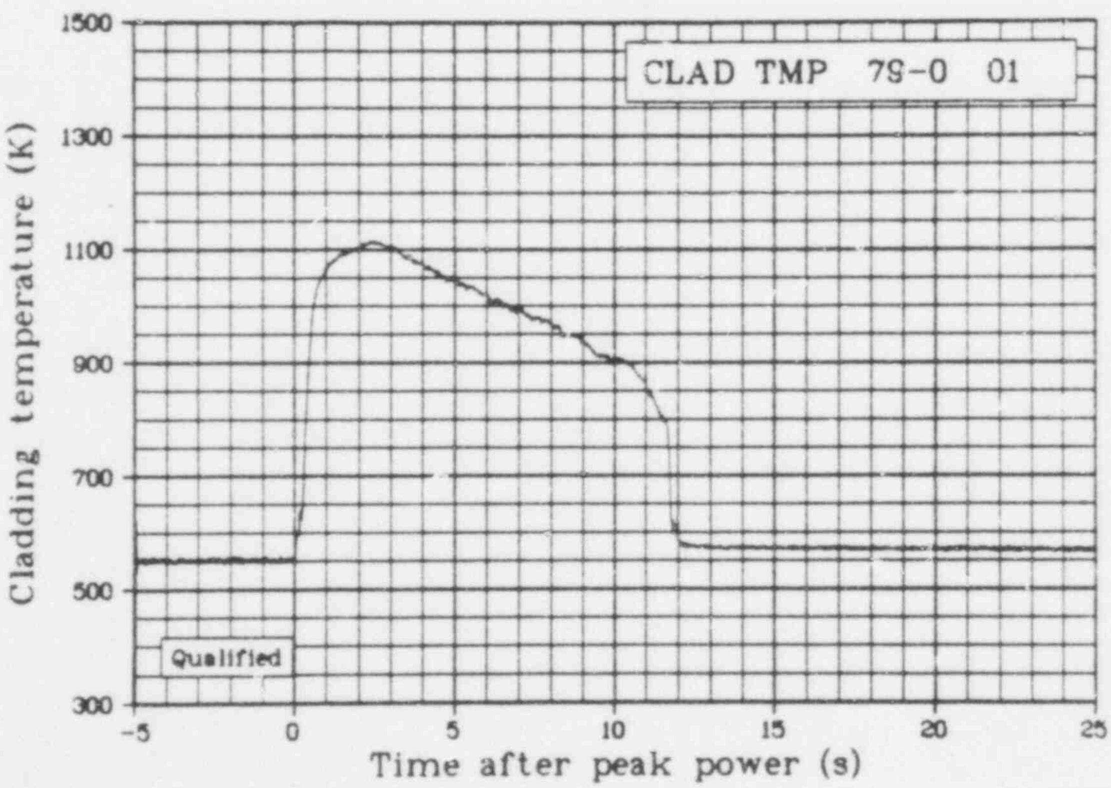

Fig. 11 Rod 802-1 cladding surface temperature at an elevation of 0.79 m above fuel stack bottom (CLAD TMP 79-0 01), from -5 to 25 s, qualified.

631 092

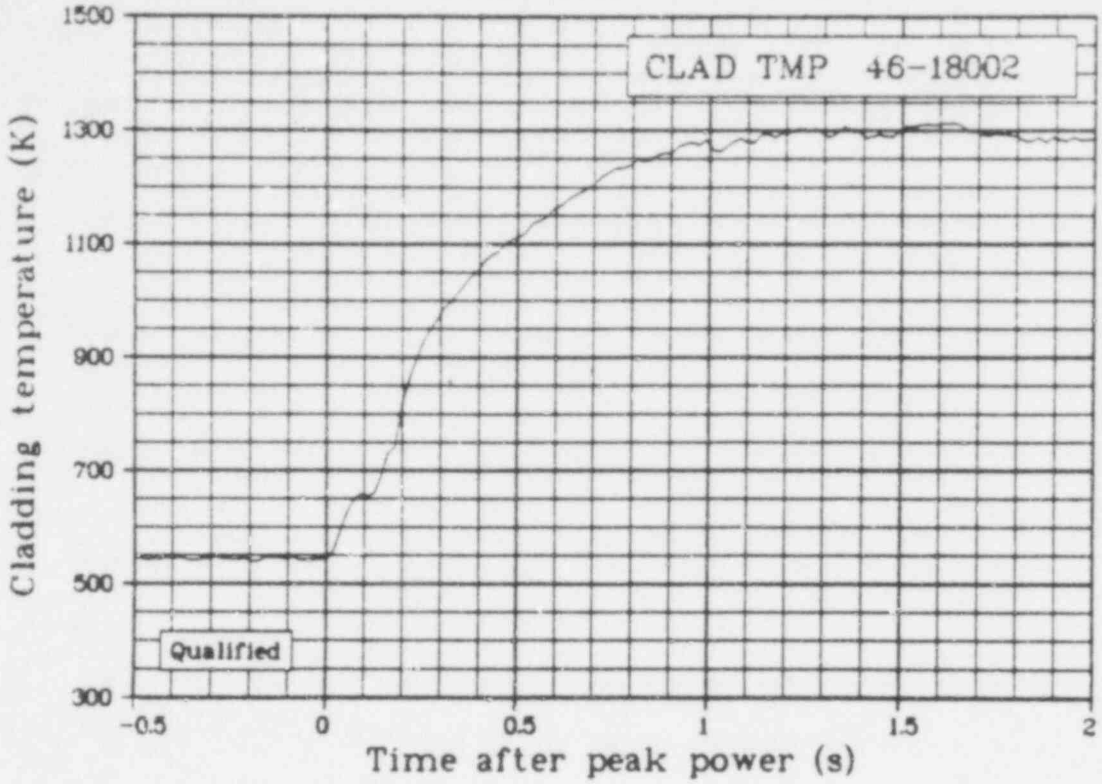

Fig. 12 Rod 802-2 cladding surface temperature at an elevation of 0.46 m above fuel stack bottom (CLAD TMP 46-18002), from -0.5 to 2 s, qualified.

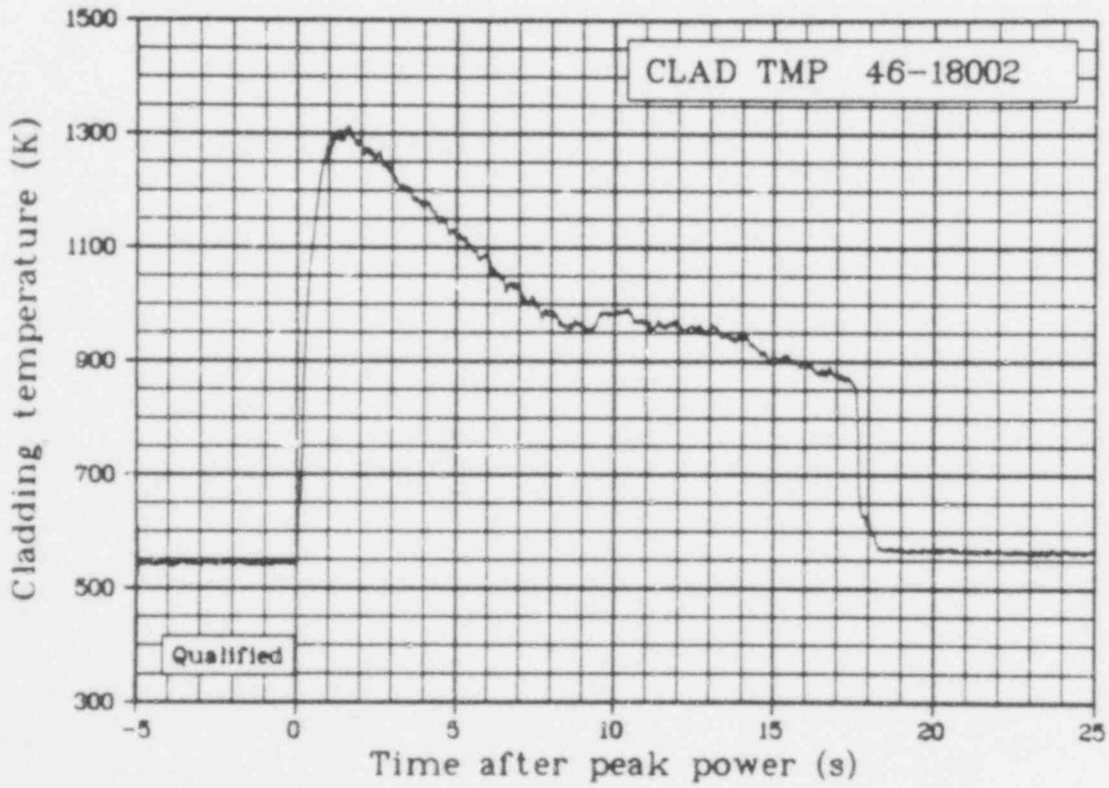

Fig. 13 Rod 802-2 cladding surface temperature at an elevation of 0.46 m above fuel stack bottom (CLAD TMP 46-18002), from -5 to 25 s, qualified.

631 093

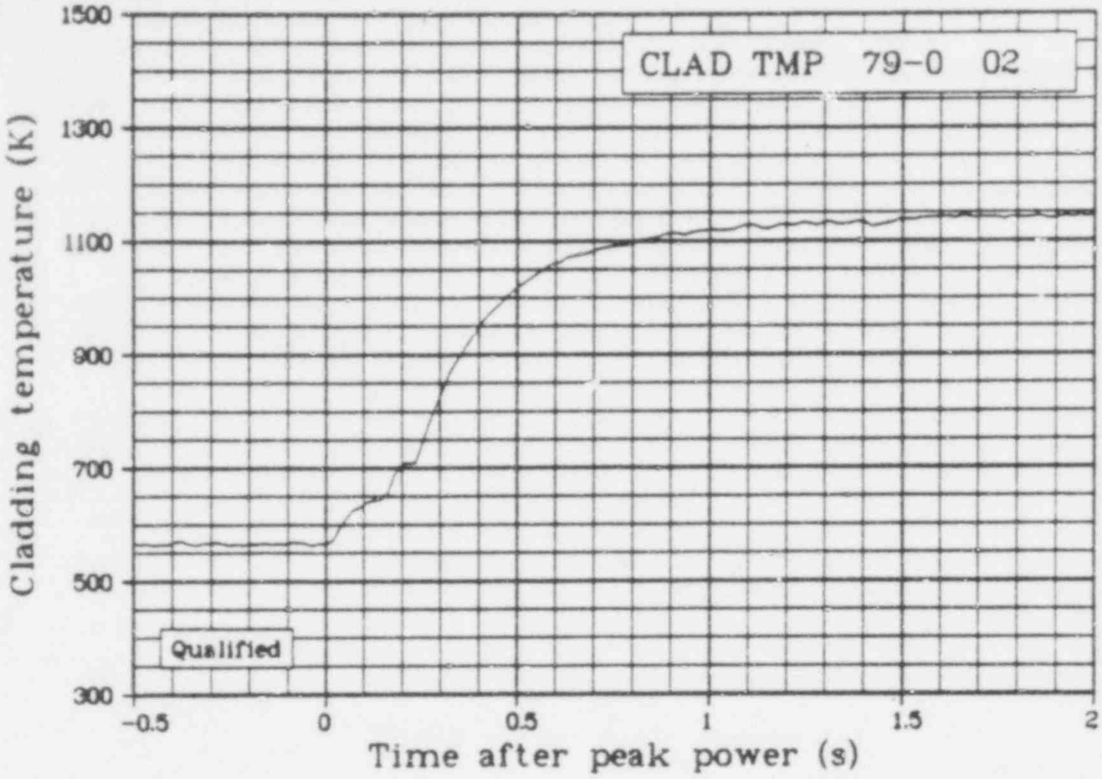

Fig. 14 Rod 802-2 cladding surface temperature at an elevation of 0.79 m above fuel stack bottom (CLAD TMP 79-0 02), from -0.5 to 2 s, qualified.

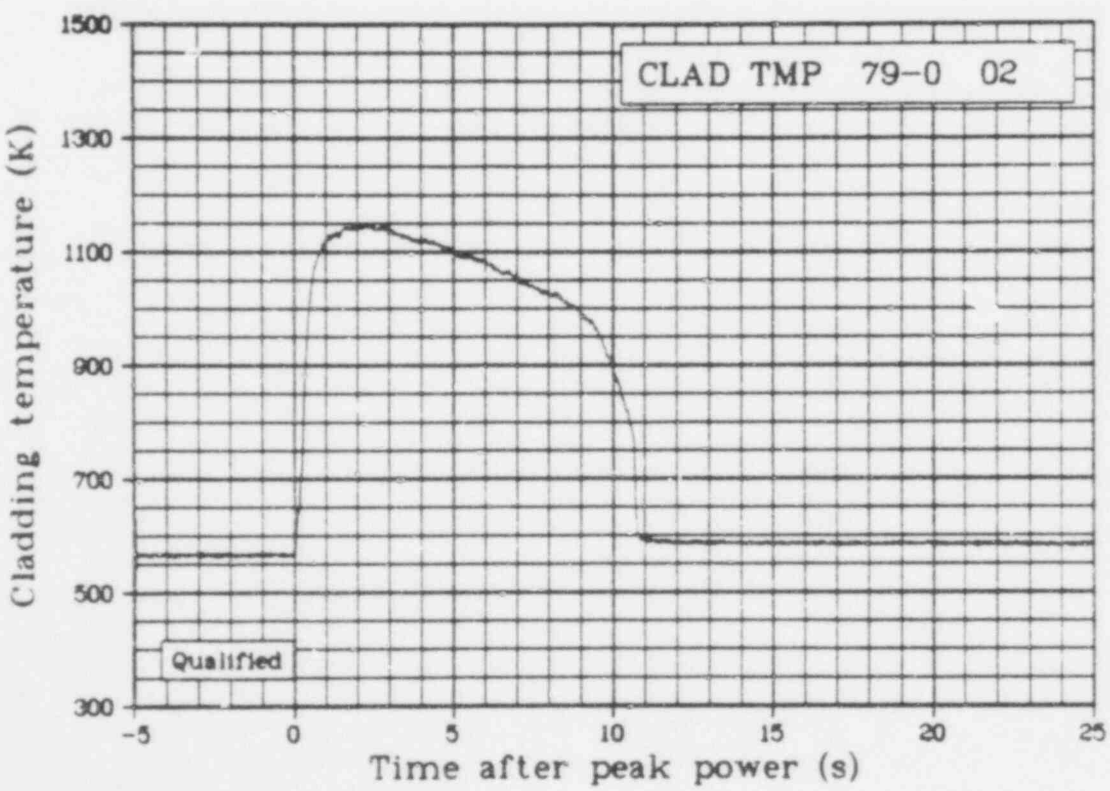

Fig. 15 Rod 802-2 cladding surface temperature at an elevation of 0.79 m above fuel stack bottom (CLAD TMP 79-0 02), from -5 to 25 s, qualified.

631 094

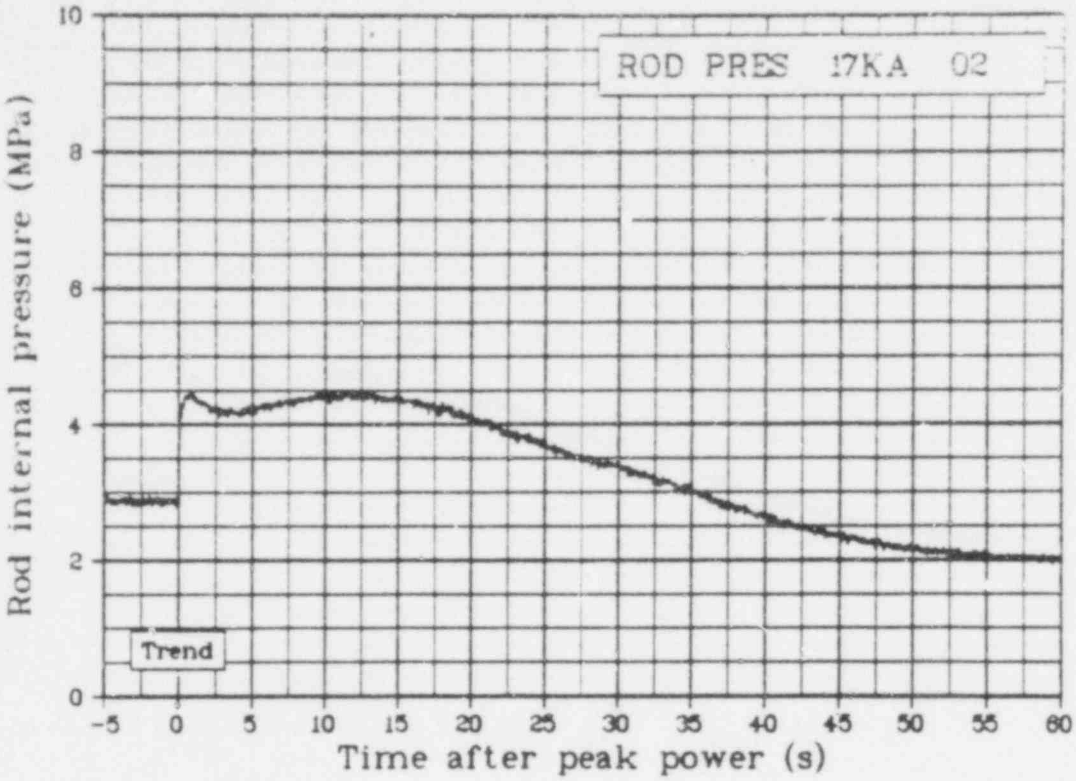

Fig. 16 Rod 802-2 plenum pressure (ROD PRES 17KA 02), trend.

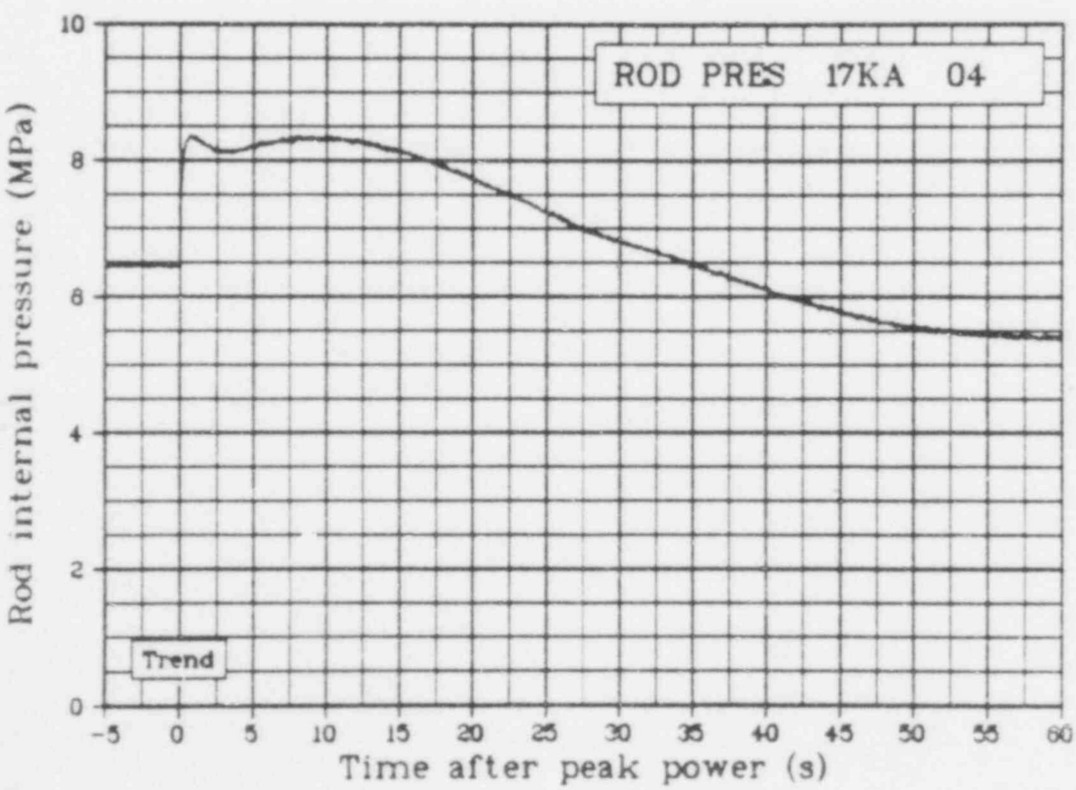

Fig. 17 Rod 802-4 plenum pressure (ROD PRES 17KA 04), trend.

631 095

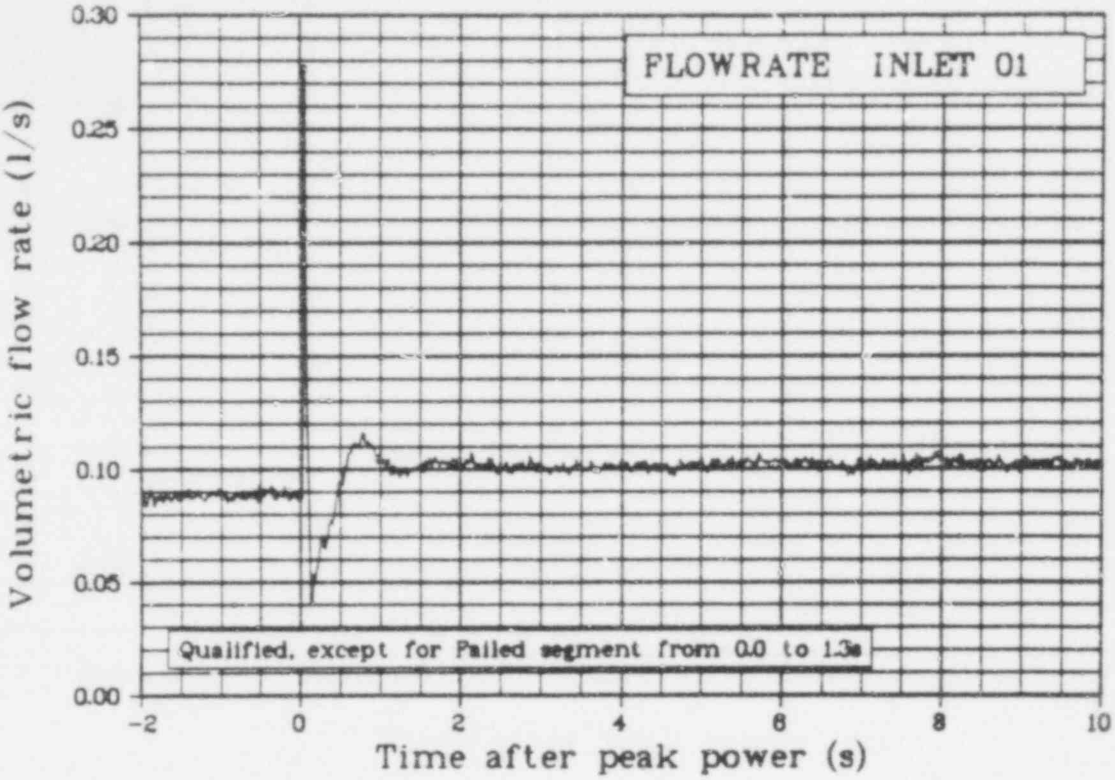

Fig. 18 Coolant flow rate at the Rod 802-1 shroud inlet (FLOWRATE INLET 01), qualified, except for failed segment from 0.0 to 1.3 s.

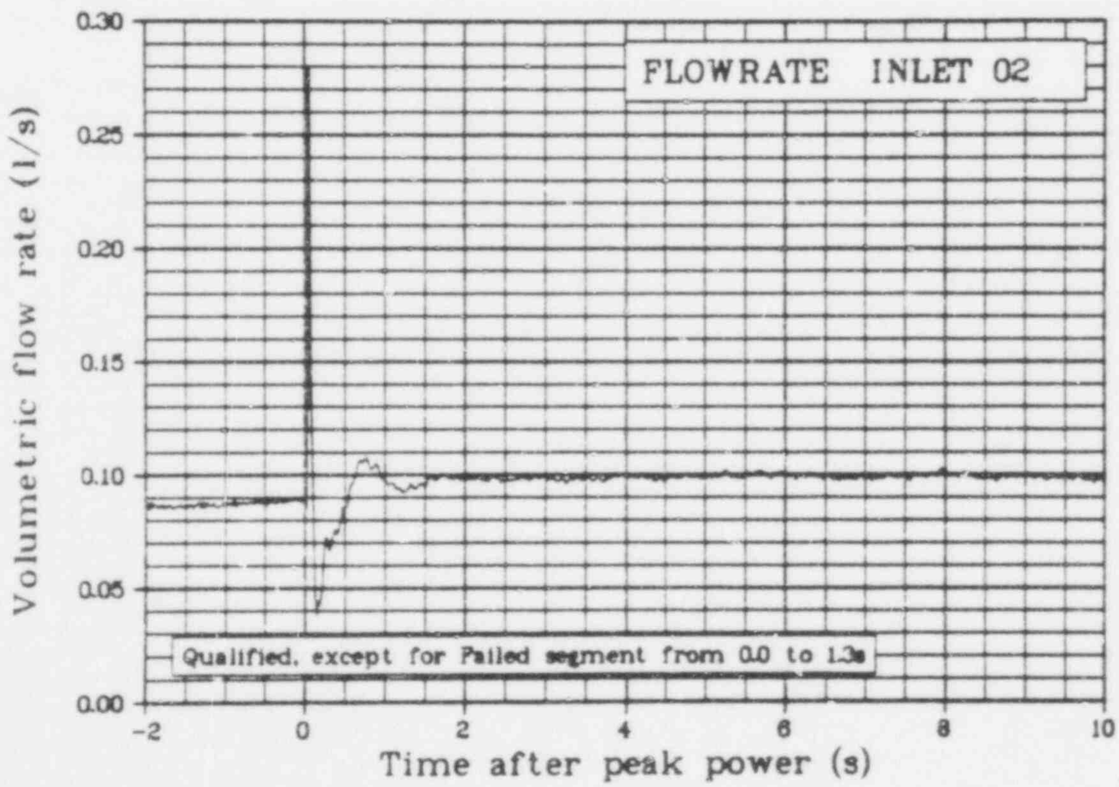

Fig. 19 Coolant flow rate at the Rod 802-2 shroud inlet (FLOWRATE INLET 02), qualified, except for failed segment from 0.0 to 1.3 s.

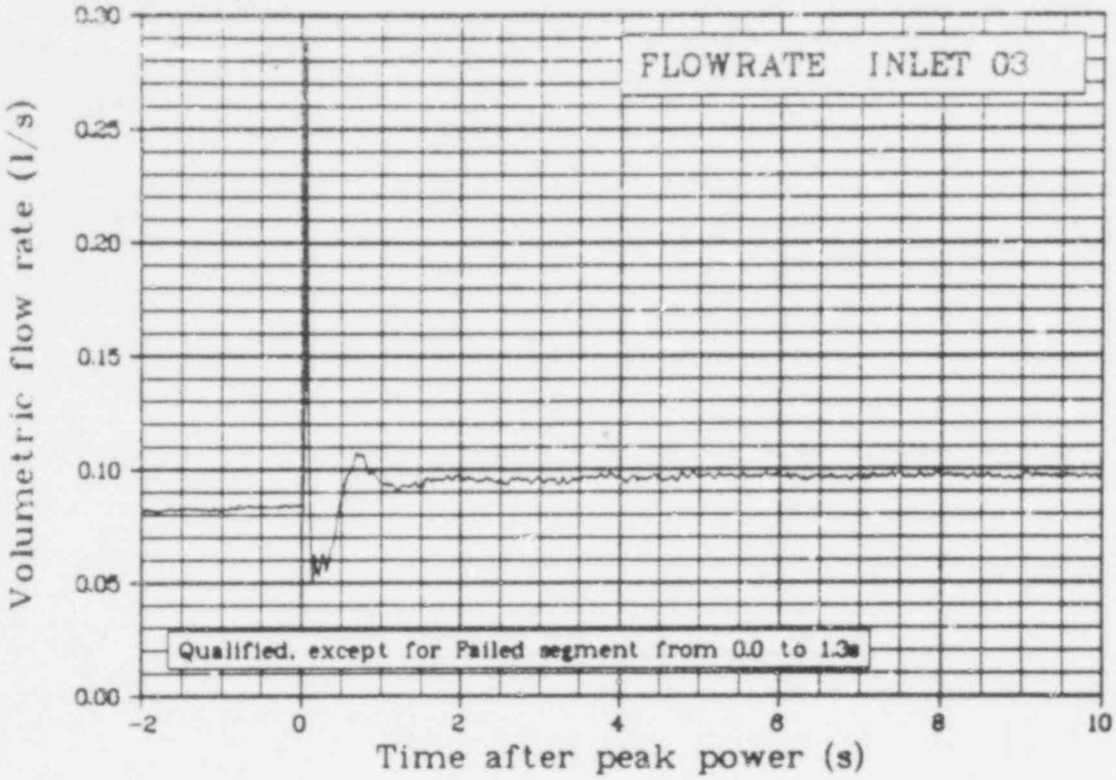

Fig. 20 Coolant flow rate at the Rod 802-3 shroud inlet (FLOWRATE INLET 03), qualified, except for failed segment from 0.0 to 1.3 s.

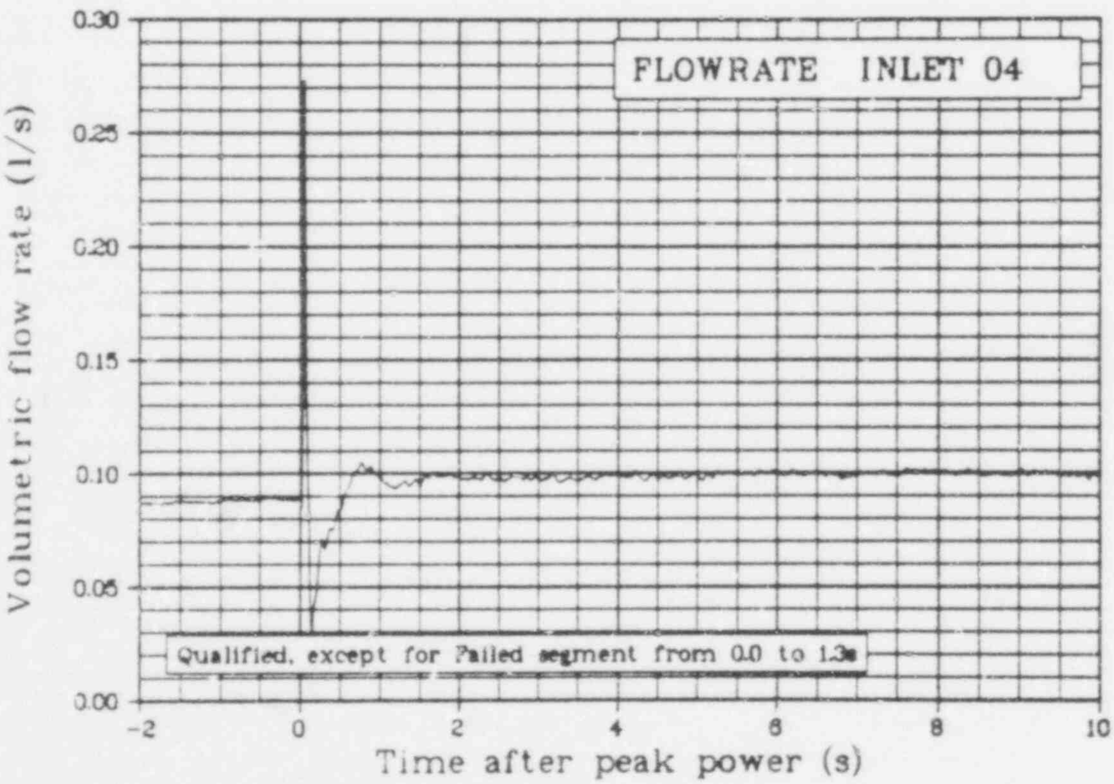

Fig. 21 Coolant flow rate at the Rod 802-4 shroud inlet (FLOWRATE INLET 04), qualified, except for failed segment from 0.0 to 1.3 s.

631 097

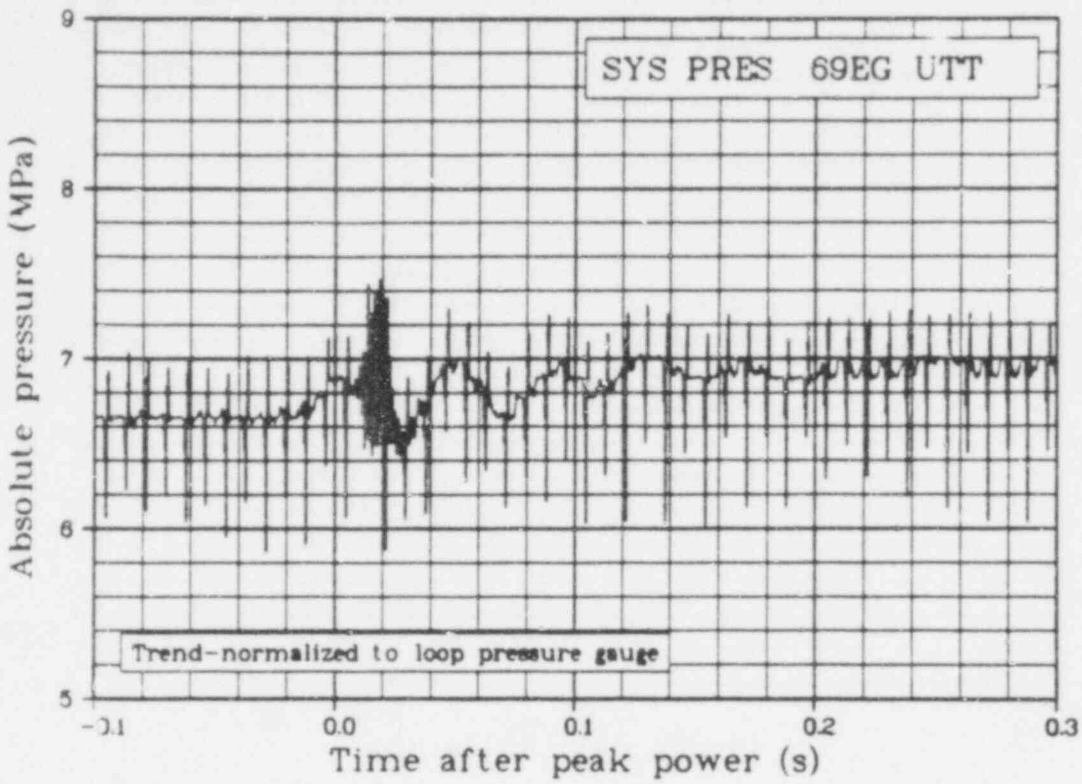

Fig. 22 Absolute system pressure in upper test train (SYS PRES 69EG UTT), from -0.1 to 0.3 s, trend.

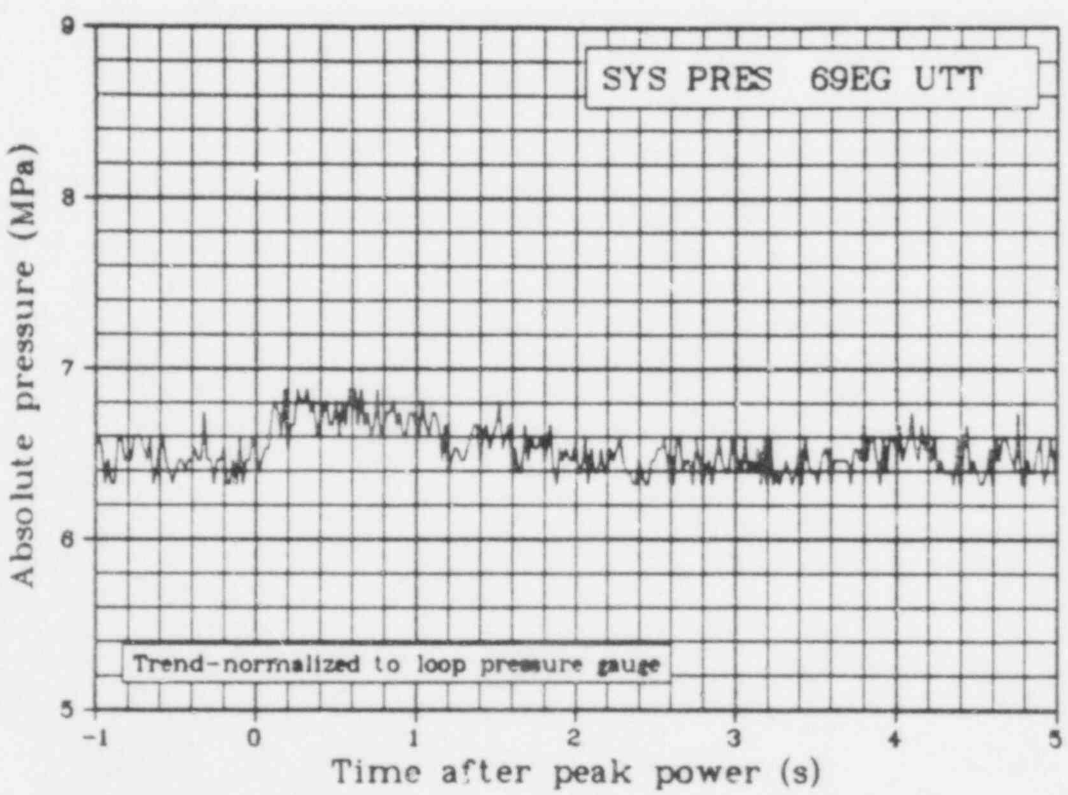

Fig. 23 Absolute system pressure in upper test train (SYS PRES 69EG UTT), from -1 to 5 s, trend.

631 098

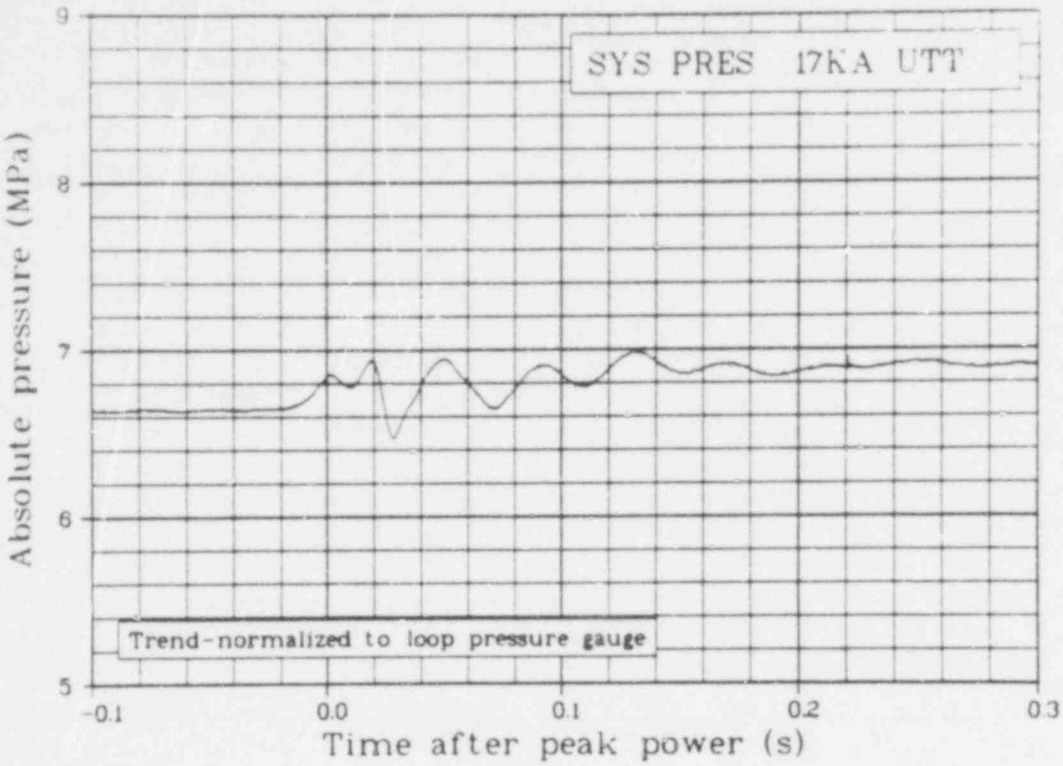

Fig. 24 Absolute system pressure in upper test train (SYS PRES 17KA UTT), from -0.1 to 0.3 s, trend.

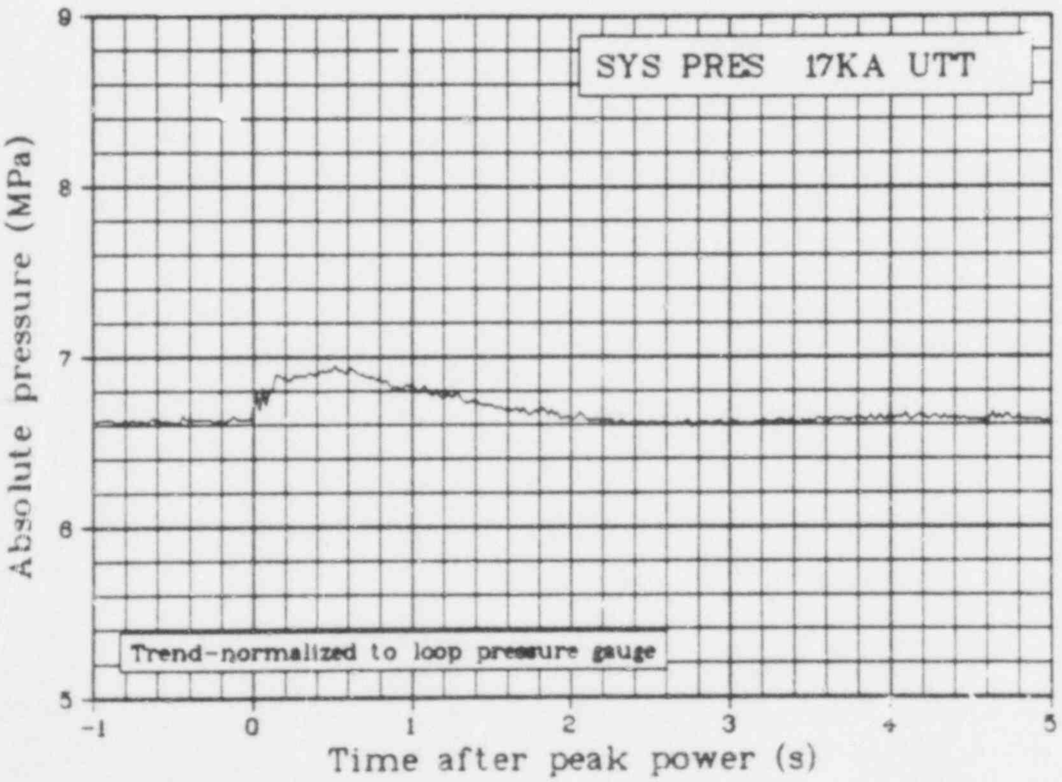

Fig. 25 Absolute system pressure in upper test train (SYS PRES 17KA UTT), from -1 to 5 s, trend.

631 099

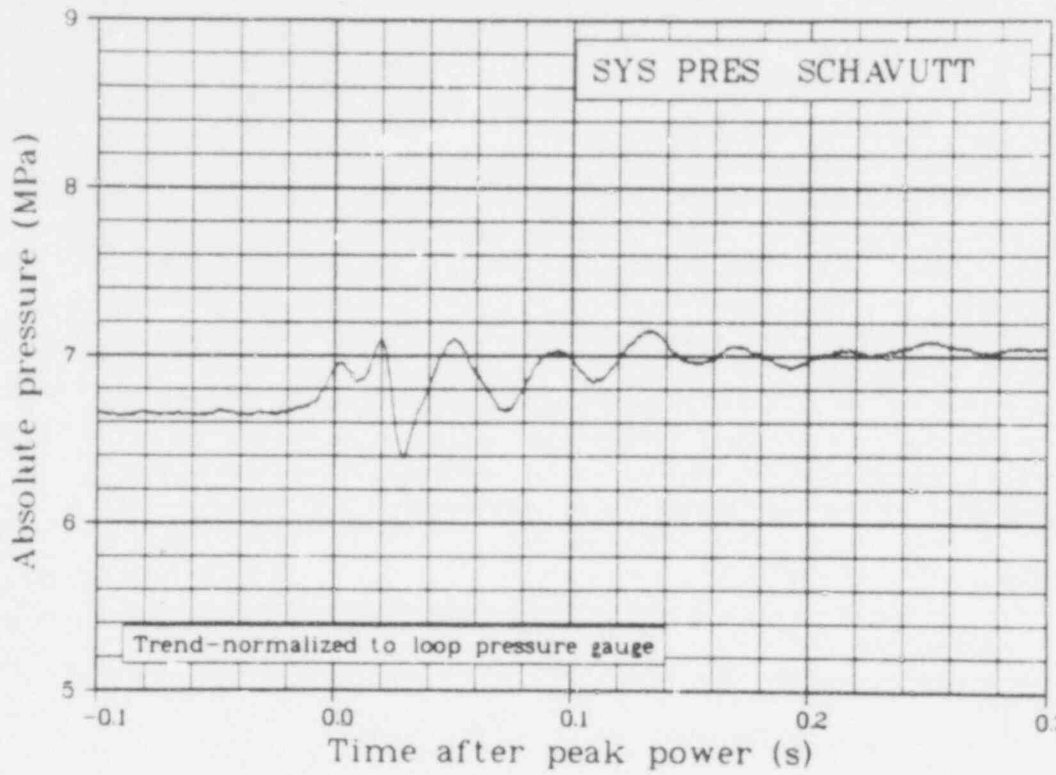

Fig. 26 Absolute system pressure in upper test train (SYS PRES SCHAVUTT), from -0.1 to 0.3 s trend.

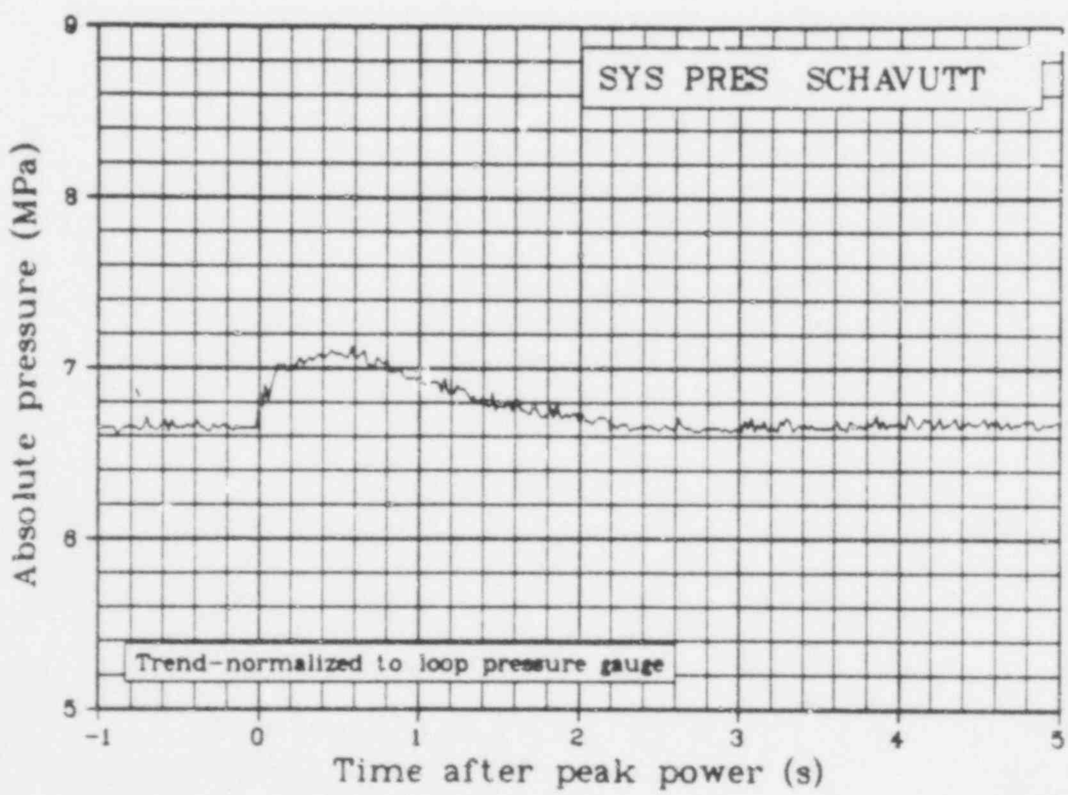

Fig. 27 Absolute system pressure in upper test train (SYS PRES SCHAVUTT), from -1 to 5 s, trend.

631 100

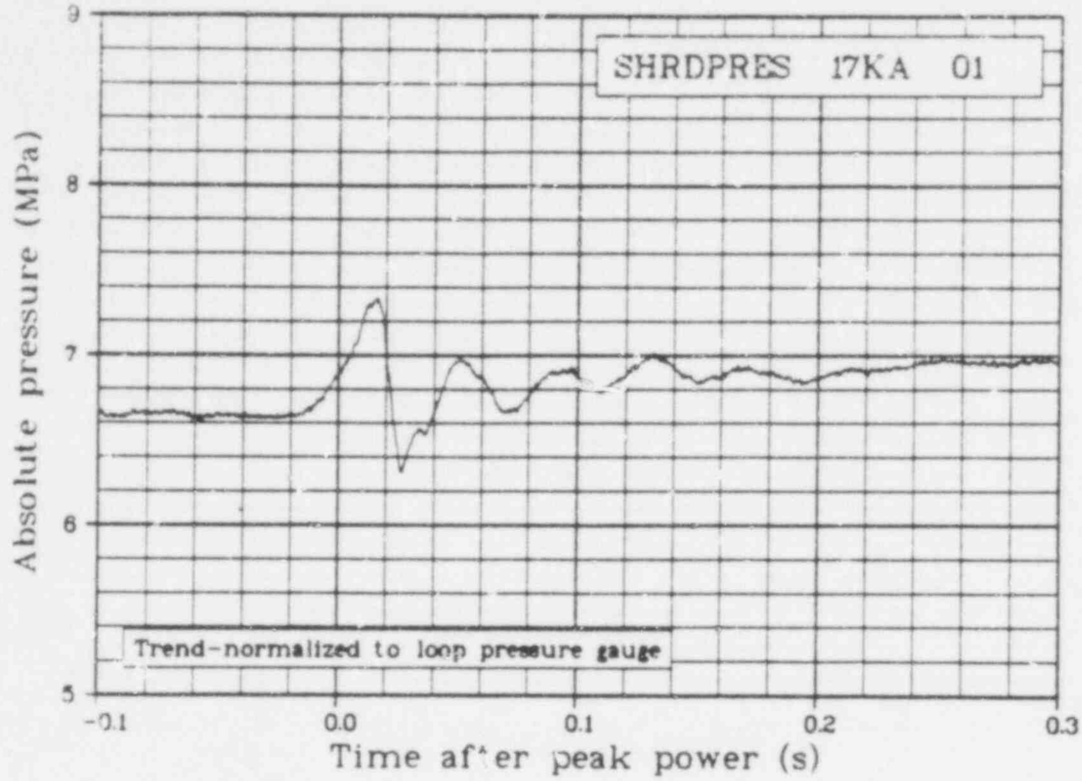

Fig. 28 Absolute pressure in the Rod 802-1 shroud (SHRDPRES 17KA 01), -0.1 to 0.3 s, trend.

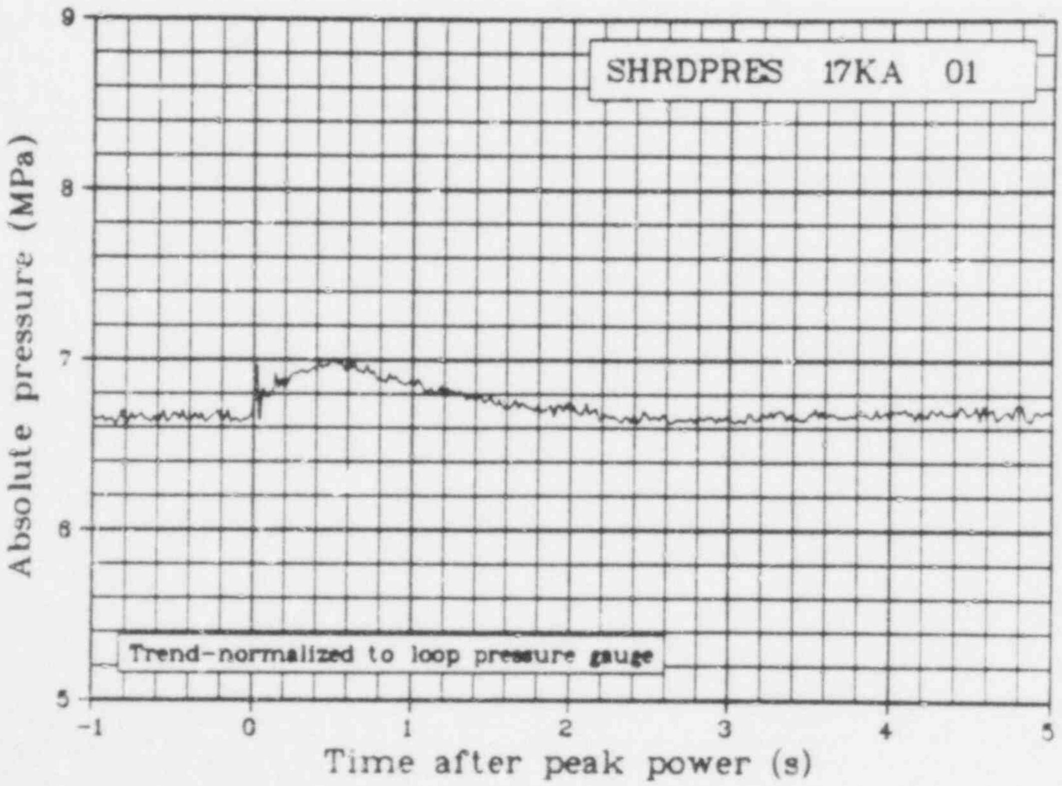

Fig. 29 Absolute pressure in the Rod 802-1 shroud (SHRDPRES 17KA 01), -1 to 5 s, trend.

631 101

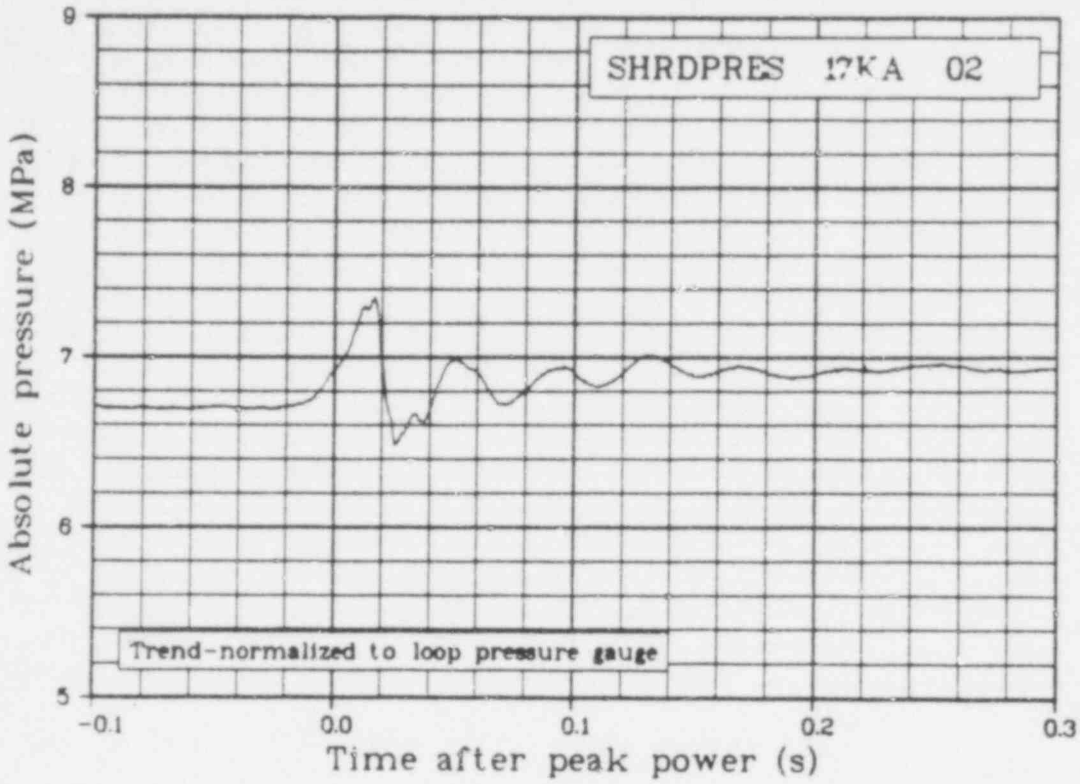

Fig. 30 Absolute pressure in the Rod 802-2 shroud (SHRDPRES 17KA 02), -0.1 to 0.3 s, trend.

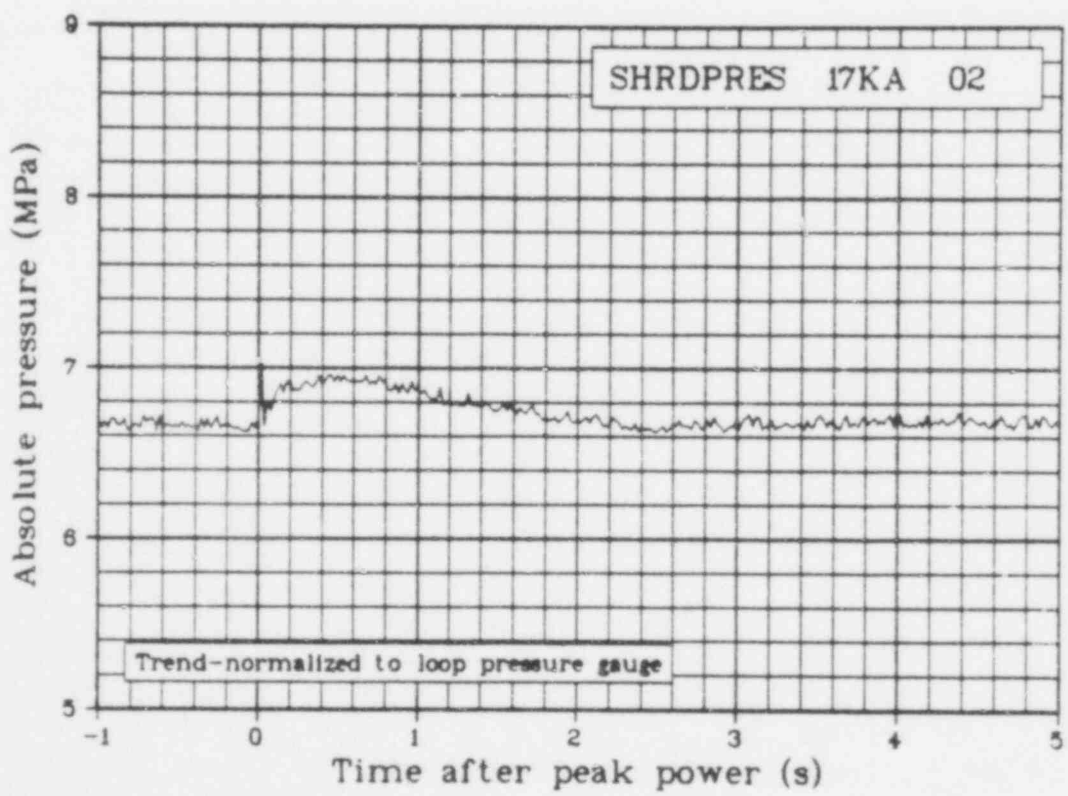

Fig. 31 Absolute pressure in the Rod 802-2 shroud (SHRDPRES 17KA 02), -1 to 5 s, trend.

631 102

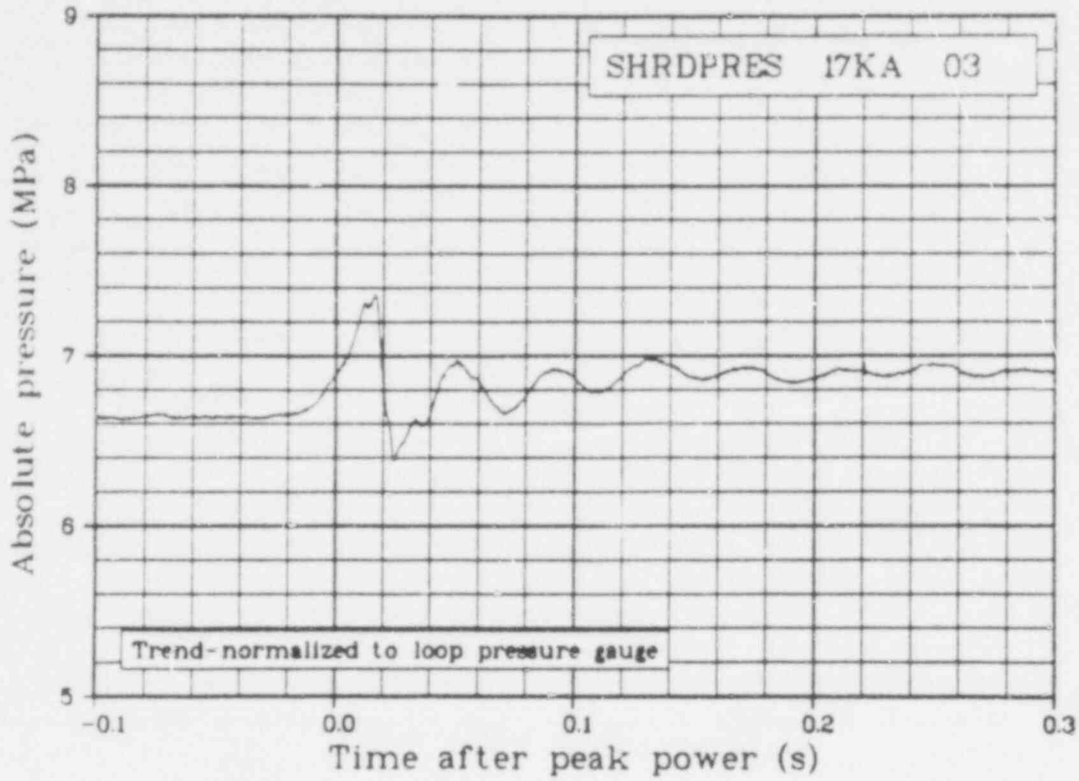

Fig. 32 Absolute pressure in the Rod 802-3 shroud (SHRDPRES 17KA 03), -0.1 to 0.3 s, trend.

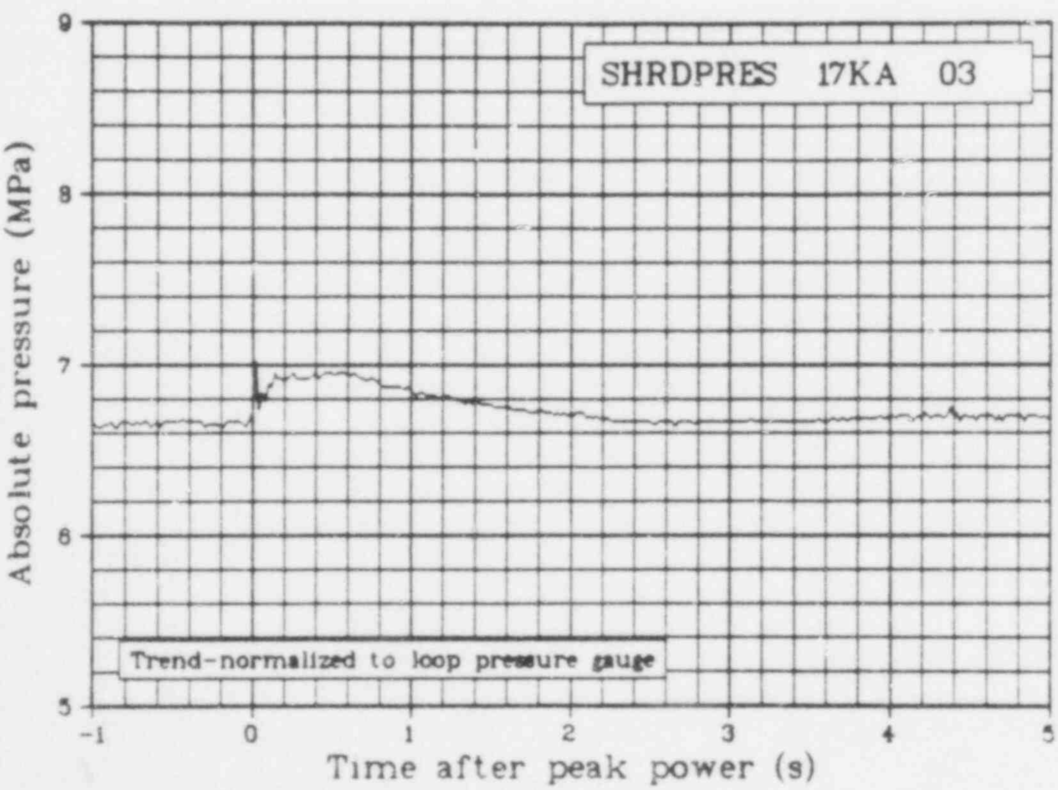

Fig. 33 Absolute pressure in the Rod 802-3 shroud (SHRDPRES 17KA 03), -1 to 5 s, trend.

631 103

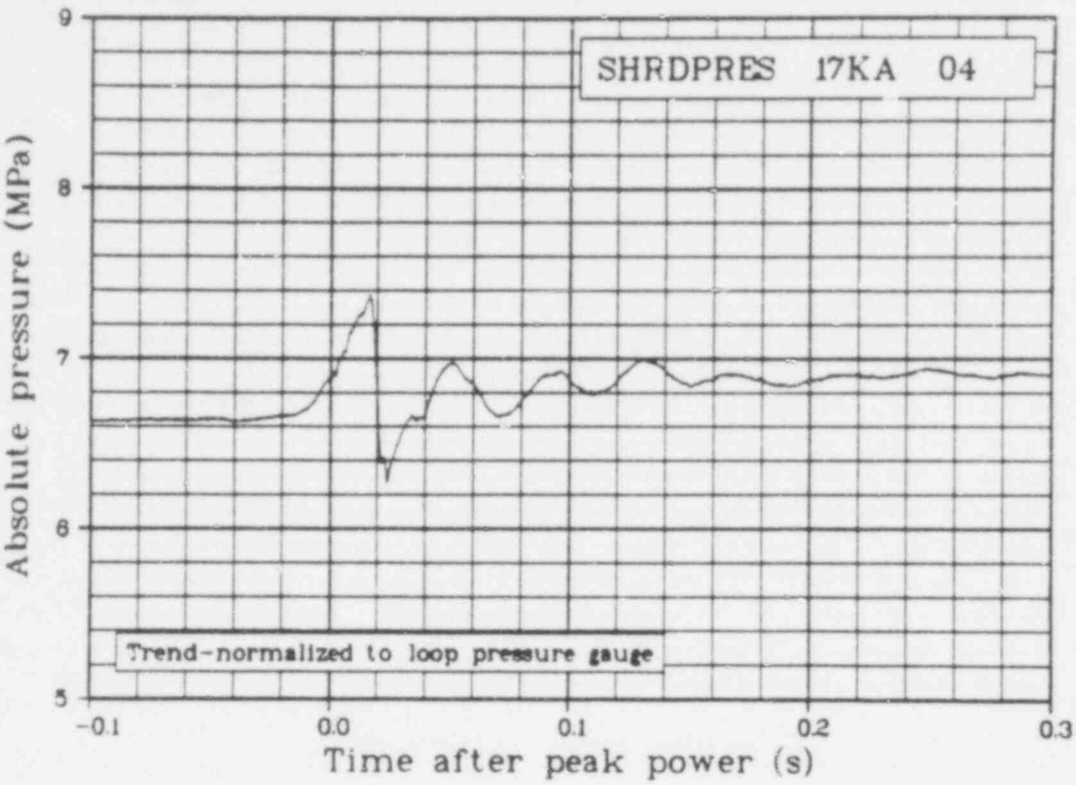

Fig. 34 Absolute pressure in the Rod 802-4 shroud (SHRDPRES 17KA 04), -0.1 to 0.3 s, trend.

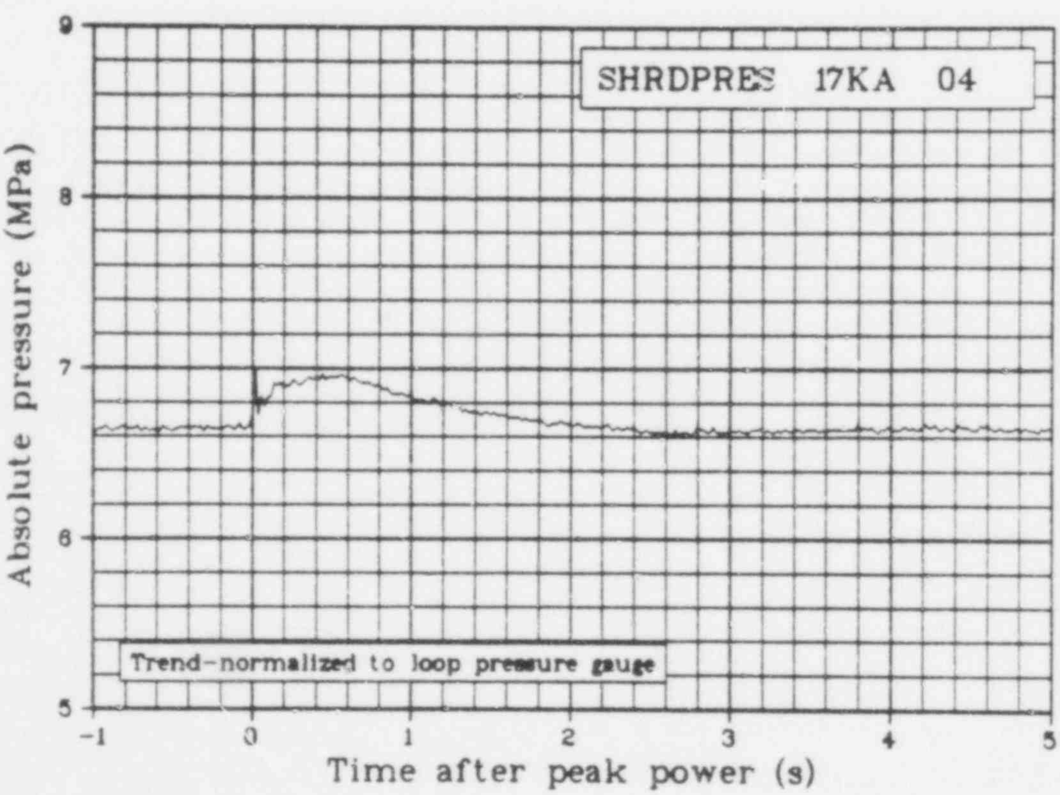

Fig. 35 Absolute pressure in the Rod 802-4 shroud (SHRDPRES 17KA 04), -1 to 5 s, trend.

631 104

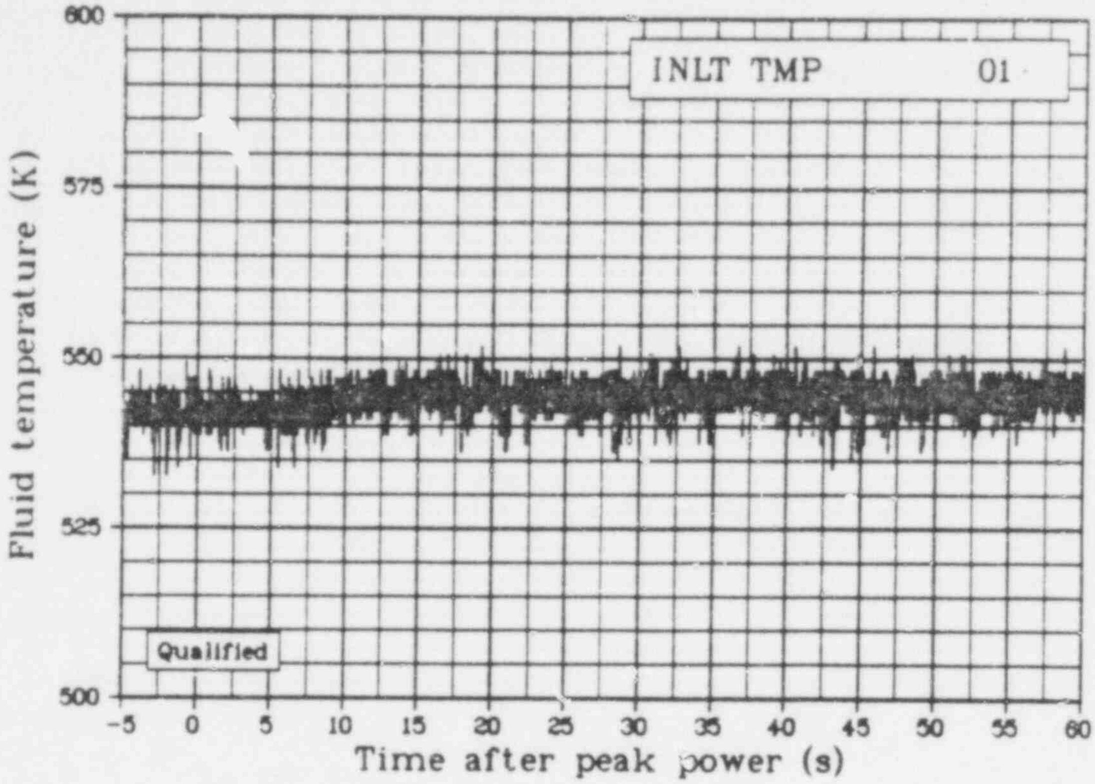

Fig. 36 Coolant temperature at the Rod 802-1 shroud inlet (INLT TMP 01), qualified.

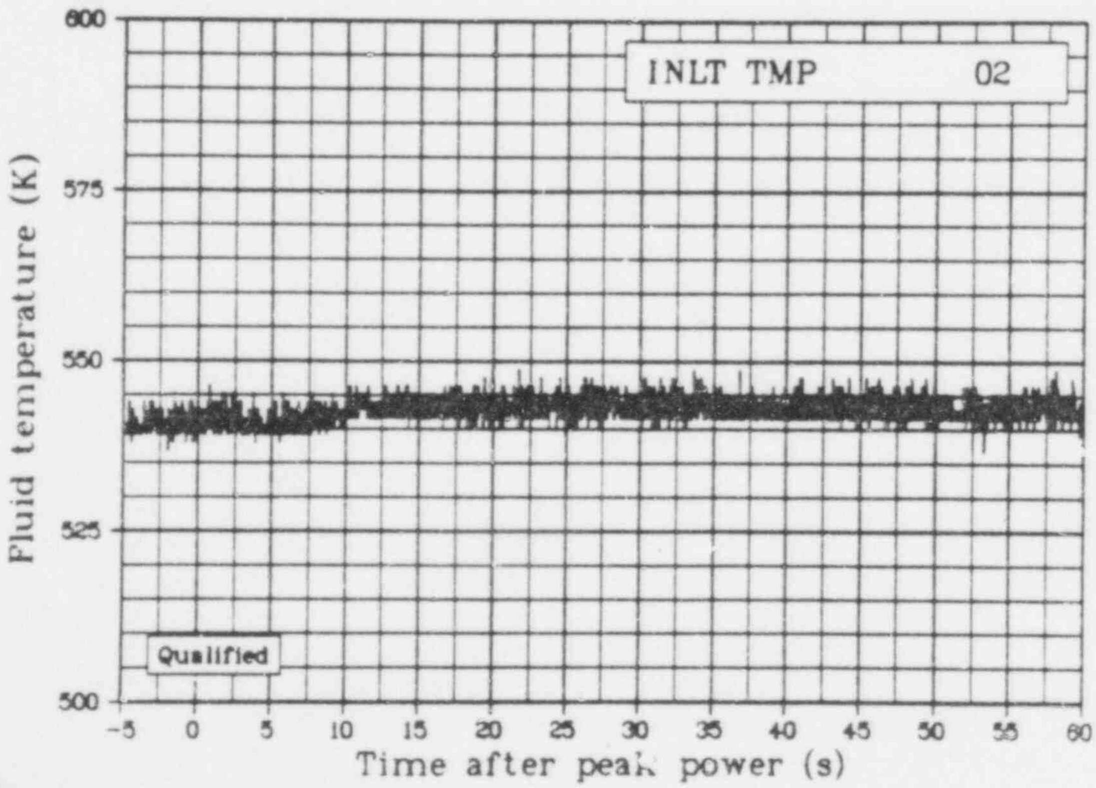

Fig. 37 Coolant temperature at the Rod 802-2 shroud inlet (INLT TMP 02), qualified.

631 105

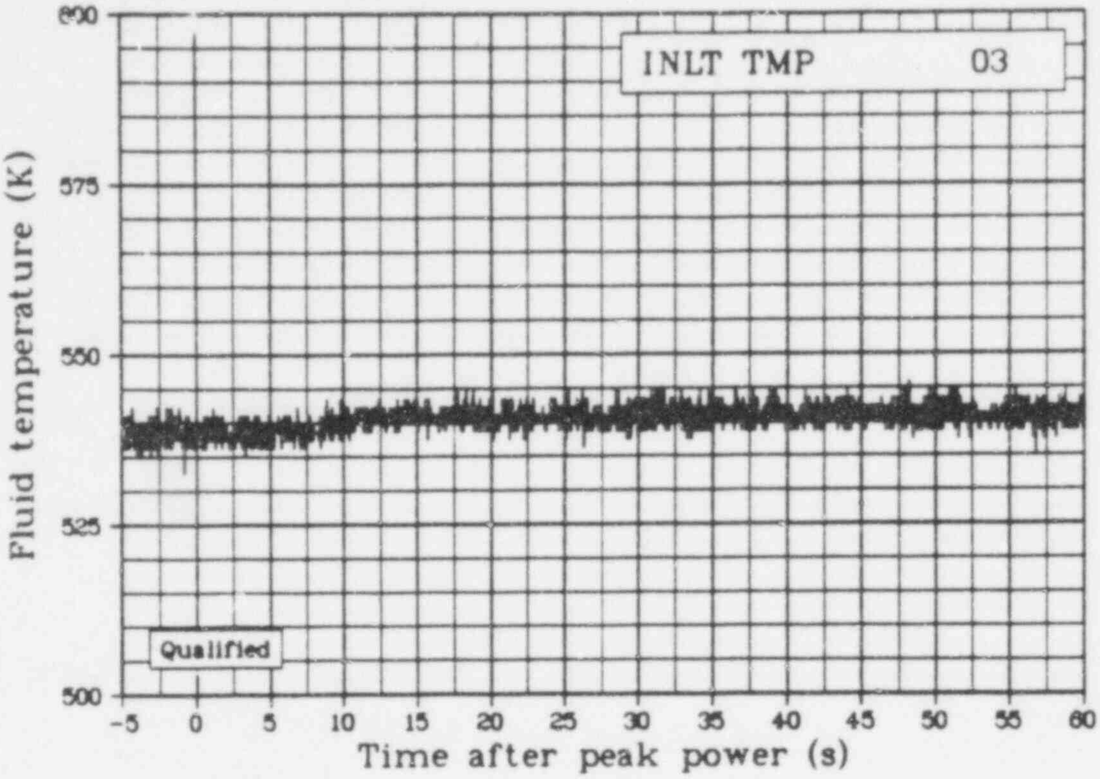

Fig. 38 Coolant temperature at the Rod 802-3 shroud inlet (INLT TMP 03), qualified.

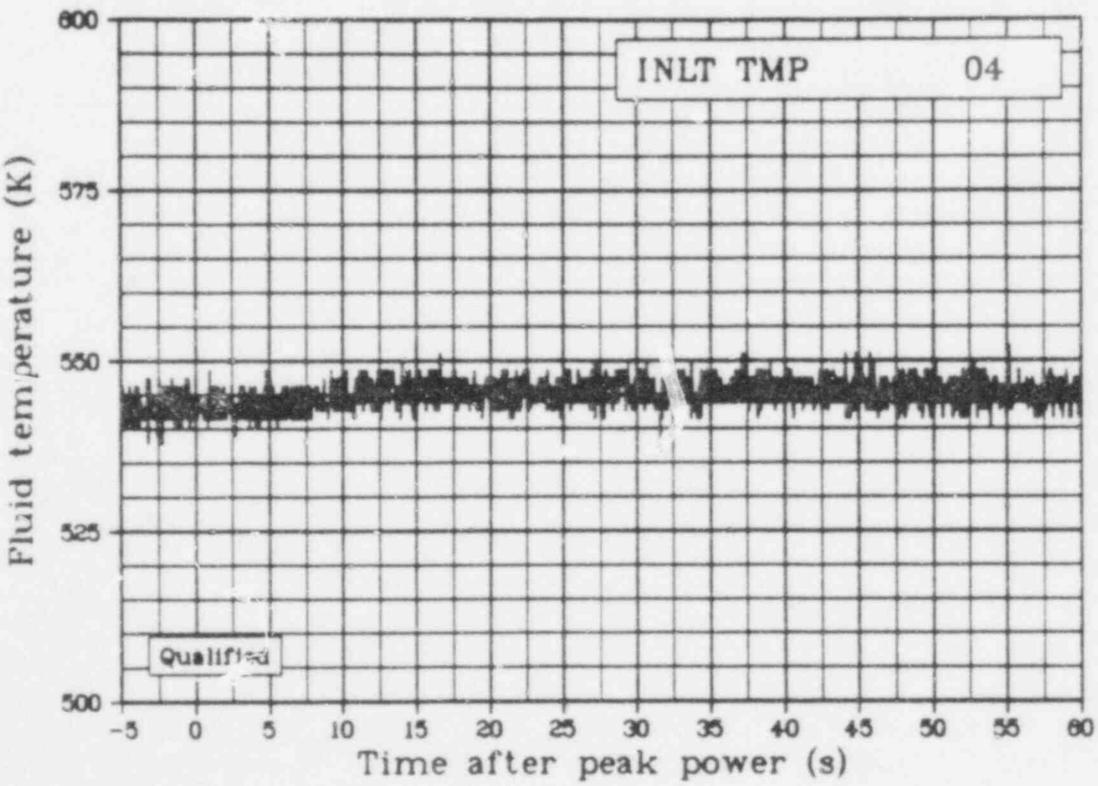

Fig. 39 Coolant temperature at the Rod 802-4 shroud inlet (INLT TMP 04), qualified.

631 106

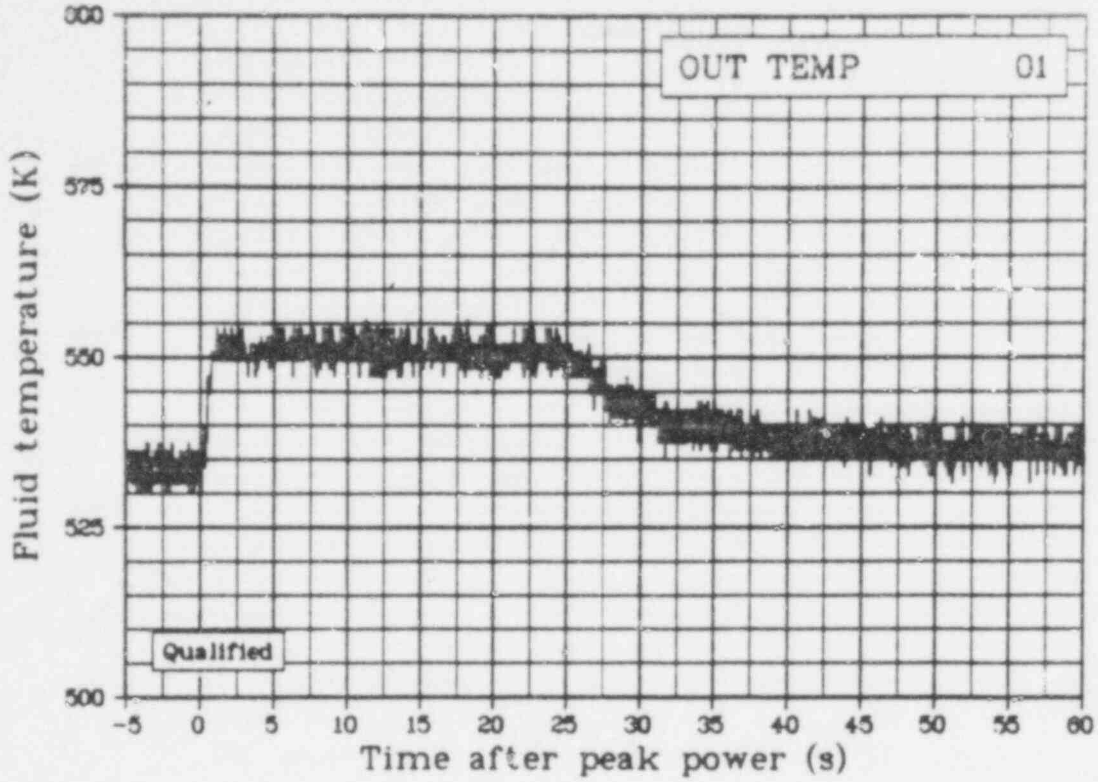

Fig. 40 Coolant temperature at the Rod 802-1 shroud outlet (OUT TEMP 01), qualified.

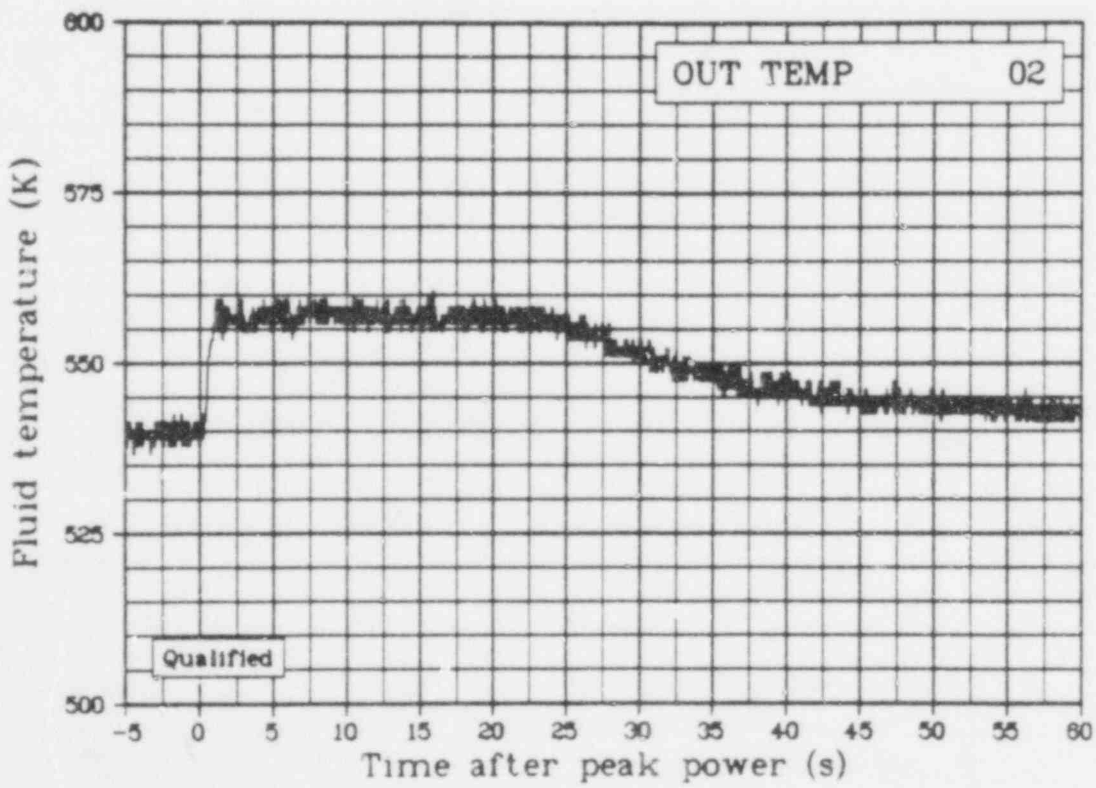

Fig. 41 Coolant temperature at the Rod 802-2 shroud outlet (OUT TEMP 02), qualified.

631 107

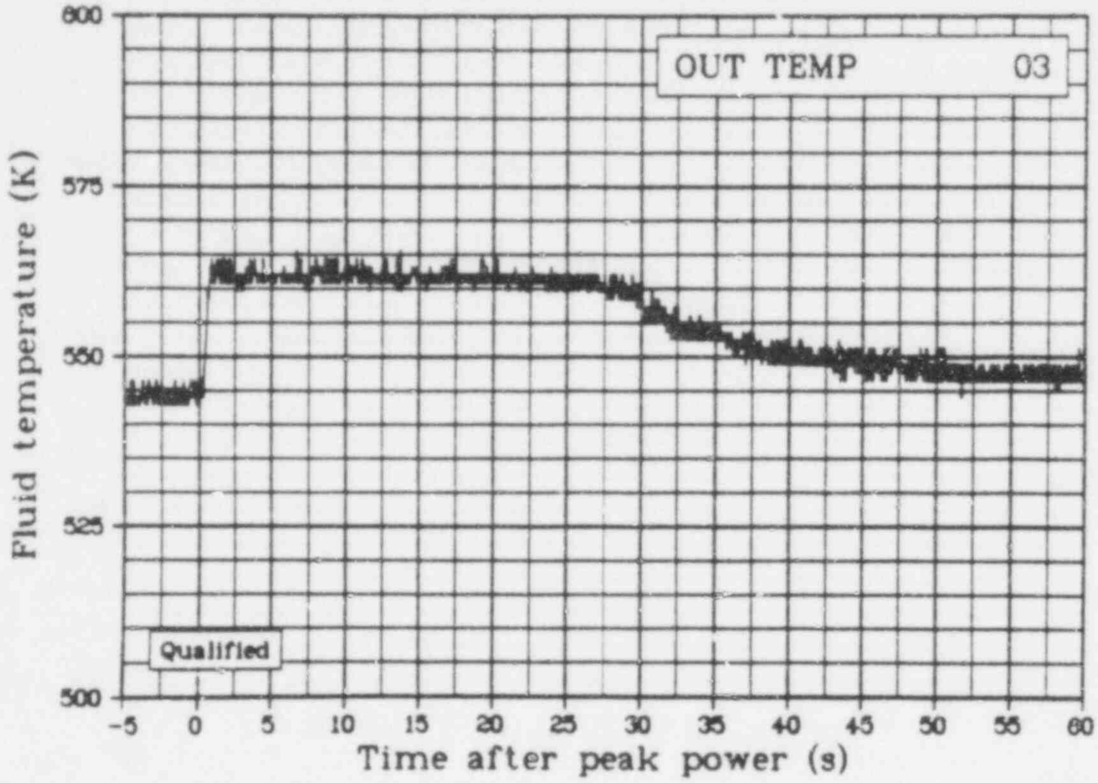

Fig. 42 Coolant temperature at the Rod 802-3 shroud outlet (OUT TEMP 03), qualified.

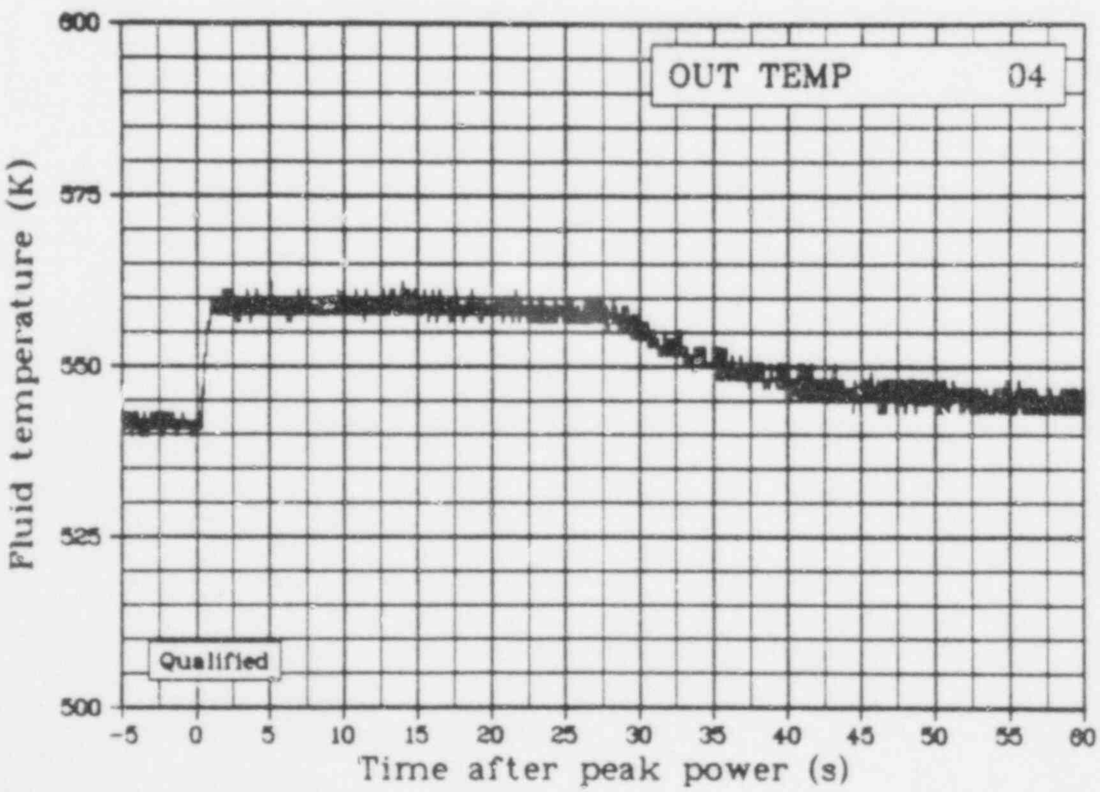

Fig. 43 Coolant temperature at the Rod 802-4 shroud outlet (OUT TEMP 04), qualified.

631 108

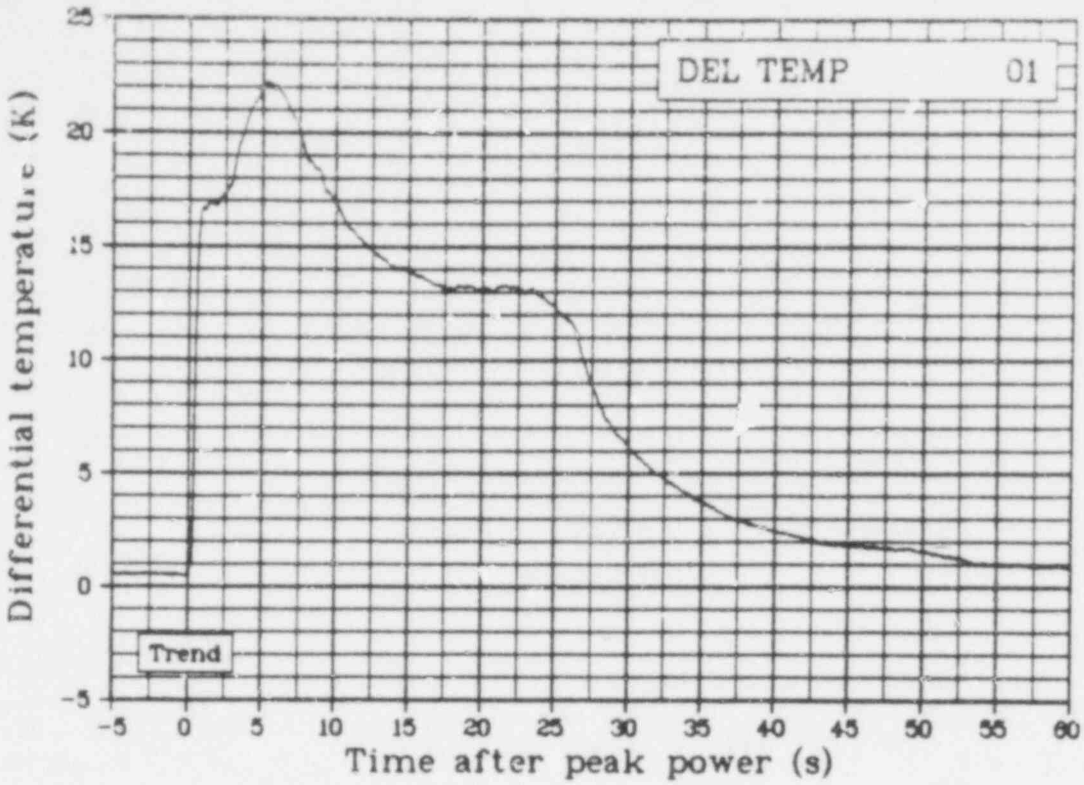

Fig. 44 Coolant temperature increase across the Rod 802-1 shroud (DEL TEMP 01), trend.

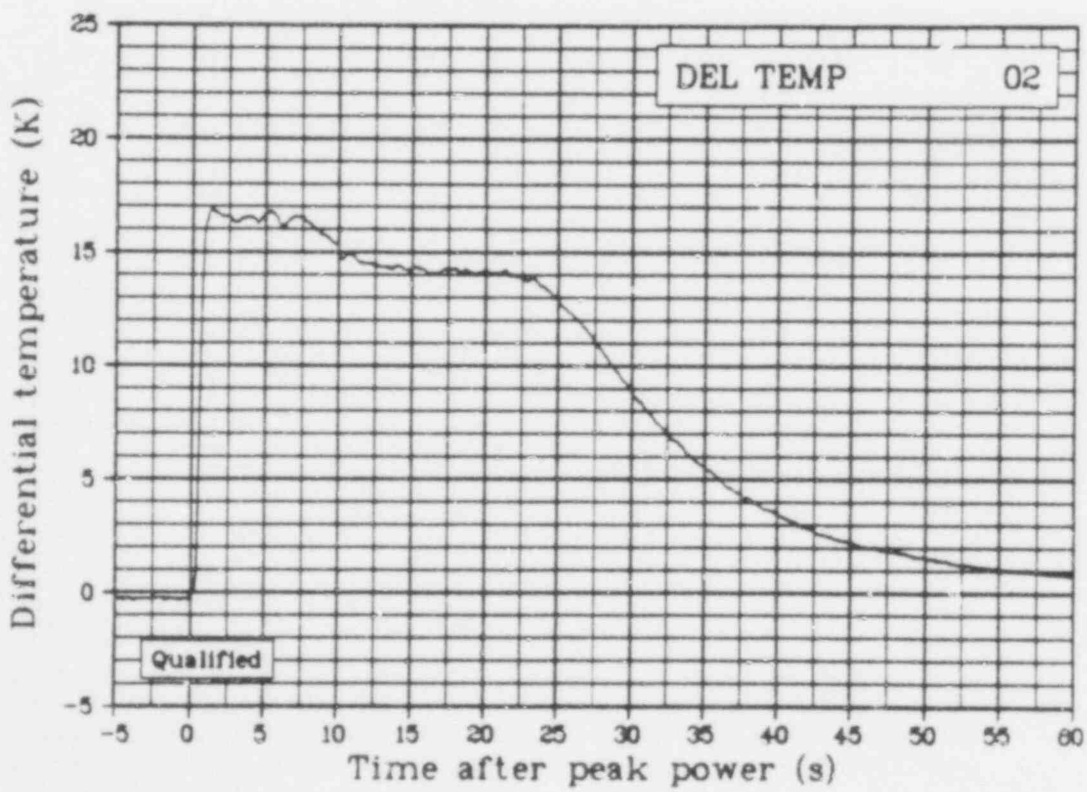

Fig. 45 Coolant temperature increase across the Rod 802-2 shroud (DEL TEMP 02), qualified.

631 109

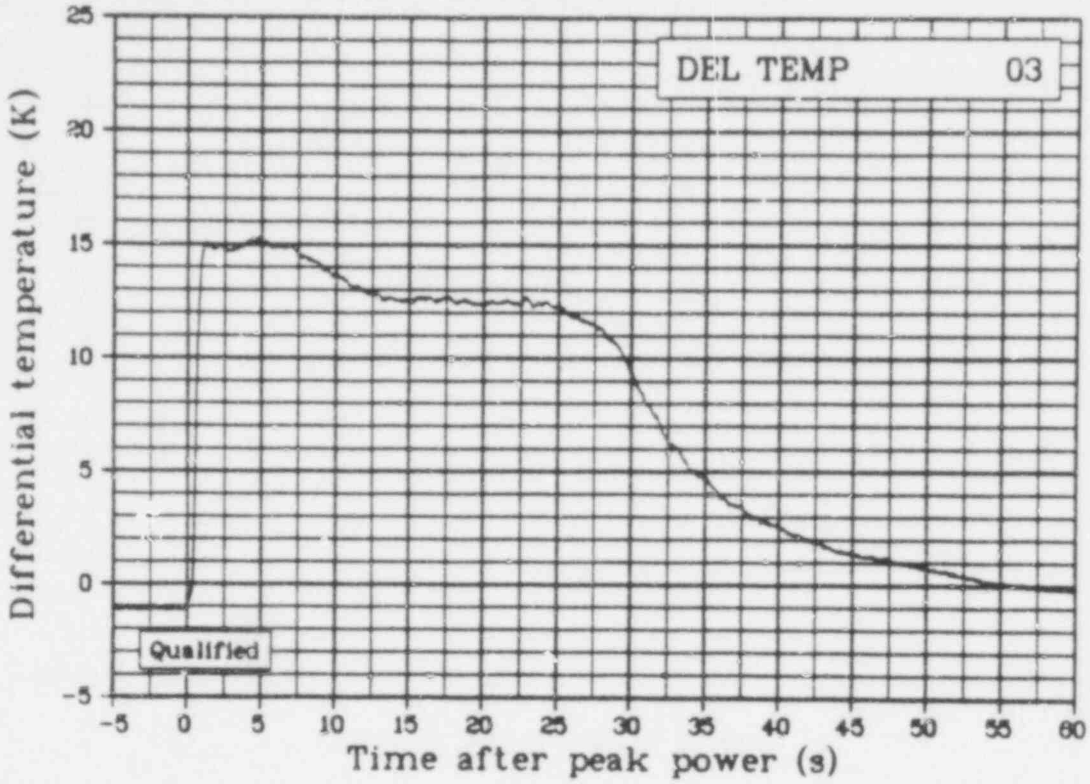

Fig. 46 Coolant temperature increase across the Rod 802-3 shroud (DEL TEMP 03), qualified.

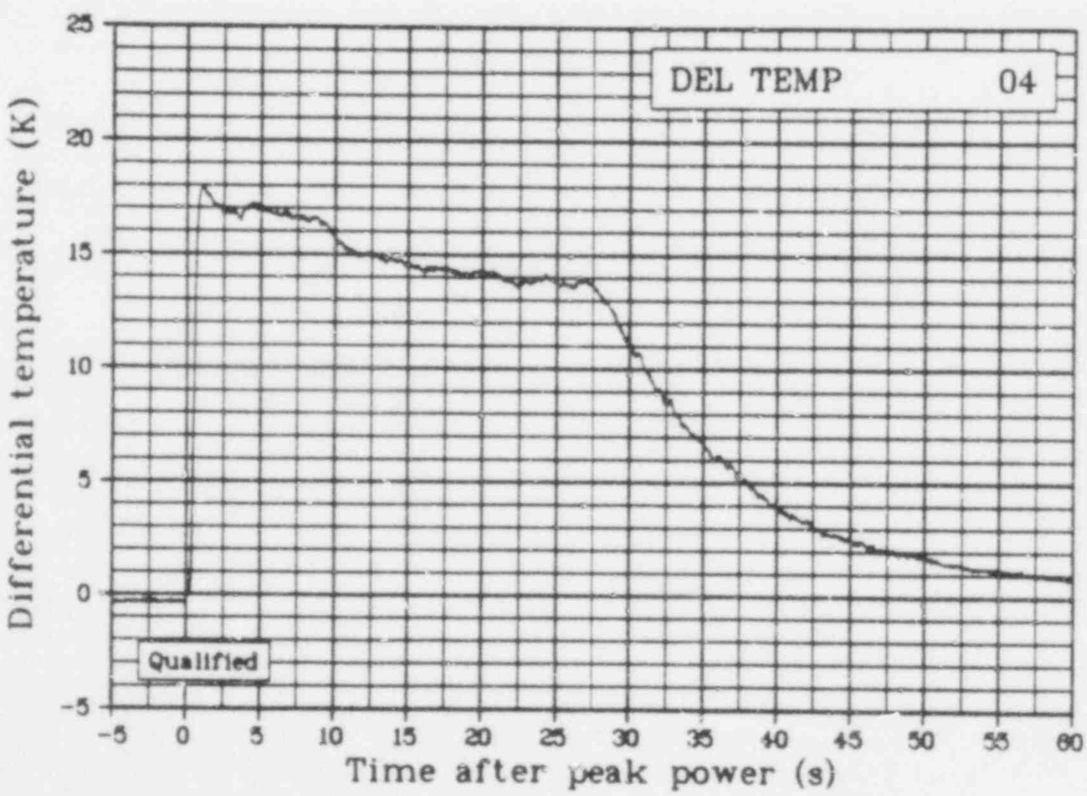

Fig. 47 Coolant temperature increase across the Rod 802-4 shroud (DEL TEMP 04), qualified.

631 110

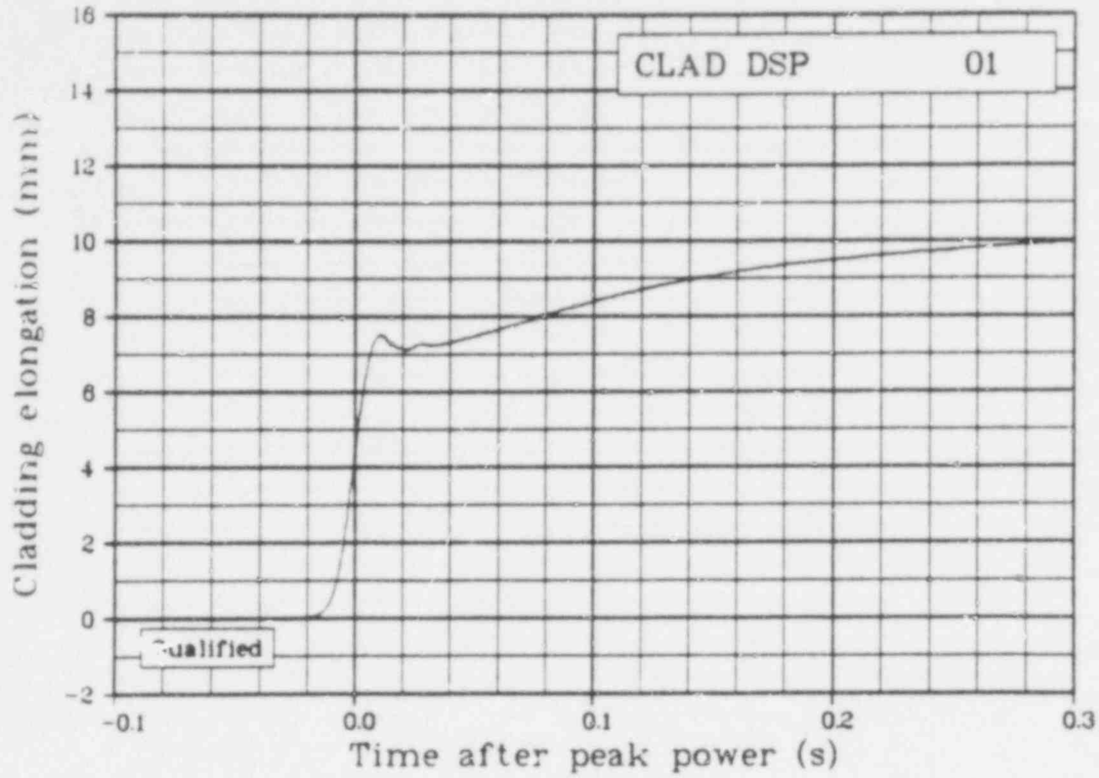

Fig. 48 Cladding elongation of Rod 802-1 (CLAD DSP 01), -0.1 to 0.3 s, qualified.

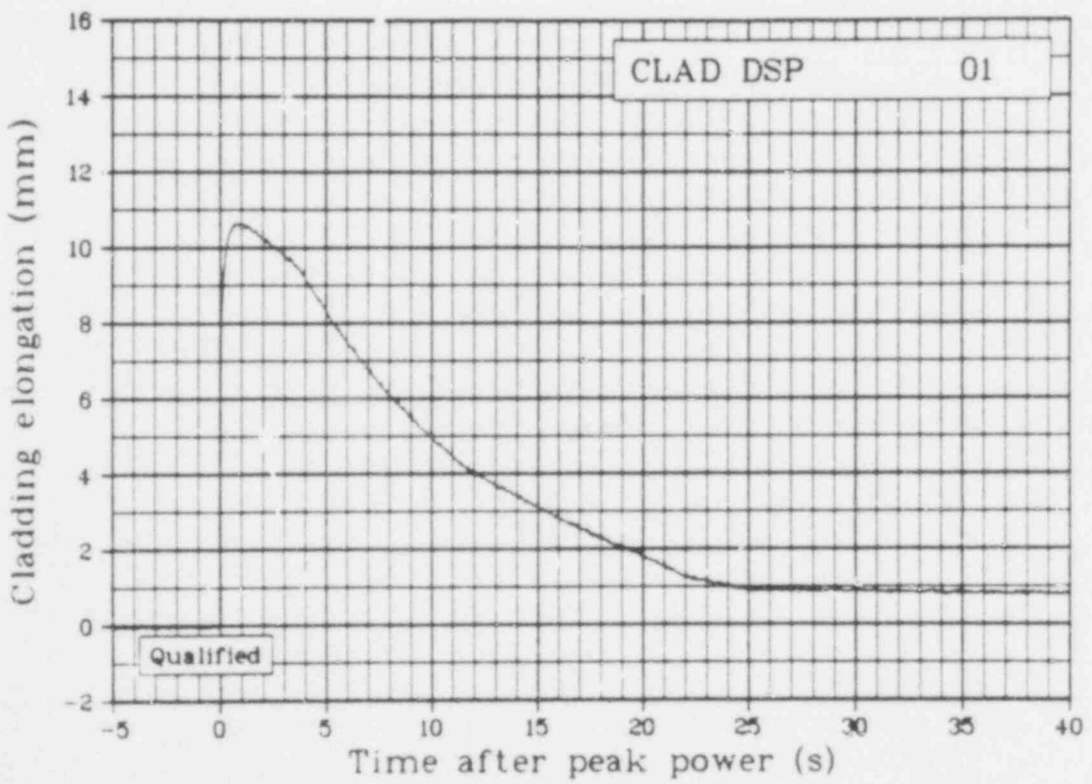

Fig. 49 Cladding elongation of Rod 802-1 (CLAD DSP 01), -5 to 40 s, qualified.

631 111

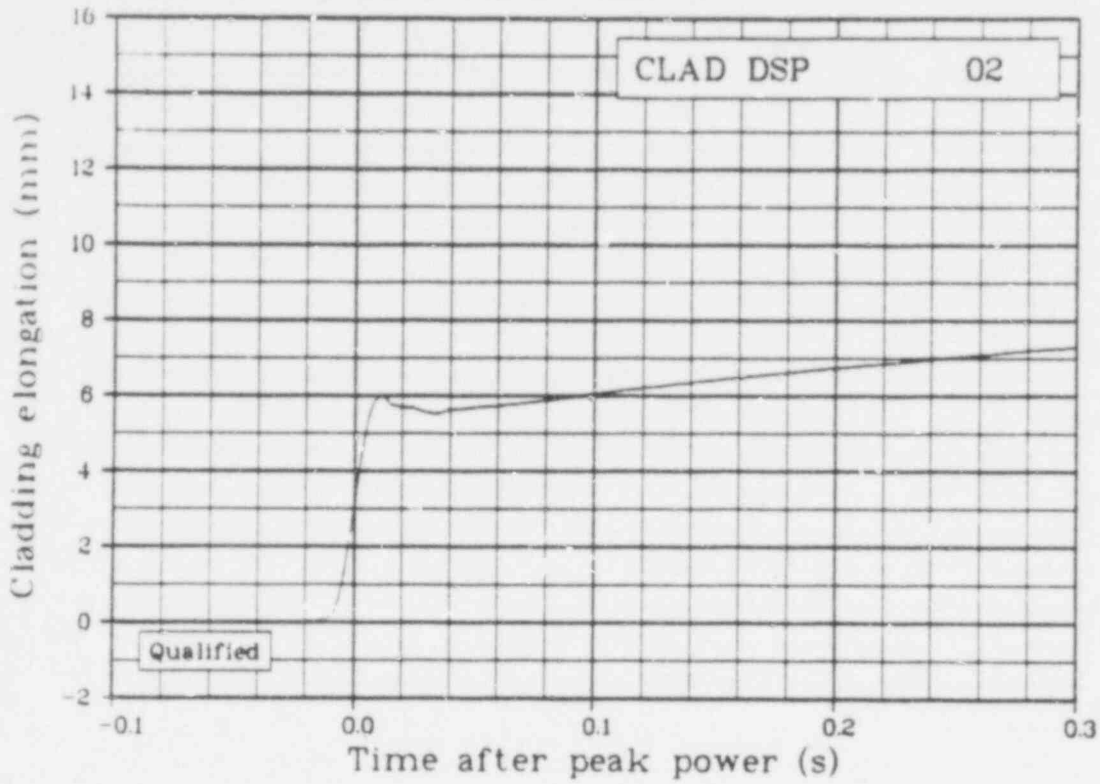

Fig. 50 C'adding elongation of Rod 802-2 (CLAD DSP 02), -0.1 to 0.3 s, qualified.

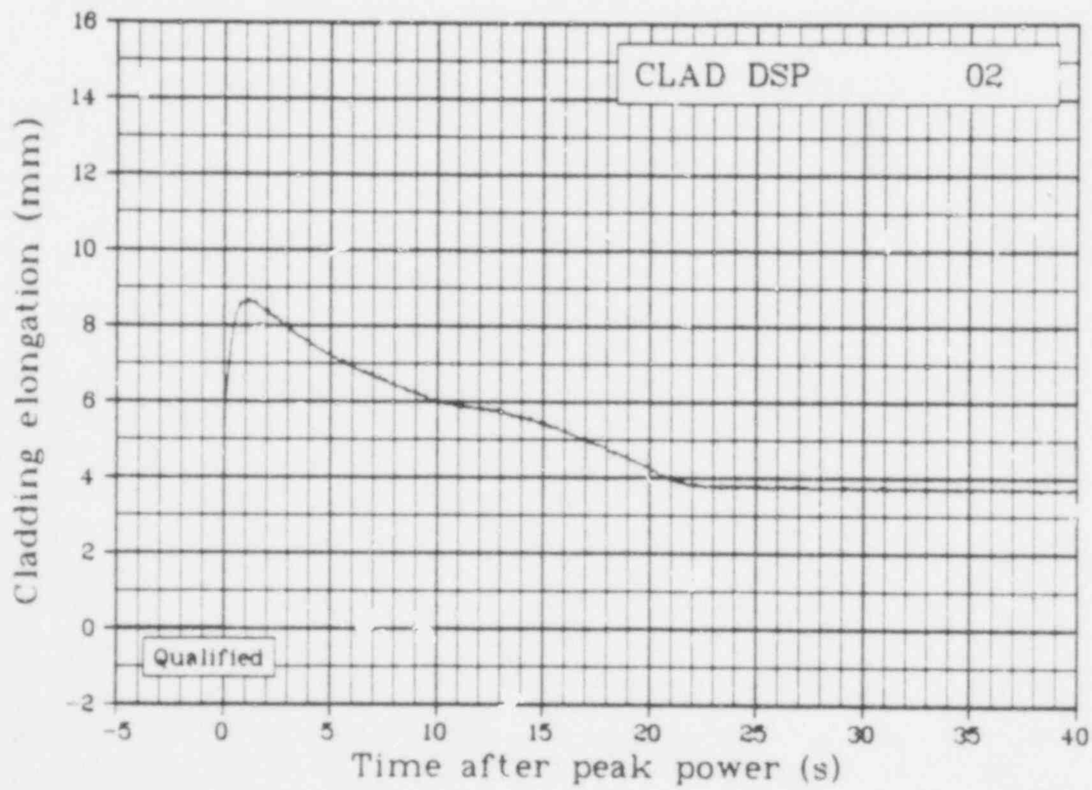

Fig. 51 Cladding elongation of Rod 802-2 (CLAD DSP 02), -5 to 40 s, qualified.

631 112

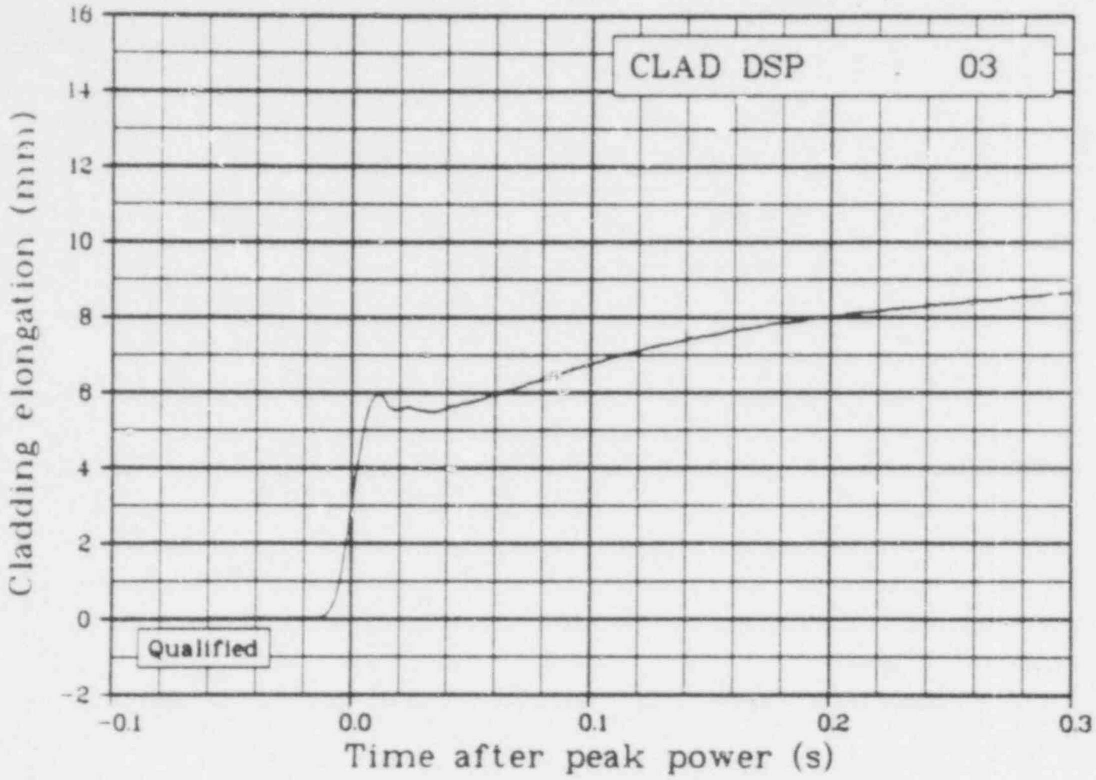

Fig. 52 Cladding elongation of Rod 802-3 (CLAD DSP 03), -0.1 to 0.3 s, qualified.

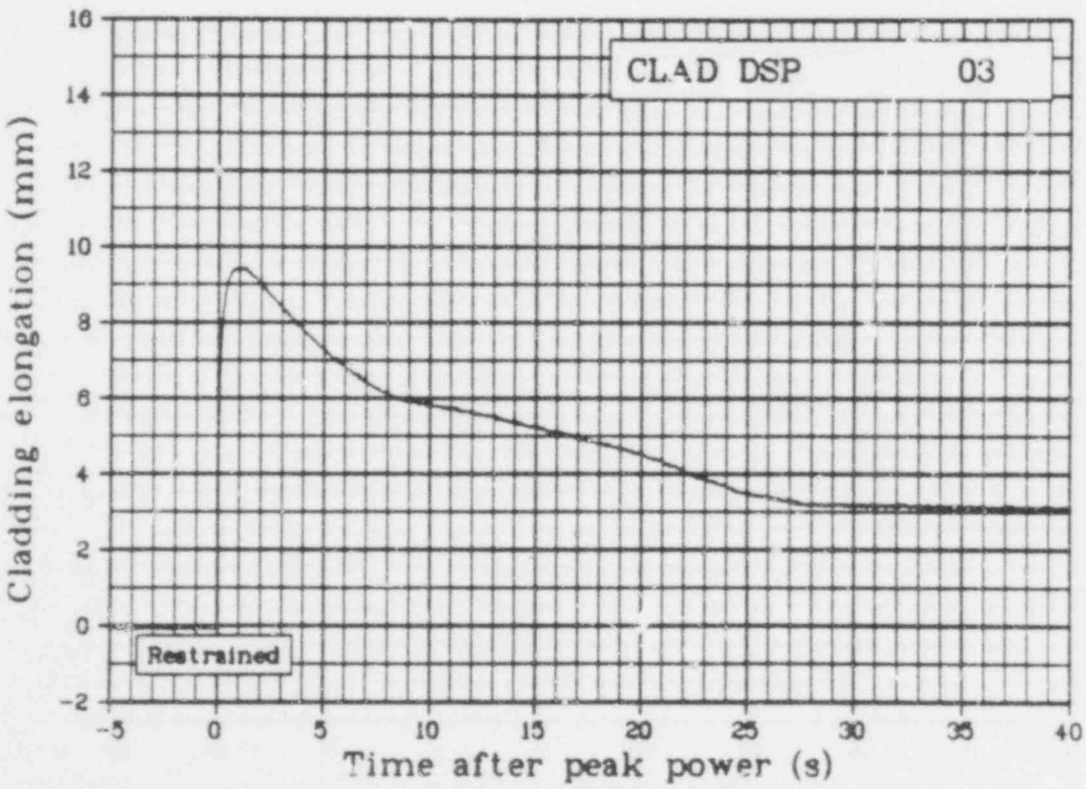

Fig. 53 Cladding elongation of Rod 802-3 (CLAD DSP 03), -5 to 40 s, restrained.

631 113

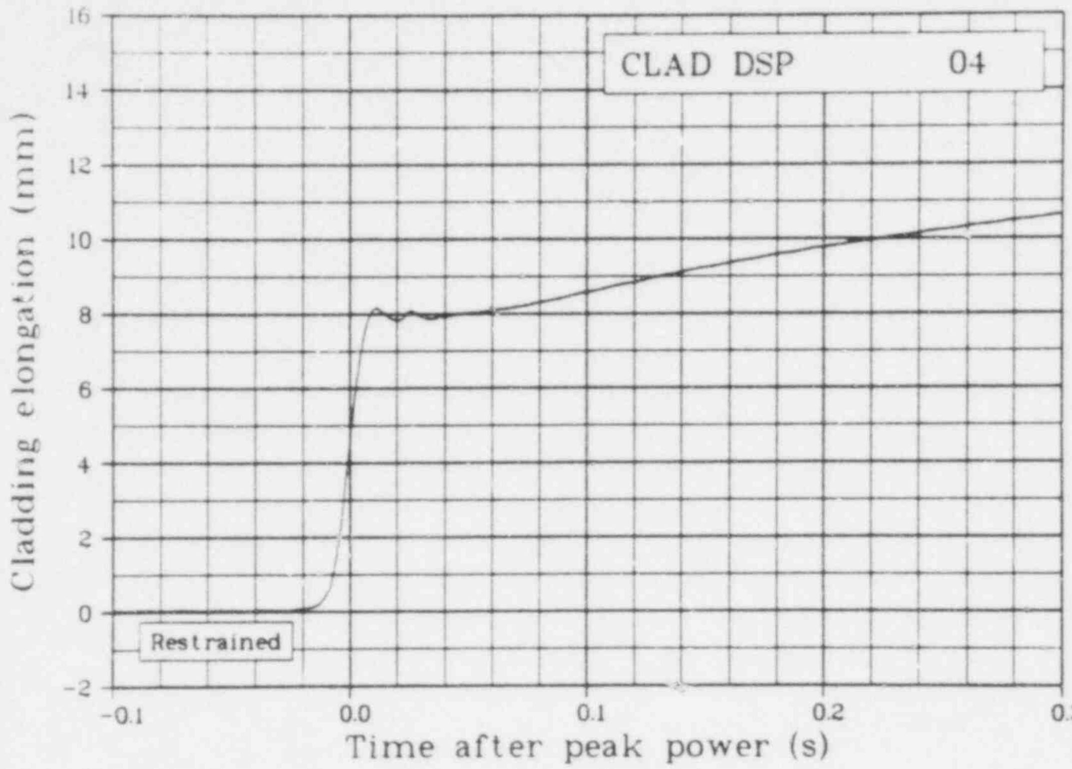

Fig. 54 Cladding elongation of Rod 802-4 (CLAD DSP 04), -0.1 to 0.3 s, restrained.

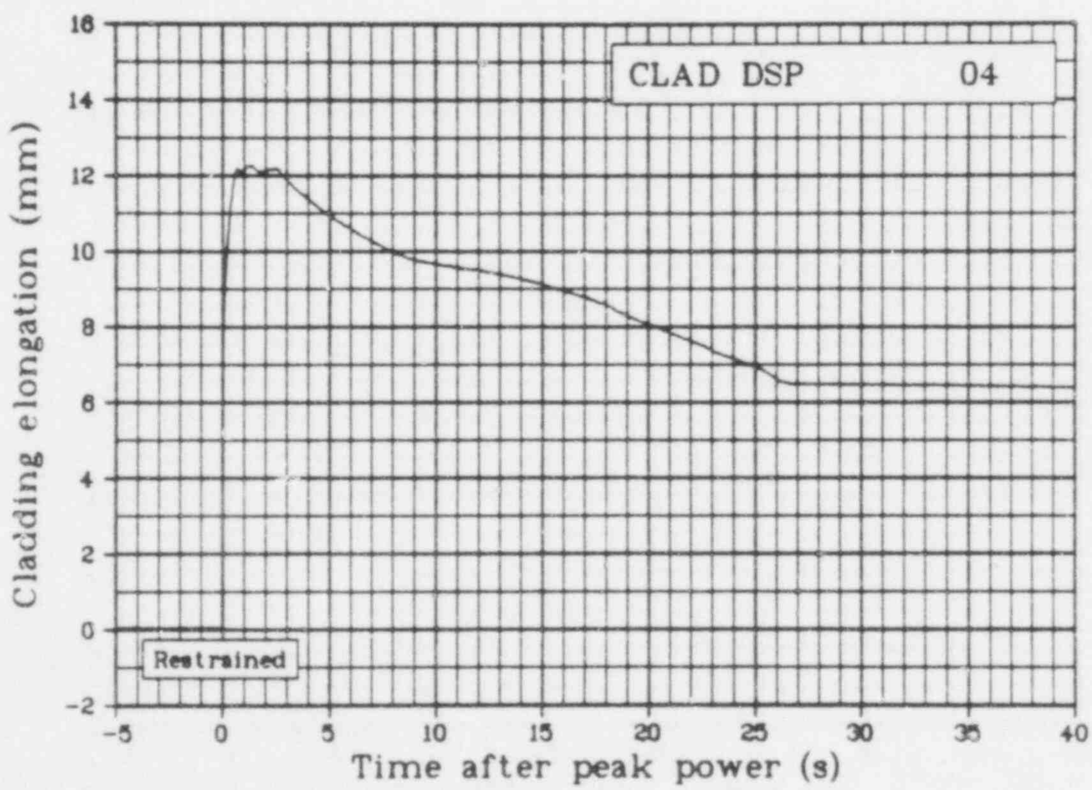

Fig. 55 Cladding elongation of Rod 802-4 (CLAD DSP 04), -5 to 40 s, restrained.

631 114

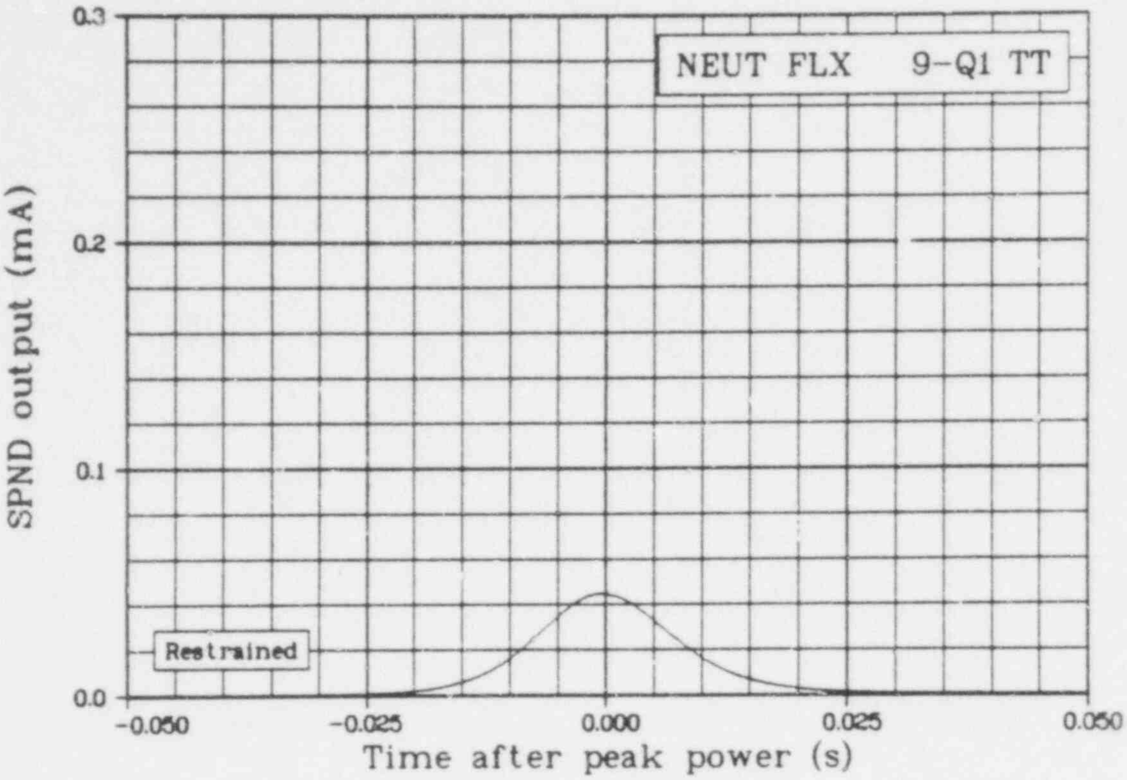

Fig. 56 Neutron flux in Quadrant 1 at an elevation of 0.09 m above fuel stack bottom (NEUT FLX 9-Q1 TT), restrained.

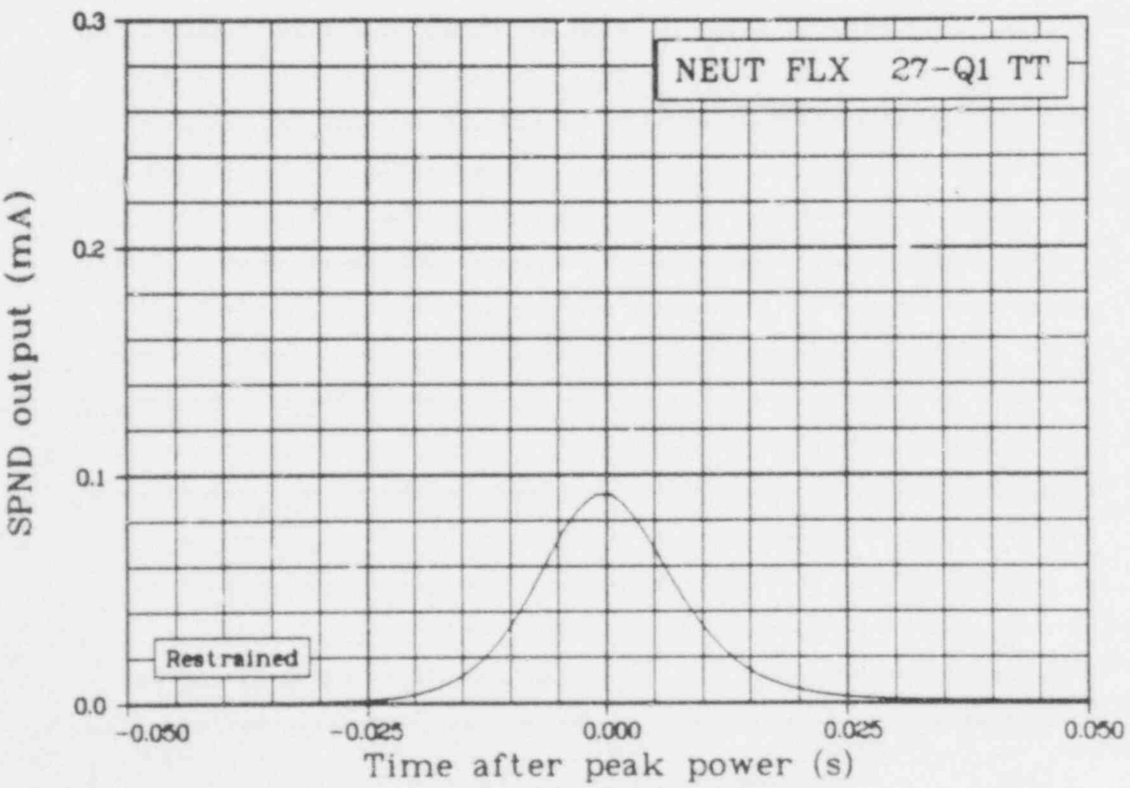

Fig. 57 Neutron flux in Quadrant 1 at an elevation of 0.27 m above fuel stack bottom (NEUT FLX 27-Q1 TT), restrained.

631 115

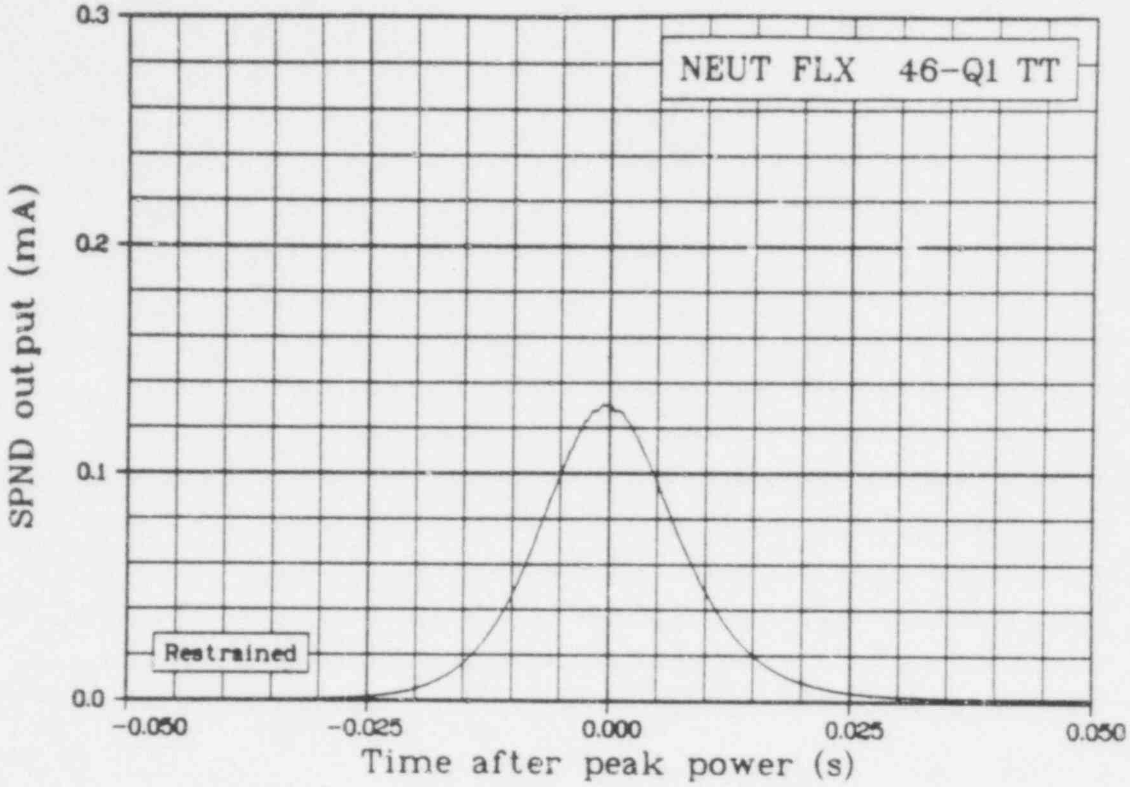

Fig. 58 Neutron flux in Quadrant 1 at an elevation of 0.46 m above fuel stack bottom (NEUT FLX 46-Q1 TT), restrained.

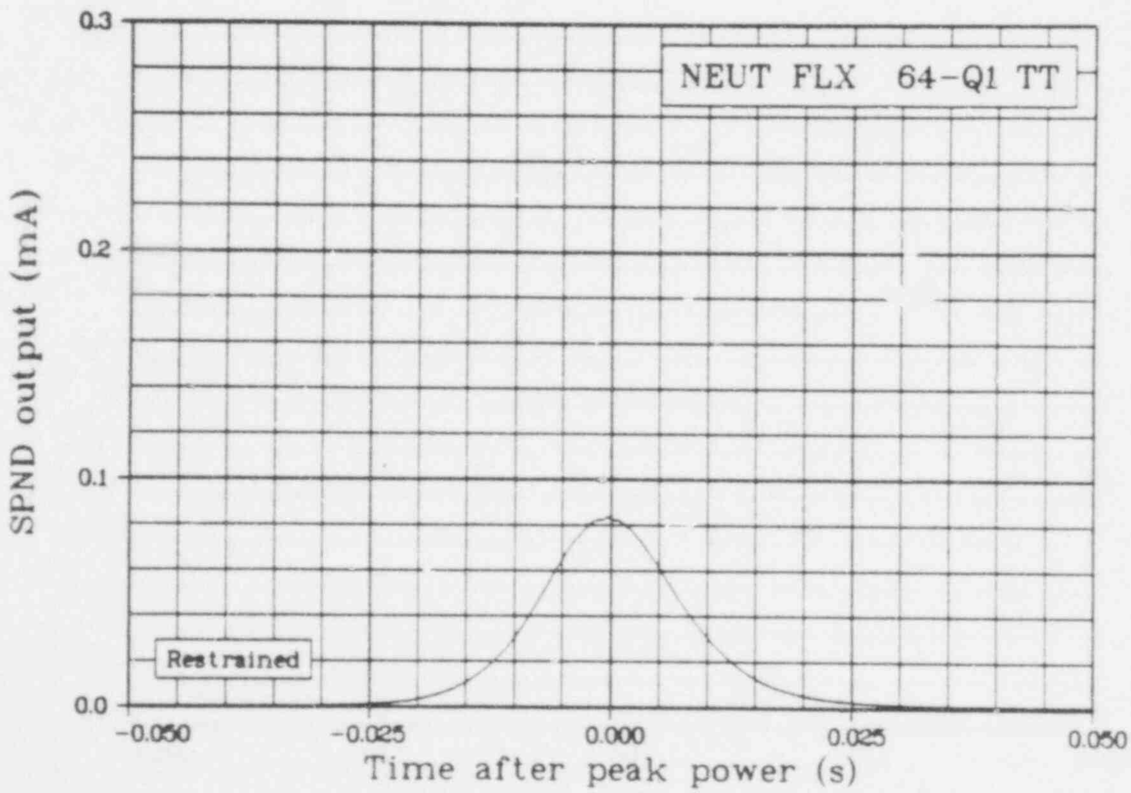

Fig. 59 Neutron flux in Quadrant 1 at an elevation of 0.64 m above fuel stack bottom (NEUT FLX 64-Q1 TT), restrained.

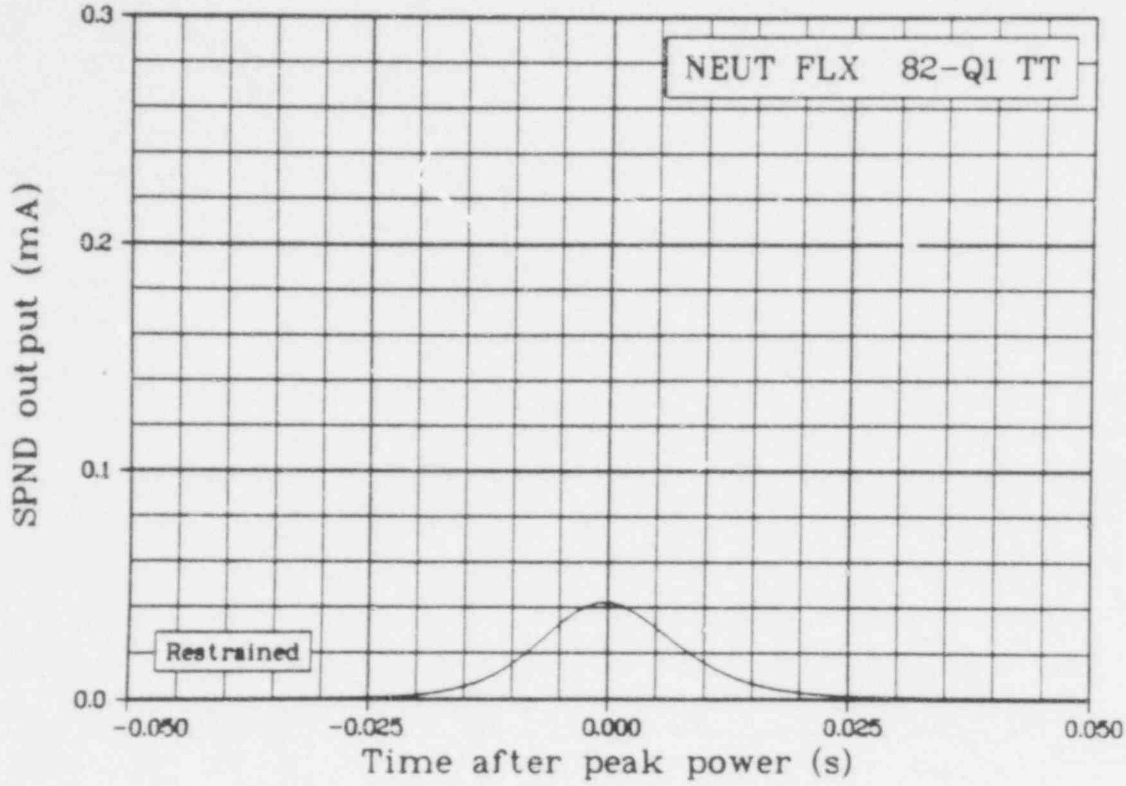

Fig. 60 Neutron flux in Quadrant 1 at an elevation of 0.82 m above fuel stack bottom (NEUT FLX 82-Q1 TT), restrained.

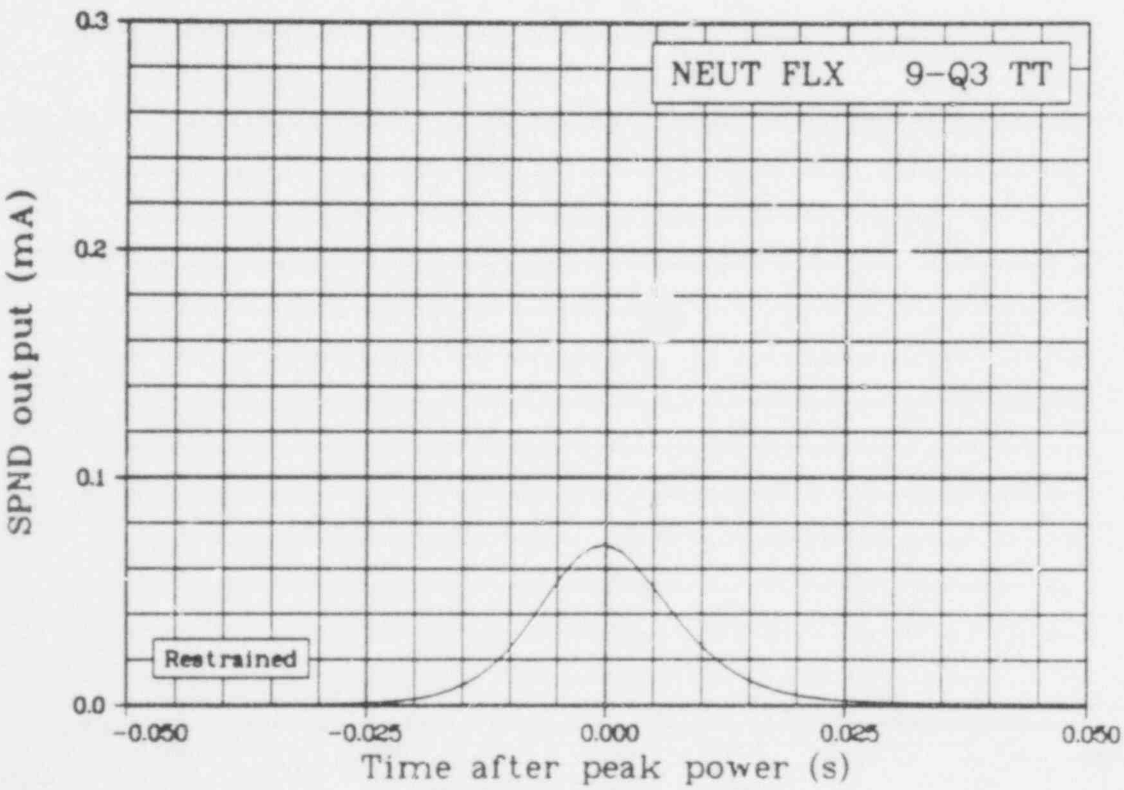

Fig. 61 Neutron flux in Quadrant 3 at an elevation of 0.09 m above fuel stack bottom (NEUT FLX 9-Q3 TT), restrained from -0.03 to 0.03 s, trend during other time segments.

631 117

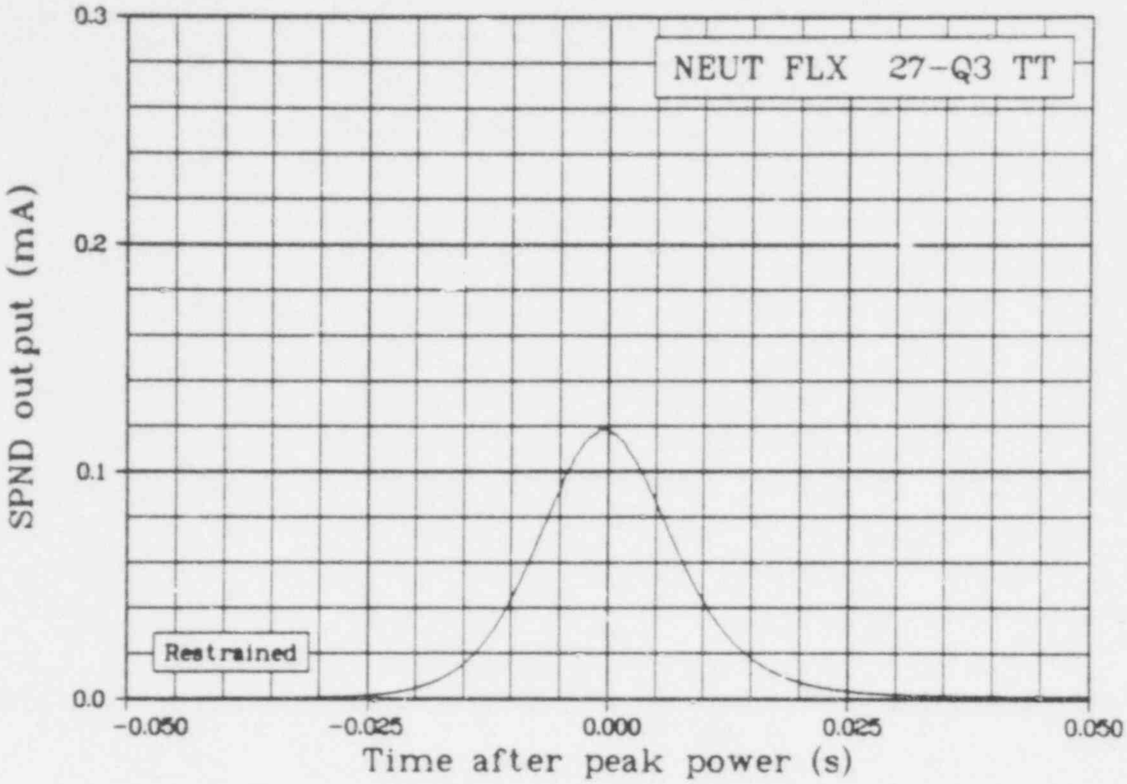

Fig. 62 Neutron flux in Quadrant 3 at an elevation of 0.27 m above fuel stack bottom (NEUT FLX 27-Q3 TT), restrained.

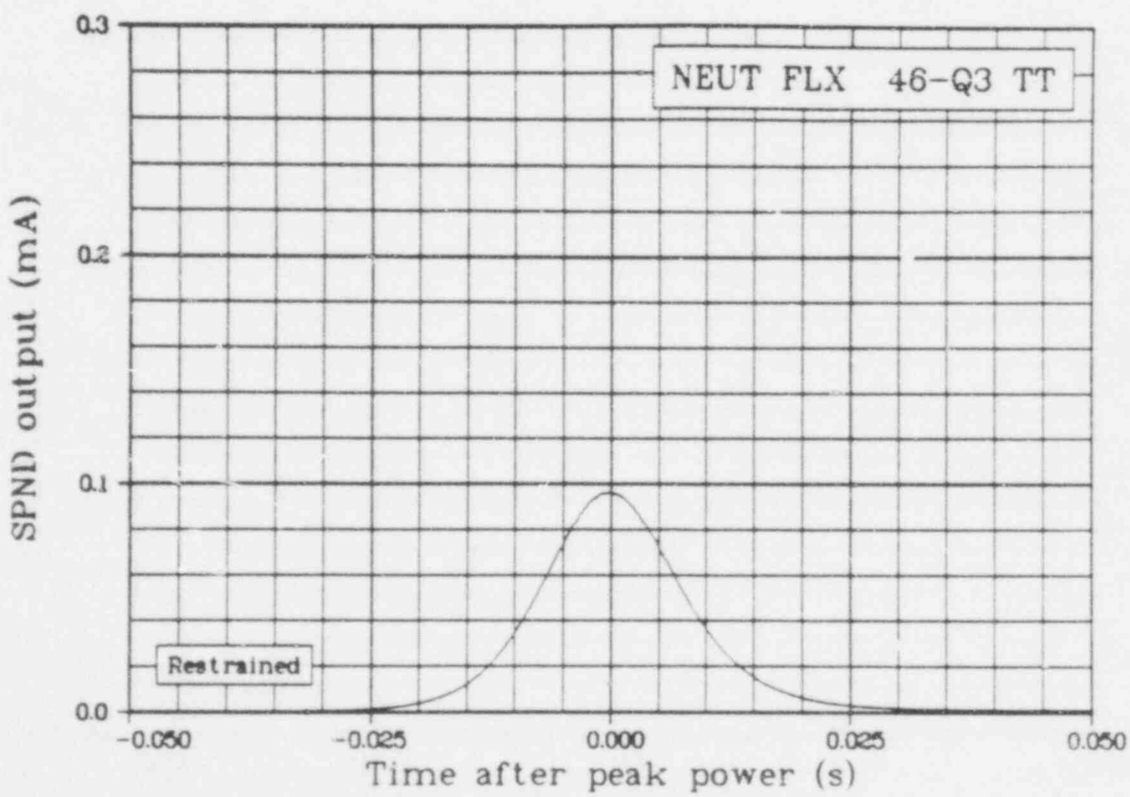

Fig. 63 Neutron flux in Quadrant 3 at an elevation of 0.46 m above fuel stack bottom (NEUT FLX 46-Q3 TT), restrained.

631 118

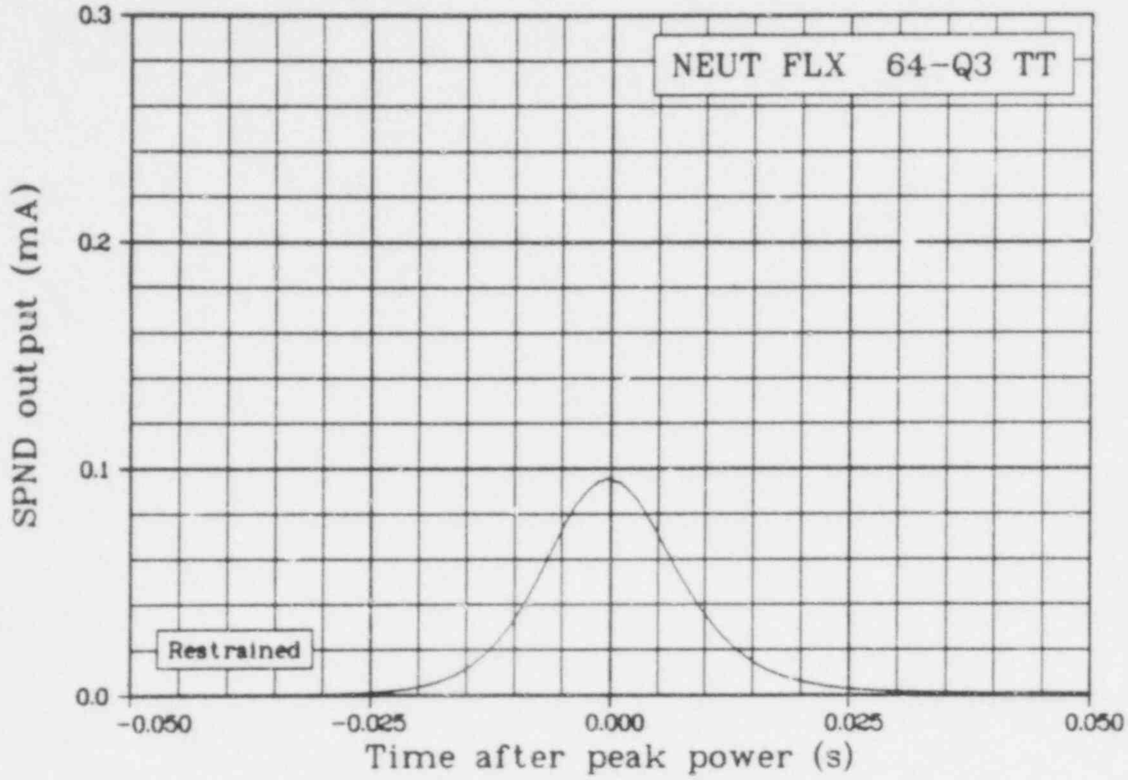

Fig. 64 Neutron flux in Quadrant 3 at an elevation of 0.64 m above fuel stack bottom (NEUT FLX 64-Q3 TT), restrained.

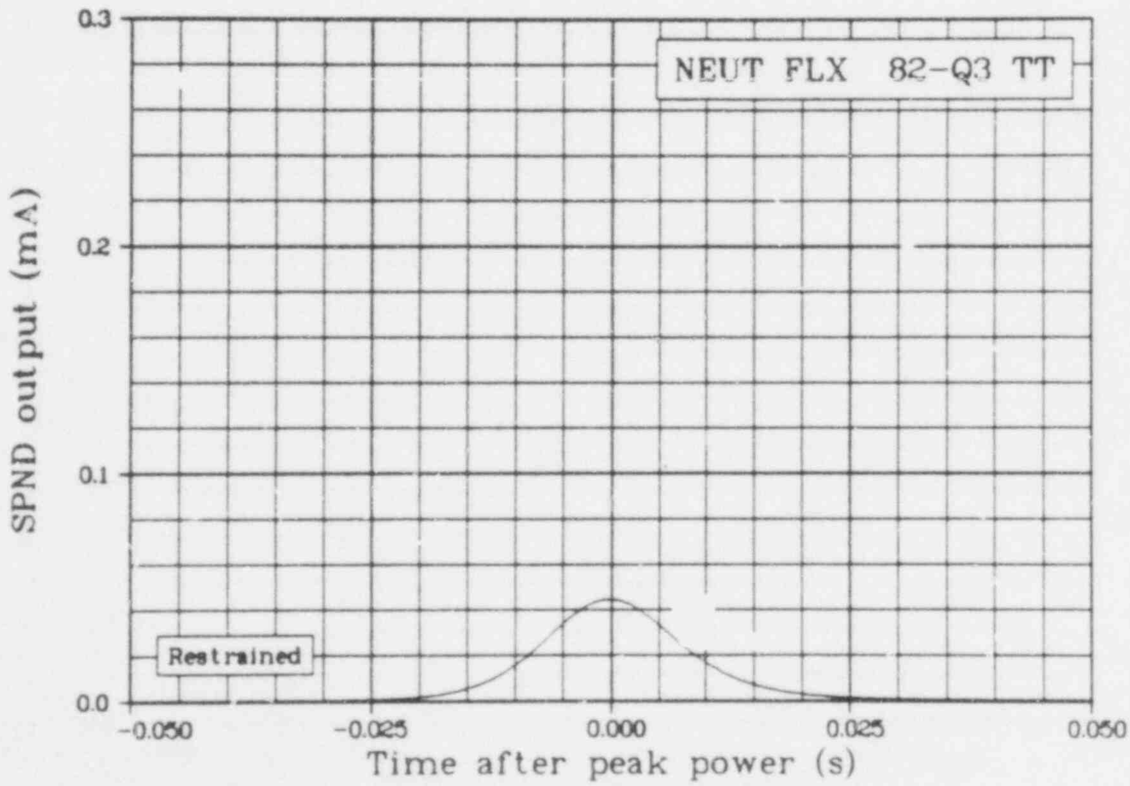

Fig. 65 Neutron flux in Quadrant 3 at an elevation of 0.82 m above fuel stack bottom (NEUT FLX 82-Q3 TT), restrained.

631 119

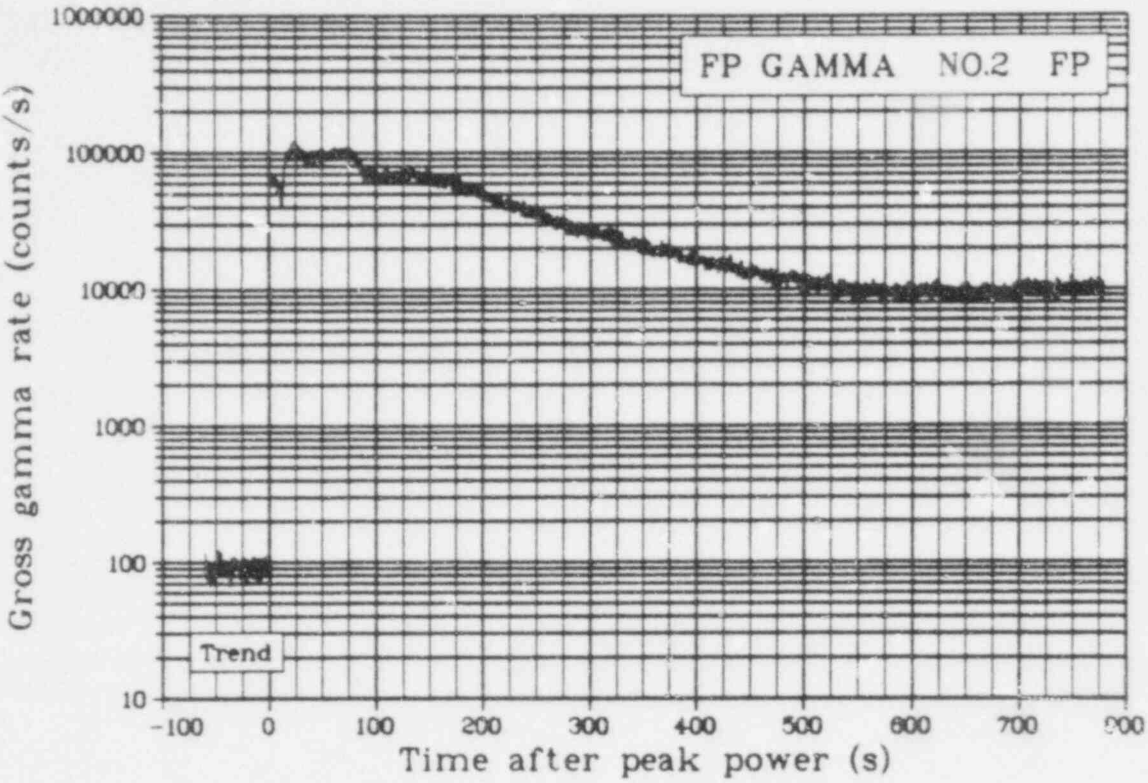

Fig. 66 Gross gamma count rate - 150 to 6300 keV range (FP GAMMA NO.2 FP), trend.

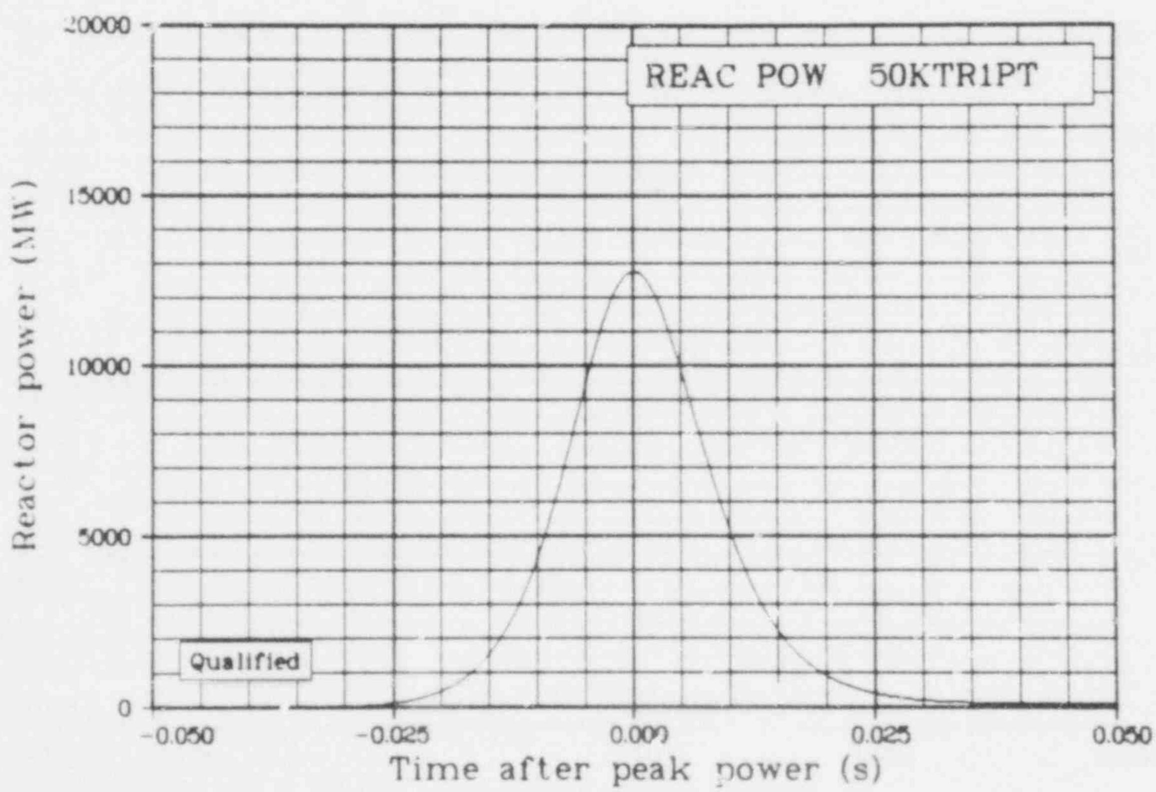

Fig. 67 Reactor power from Transient Ionization Chamber 1 (REAC POW 50KTR1PT), qualified.

631 120

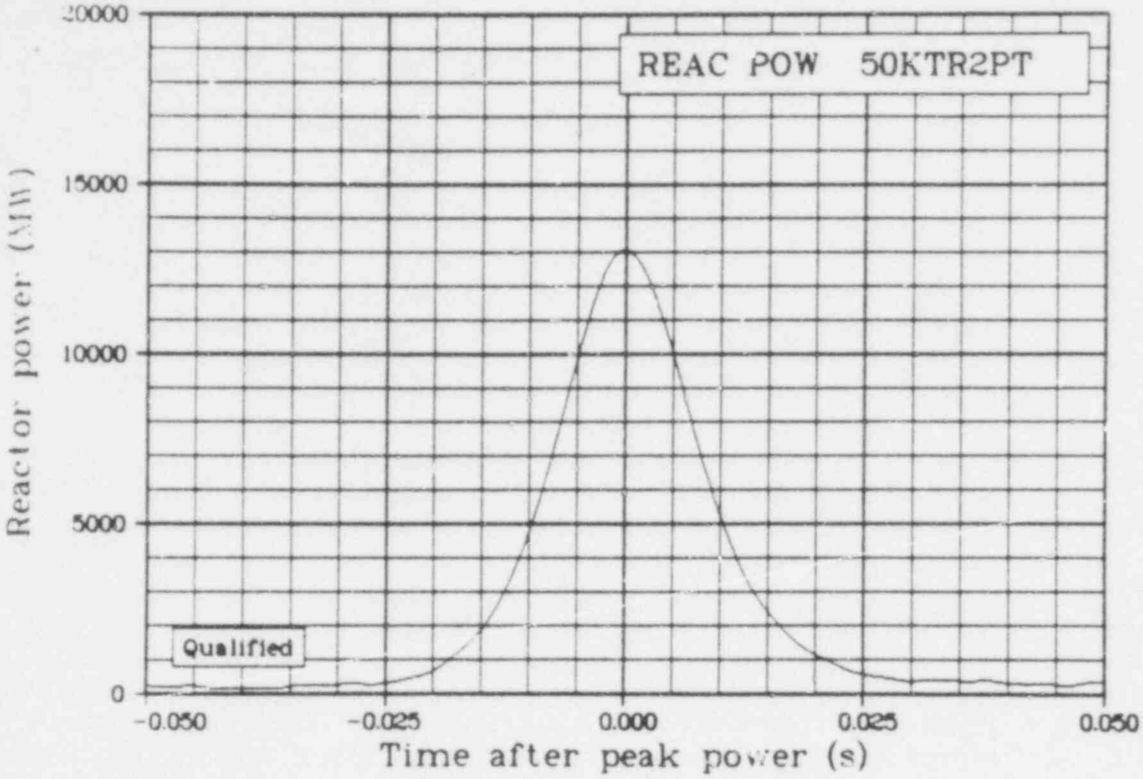

Fig. 68 Reactor power from Transient Ionization Chamber 2 (REAC POW 50KTR2PT), qualified.

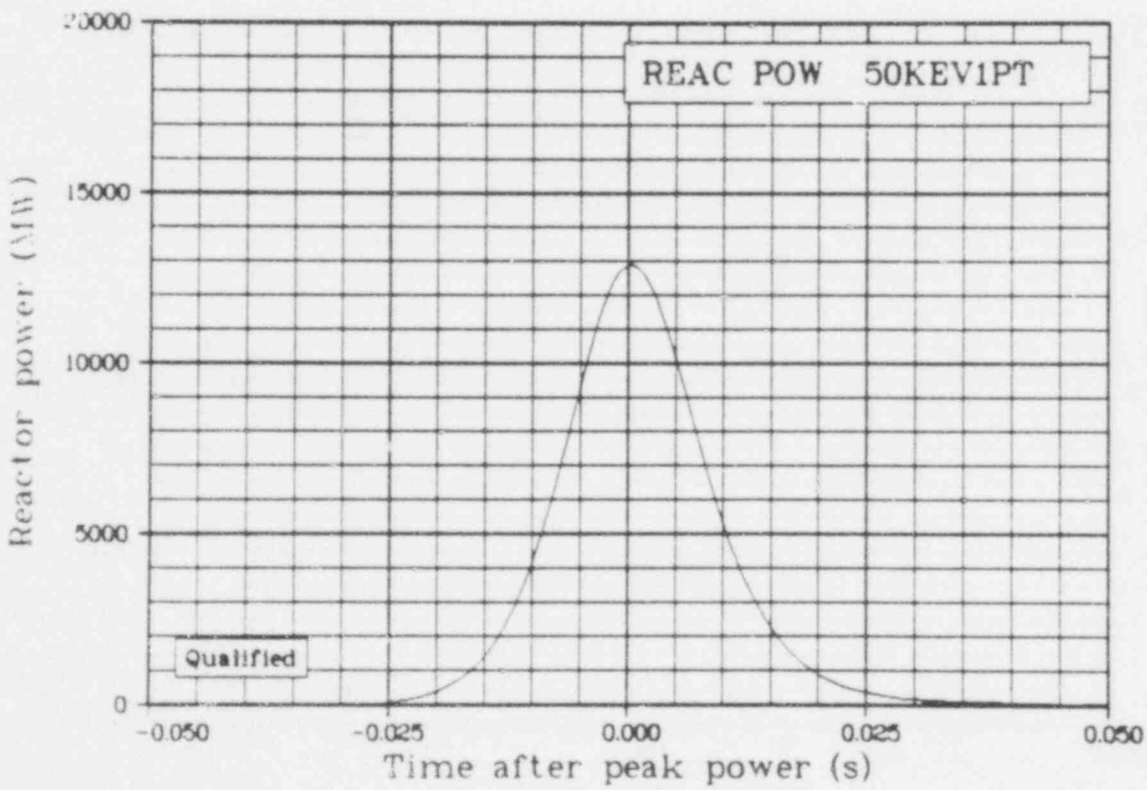

Fig. 69 Reactor power from Evacuated Ionization Chamber 1 (REAC POW 50KEV1PT), qualified.

631 121

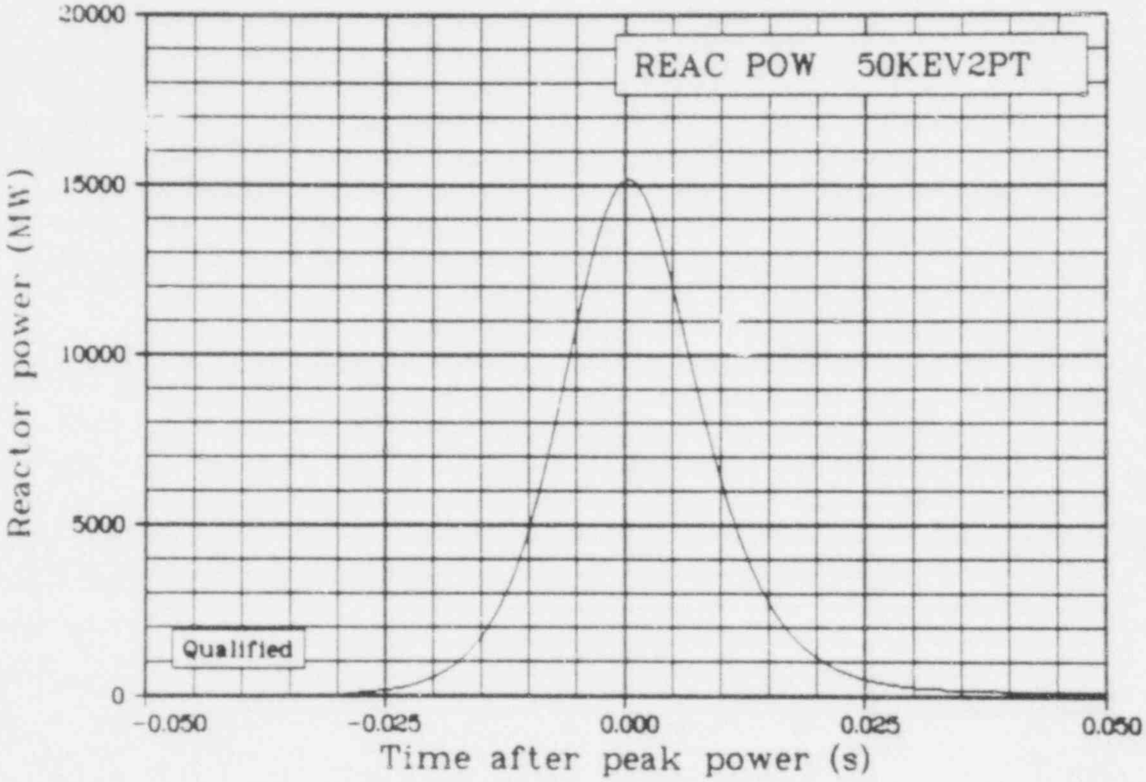

Fig. 70 Reactor power from Evacuated Ionization Chamber 2 (REAC POW 50KEV2PT), qualified.

VI. REFERENCE

1. *Characteristics of UO_2 - Zircaloy Fuel Rod Materials from Saxton Reactor for Use in Power Burst Facility*, ANCR-NUREG-1321 (September 1976).

631 123

APPENDIX A

POSTTEST DATA ADJUSTMENTS AND QUALIFICATION

631 124

APPENDIX A

POSTTEST DATA ADJUSTMENTS AND QUALIFICATION

Many of the instrumentation transducers used during the conduct of an experiment at the Power Burst Facility (PBF) are recognized to have responded erroneously, in varying degrees, to extraneous environmental stimuli such as pressure, temperature, neutron flux, gamma radiation, vibration, and mechanical strain. In addition, the data acquisition and recording system (DARS) and the signal conditioning equipment may also have contributed unwanted or distorted signals to the measurement channel while the transducer output was being processed and recorded.

Although the errors introduced into the data by these spurious secondary inputs generally do not exceed the specified error ranges of the transducers, significant improvement in measurement accuracy can be achieved if the secondary sensitivity can be identified and removed. Since the exact values of the spurious inputs to which different transducers might be sensitive cannot be easily predicted and are sometimes inconvenient to measure, secondary effects have been accounted for by correcting the data after the test.

After Test RIA 1-2, an error due to the electronic drift of the DARS signal conditioning units was removed from the data by a linear correction of offset versus time as follows:

$$F^1(t) = [F(t) + A]B$$

where

$F^1(t)$	=	corrected engineering unit value at time τ
$F(t)$	=	measured engineering unit value at time τ
A	=	total offset correction form voltage insertion calibration
B	=	electronic gain correction.

The values for A and B are given in Table A-I.

Data acquired at the PBF during the performance of the Thermal Fuels Behavior Program testing are appraised by a data integrity review committee for quality and validity. The appraisal process determines whether the measurement channel output represents the phenomenon being measured. The data review and examination process ascertains that verified calibration equations have been applied and that offsets and corrections have also been applied to remove any identifiable spurious secondary effects from the data. As a result of the review and examination by the review committee, each measurement is assigned one or more of the following classifications as a function of time.

(1) *Qualified engineering unit data (Qualified).* These data represent the phenomenon measured within the defined uncertainty limits. Data must meet the following criteria: (a) verified calibrations and all corrections have been applied, (b) independent data were used for comparison with these data and agreement was found between the data during the period of interest within specified uncertainty limits, (c) verified engineering unit conversion equations have been applied, and (d) uncertainty limits have been established and can be verified.

(2) *Restrained.* These data represent the phenomenon measured with one or more of the following constraints: (a) verified calibrations have been applied but not all corrections have been made, (b) offsets and corrections cannot be adequately determined, and (c) uncertainty limits have been established but cannot be adequately verified.

631 125

TABLE A-I

LINEAR OFFSET CORRECTION EQUATION CONSTANTS

	Power Calibration and Preconditioning		Power Burst	
Measurement	A	B	A	B
FUEL ROD				
CLAD TMP 46-18001	-9 K	1.0032	6 K	1.0008
CLAD TMP 79-0 01	-3 K	0.9941	3 K	0.9941
CLAD TMP 46-18002	-3 K	0.9995	15 K	0.9967
CLAD TMP 79-0 02	-13 K	0.9985	-13 K	1.0040
ROD PRES 6.9KA 01	Failed		Failed	
ROD PRES 17KA 02	0.57 MPa	0.9867	0.57 MPa	0.9834
ROD PRES 17KA 04	0.316 MPa	0.[illegible]933	0.316 MPa	0.9882
PLNM TMP 02	Failed		Failed	
TEST TRAIN				
FLOWRATE INLET 01	0	0.9925	0	0
FLOWRATE INLET 02	0	1.0	0	0
FLOWRATE INLET 03	0	1.0	0	0
FLOWRATE INLET 04	0	0.9939	0	0
SYS PRES 69EG UTT	-4.2 MPa	0.9960	-1.69 MPa[a] -3.60 MPa[b]	1.0039 0.9920
SYS PRES 17KA UTT	-1.32 MPa	1.0034	-1.25 MPa[c] -1.36 MPa[b]	1.0014 0.9960
SYS PRES SCHAVUTT	1.62 MPa	1.2153	-0.07 MPa[c] 1.55 MPa[b]	1.2075 1.2189
SHRDPRES 17KA 01	-3.84 MPa	0.9916	-3.26 MPa[a] -3.21 MPa[b]	1.0092 0.9994
SHRDPRES 17KA 02	1.56 MPa	0.9442	1.63 MPa[a] 1.66 MPa[b]	0.9351 0.9273
SHRDPRES 17KA 03	5.07 MPa	0.8957	3.04 MPa[a] 3.05 MPa[b]	0.9995 0.9973
SHRDPRES 17KA 04	-3.66 MPa	0.9929	-3.56 MPa[a] -3.66 MPa[b]	1.0170 0.9929

TABLE A-I (continued)

Measurement		Power Calibration and Preconditioning A	B	Power Burst A	B
TEST TRAIN (continued)					
INLT TMP	01	-1 K	0.9953	5 K	0.9962
INLT TMP	02	9 K	0.9953	6 K	1.0000
INLT TMP	03	-1 K	1.0000	1 K	1.0047
INLT TMP	04	4 K	1.0000	4 K	0.9972
OUT TEMP	01	-1 K	1.0038	6 K	1.0038
OUT TEMP	02	4 K	1.0000	1 K	1.0000
OUT TEMP	03	-1 K	1.0009	9 K	0.9972
OUT TEMP	04	5 K	0.9991	3 K	0.9991
DEL TEMP	01	0.55 K	0.9471	6 K	0.9482
DEL TEMP	02	-1.27 K	1.0000	-0.21 K	0.9524
DEL TEMP	03	-0.28 K	0.9983	0.14 K	0.9861
DEL TEMP	04	-0.61 K	1.0049	-0.91 K	0.9969
CLAD DSP	01	-5.75 mm	0.9911	-5.53 mm[c] -5.75 mm[d]	0.9947 0.9947
CLAD DSP	02	-5.90 mm	0.9960	-5.75 mm[c] -5.95 mm[d]	0.9938 1.0004
CLAD DSP	03	-5.87 mm	1.0076	-5.57 mm[c] -5.77 mm[d]	0.9934 1.0022
CLAD DSP	04	-3.18 mm		5.57 mm[c] 5.57 mm[d]	
NEUT FLX 9-Q1	TT	0	1	0.1 Log A	1
NEUT FLX 27-Q1	TT	-0.1 Log A	1	0	1
NEUT FLX 46-Q1	TT	0	1	0	0.9877
NEUT FLX 64-Q1	TT	0	0.9938	0.1 Log A	1.0127
NEUT FLX 82-Q1	TT	0	1	0	1

631 127

TABLE A-I (continued)

Measurement	Power Calibration and Preconditioning		Power Burst	
	A	B	A	B
TEST TRAIN (continued)				
NEUT FLX 9-Q3 TT	0	1	0	0.9877
NEUT FLX 27-Q3 TT	0	1	0.1 Log A	0.9756
NEUT FLX 46-Q3 TT	0	1	0	1
NEUT FLX 64-Q3 TT	0	1	0.1 Log A	0.9756
NEUT FLX 82-Q3 TT	0	1	0	1
PLANT				
REAC POW 50TR1PT	-0.24 MW	1.000		
REAC POW 50KTR1PT			0	1.0048
REAC POW 50TR2PT	-0.30 MW	1.0077		
REAC POW 50KTR2PT			-0.22 GW	1.0022
REAC POW 50EV1PT	-0.09 MW	-0.9991		
REAC POW 50KEV1PT			0	1.0002
REAC POW 50EV2PT	0	1.0017		
REAC POW 50KEV2PT			-0.24 GW	1.0059

a. The data were recorded at two different bandwidths. The specified constants were used to correct data recorded at a bandwidth of 20 kHz and presented in a -0.1 to 0.3 s plot.

b. The data were recorded at two different bandwidths. The specified constants were used to correct data recorded at a bandwidth of 10 Hz and presented in a -1 to 5 s plot.

c. The data were recorded at two different bandwidths. The specified constants were used to correct data recorded at a bandwidth of 5 kHz and presented in a -0.1 to 0.3 s plot.

d. The data were recorded at two different bandwidths. The specified constants were used to correct data recorded at a bandwidth of 10 Hz and presented in a -5 to 40 s plot.

(3) *Trend.* These data have been verified to represent the relative changes in the phenomenon but do not necessarily represent the absolute level in the measured phenomenon due to: (a) instrument calibrations do not adequately represent the environment measured by the transducer, (b) the calibration and performance of the DARS are questionable but known errors have been eliminated, (c) uncertainty limits cannot be adequately quantified, (d) transducer performance is questionable but relatively correct, or (e) no corrections can be made to adequately compensate for environmental effects. The data have met the following criteria: (a) instrument and DARS calibrations have been applied, (b) wild points have been removed, (c) data have been appropriately filtered, and (d) relative uncertainty limits have been defined.

(4) *Failed.* Data are irretrievable due to a transducer, signal conditioning, or data channel failure or inadequate rejection of extraneous noise, transients, or frequencies.

APPENDIX B

UNCERTAINTY ANALYSIS

APPENDIX B

UNCERTAINTY ANALYSIS

To provide a guide to the uncertainty associated with data measurements in the PBF facility, three possible sources of data measurement uncertainty were analyzed for Test RIA 1-2 data - conversion to engineering unit uncertainties, bias uncertainties for the applied offsets, and random variations in the data. These sources of uncertainty do not include all the uncertainties that may exist in most measurements and therefore they should not be considered indicative of the total uncertainty levels in the Test RIA 1-2 data. The uncertainty values ($\pm 2\sigma$) given in Table B-I are the upper and lower limits for a 95% confidence level.

(1) *Conversion to Engineering Unit Uncertainties.* During the calibration and development of engineering unit conversion polynomials for each instrument, the standard deviation (σ) for a measurement was determined. In the first column of Table B-I, an uncertainty value of $\pm 2\sigma$ is given for each measurement.

(2) *Bias Uncertainties for Applied Offsets.* All data in this report were reviewed to determine the quality and validity of the data. Each measurement was compared with initial conditions, redundant or similar measurements, and calculated values to determine the required offsets or adjustments. The bias uncertainties are the expected errors in the offsets that were applied to the data. They are given in the second column of Table B-I.

(3) *Random Variations in the Data.* The Box-Jenkins time series analysis technique for estimating process variability was used to determine random variations in selected data from Test RIA 1-2. Each selected data curve was segmented and each segment was empirically fitted with a linear difference equation to characterize the white noise input at each sampling time point. The procedures for fitting difference equations are discussed in depth in Reference B-1. The white noise input was assumed to originate from a normally distributed population and to represent the random error. The standard deviation of the white noise as derived from the fitting procedures was used as an estimate of the standard deviation for the random uncertainty. Upper and lower uncertainty bands for a 95% confidence level have been plotted and represent uncertainty values of $\pm 2\sigma$. Since the uncertainty bands were found to be small, they are presented in this appendix in Figures B-1 through B-22 without the corresponding data which fits inside the uncertainty bands. The random uncertainty obtained from the original data is not valid for any filtering process applied to the original data. The Box-Jenkins analysis method has a tendency to reflect the total noise content of the data that originated from sample repeatability, electrical noise, the measured event, and extraneous phenomenon occurring during the test. To rigorously characterize the separate random components of a measurement would be difficult, although one or more of these components could possibly be filtered from the noise which was used to determine the random uncertainty.

(4) *Excluded Uncertainties.* Other random and systematic uncertainties exist in the data but they could not be adequately analyzed for this report. These uncertainties include measurement dependent and independent uncertainties. The measurement dependent errors are the most difficult errors to analyze and will probably never be rigorously presented in an experiment data report (EDR). A detailed and comprehensive measurement independent uncertainty analysis of the PBF measurement systems is currently in progress. The results are expected to be invaluable for determining engineering confidence limits on future data published by the Thermal Fuels Behavior Program.

TABLE B-I

MEASUREMENT UNCERTAINTIES FOR TEST RIA 1-2

Measurement	Engineering Unit Conversion Uncertainties	Bias for Applied Offsets	Figure Showing Random Uncertainty for Selected Data
FUEL ROD			
CLAD TMP 46-18001	± 1.06 K	± 2 K	B-1, B-2
CLAD TMP 79-0 01	± 1.06 K	± 2 K	B-3, B-4
CLAD TMP 46-18002	± 1.06 K	± 2 K	B-5, B-6
CLAD TMP 79-0 02	± 1.06 K	± 2 K	B-7, B-8
ROD PRES 6.9KA 01	± 0.15 MPa	± 0.05 MPa	
ROD PRES 17KA 02	± 0.10 MPa	± 0.05 MPa	
ROD PRES 17KA 04	± 0.13 MPa	± 0.05 MPa	
PLNM TMP 02	Failed	Failed	
TEST TRAIN			
FLOWRATE INLET 01	± 0.00124 l/s	± 0.002 l/s	B-9
FLOWRATE INLET 02	± 0.00105 l/s	± 0.002 l/s	B-10
FLOWRATE INLET 03	± 0.00204 l/s	± 0.002 l/s	
FLOWRATE INLET 04	± 0.00179 l/s	± 0.002 l/s	
SYS PRES 69EG UTT	NA	± 0.01 MPa	
SYS PRES 17KA UTT	NA	± 0.05 MPa	B-11, B-12
SYS PRES SCHAVUTT	NA	± 0.05 MPa	
SHRDPRES 17KA 01	± 0.149 MPa	± 0.05 MPa	B-13, B-14
SHRDPRES 17KA 02	± 0.145 MPa	± 0.05 MPa	B-15, B-16
SHRDPRES 17KA 03	± 0.176 MPa	± 0.05 MPa	
SHRDPRES 17KA 04	± 0.094 MPa	± 0.05 MPa	
INLT TMP 01	± 1.47 K	± 2 K	B-17
INLT TMP 02	± 1.47 K	± 2 K	B-18
INLT TMP 03	± 1.47 K	± 2 K	
INLT TMP 04	± 1.47 K	± 2 K	
OUT TEMP 01	± 1.47 K	± 2 K	B-19
OUT TEMP 02	± 1.47 K	± 2 K	B-20
OUT TEMP 03	± 1.47 K	± 2 K	
OUT TEMP 04	± 1.47 K	± 2 K	

TABLE B-I (continued)

Measurement	Engineering Unit Conversion Uncertainties	Bias for Applied Offsets	Figure Showing Random Uncertainty for Selected Data
TEST TRAIN (continued)			
DEL TEMP 01	± 0.92 K	± 0.1 K	B-21
DEL TEMP 02	± 0.0578 K	± 0.1 K	B-22
DEL TEMP 03	± 0.174 K	± 0.1 K	
DEL TEMP 04	± 0.527 K	± 0.1 K	
CLAD DSP 01	± 0.18 mm	± 0.1 mm	
CLAD DSP 02	± 0.18 mm	± 0.1 mm	
CLAD DSP 03	± 0.18 mm	± 0.1 mm	
CLAD DSP 04	± 0.18 mm	± 0.1 mm	
NEUT FLX 9-Q1 TT	--	± 0.02 ma	
NEUT FLX 27-Q1 TT	--	± 0.02 ma	
NEUT FLX 46-Q1 TT	--	± 0.02 ma	
NEUT FLX 64-Q1 TT	--	± 0.02 ma	
NEUT FLX 82-Q1 TT	--	± 0.02 ma	
NEUT FLX 9-Q3 TT	--	± 0.02 ma	
NEUT FLX 27-Q3 TT	--	± 0.02 ma	
NEUT FLX 46-Q3 TT	--	± 0.02 ma	
NEUT FLX 64-Q3 TT	--	± 0.02 ma	
NEUT FLX 82-Q3 TT	--	± 0.02 ma	
PLANT			
REAC POW 50TR1PT	--	± 0.1 MW	
REAC POW 50KTR1PT	--	± 0.1 GW	
REAC POW 50TR2PT	--	± 0.1 MW	
REAC POW 50KTR2PT	--	± 0.1 GW	
REAC POW 50EV1PT	--	± 0.1 MW	
REAC POW 50KEV1PT	--	± 0.1 GW	
REAC POW 50EV2PT	--	± 0.1 MW	
REAC POW 50KEV2PT	--	± 0.1 GW	

631 133

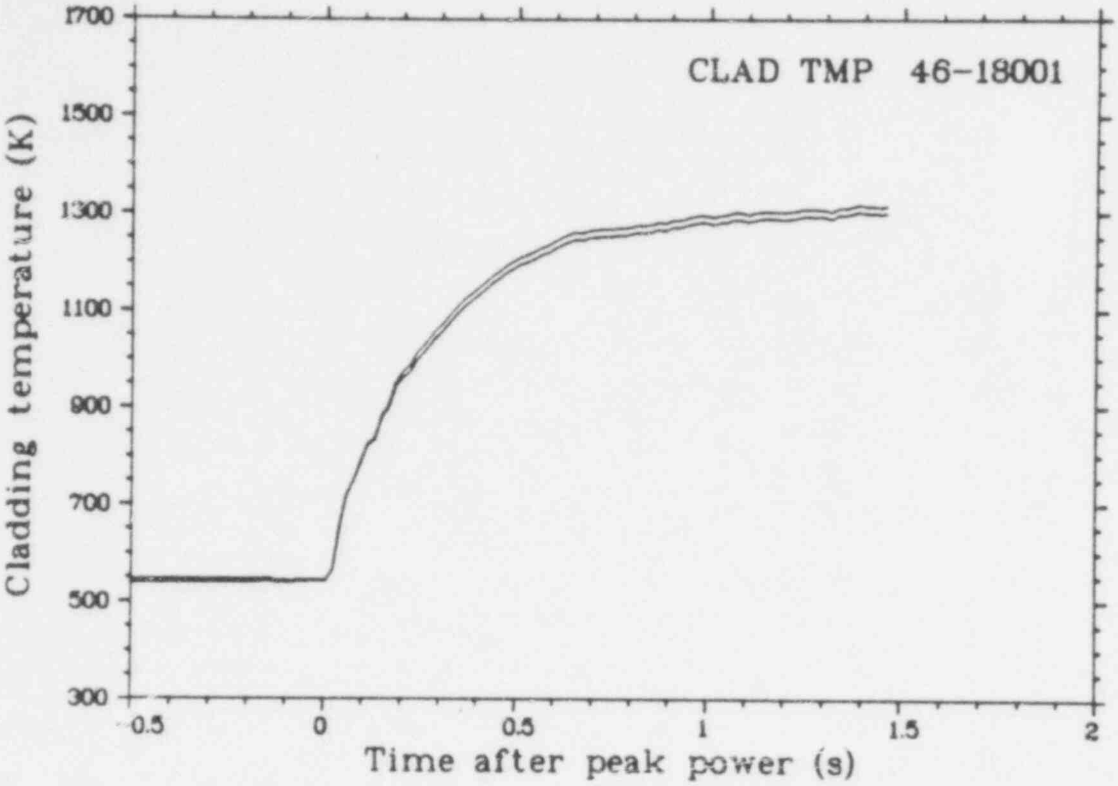

Fig. B-1 Uncertainty bands for the random variation component of the measurement uncertainty for the Rod 802-1 cladding surface temperature at an elevation of 0.46 m above fuel stack bottom (CLAD TMP 46-18001), from -0.5 to 2 s.

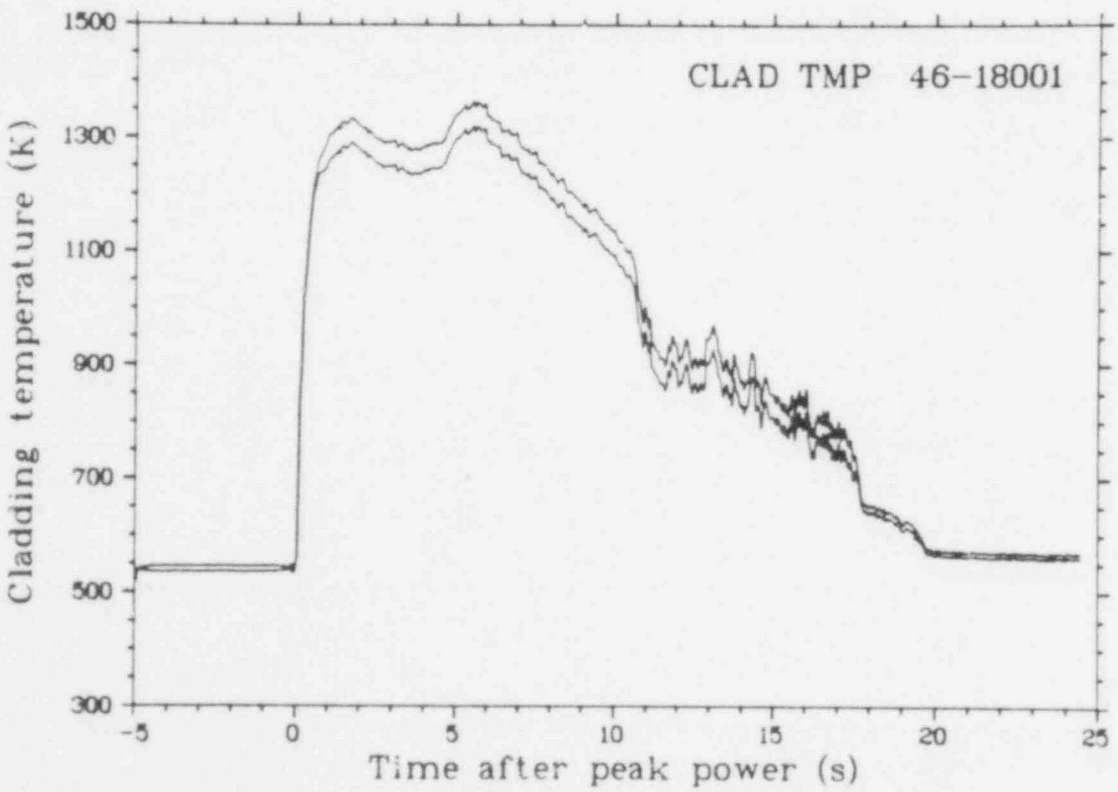

Fig. B-2 Uncertainty bands for the random variation component of the measurement uncertainty for the Rod 802-1 cladding surface temperature at an elevation of 0.46 m above fuel stack bottom (CLAD TMP 46-18001), from -5 to 25 s.

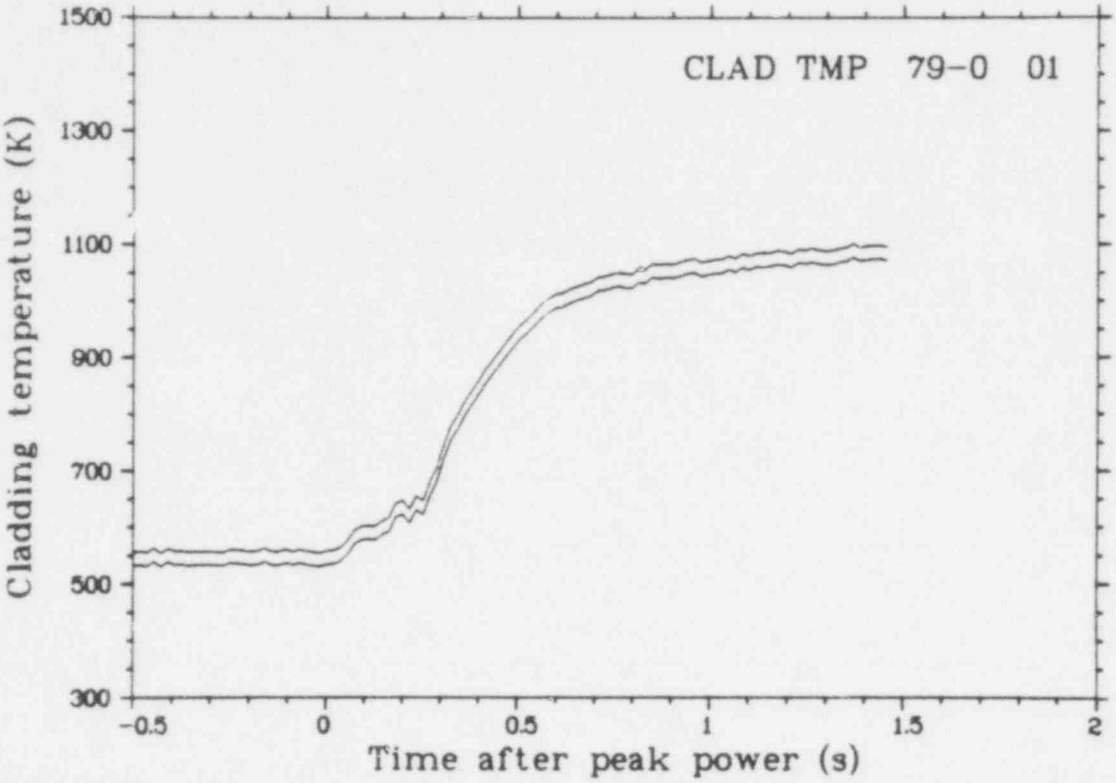

Fig. B-3 Uncertainty bands for the random variation component of the measurement uncertainty for the Rod 802-1 cladding surface temperature at an elevation of 0.79 m above fuel stack bottom (CLAD TMP 79-0 01), from -0.5 to 2 s.

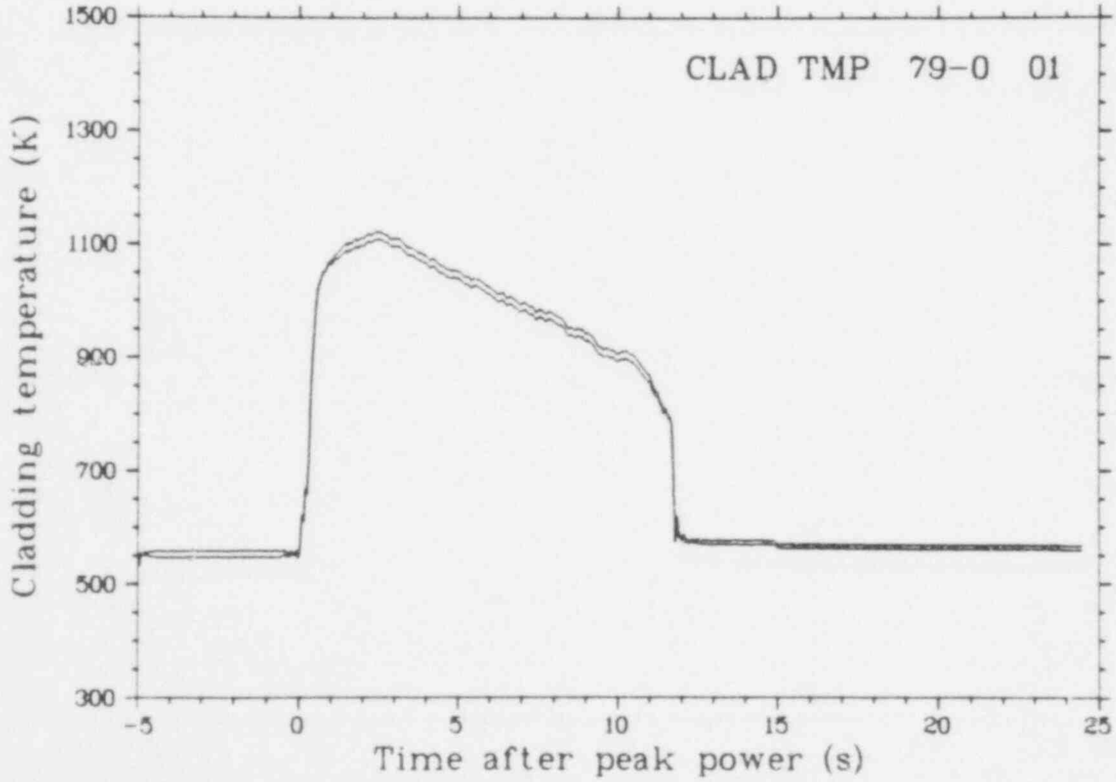

Fig. B-4 Uncertainty bands for the random variation component of the measurement uncertainty for the Rod 802-1 cladding surface temperature at an elevation of 0.79 m above fuel stack bottom (CLAD TMP 79-0 01), from -5 to 25 s.

631 135

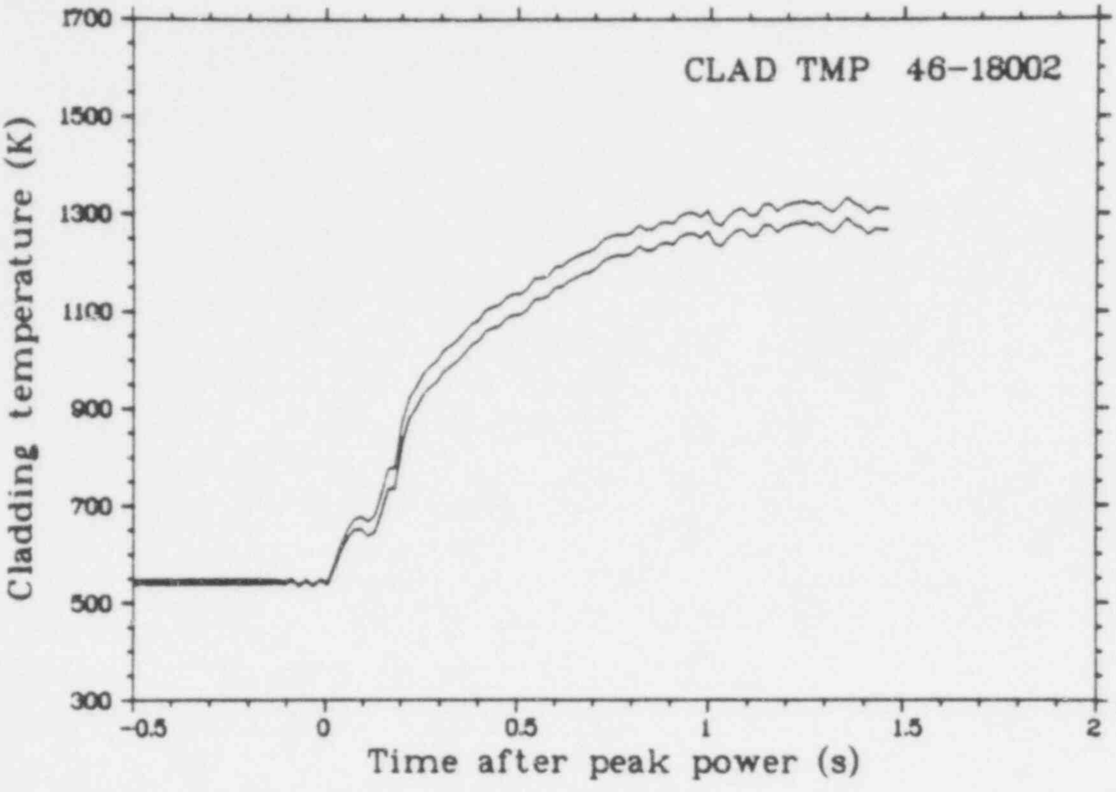

Fig. B-5 Uncertainty bands for the random variation component of the measurement uncertainty for the Rod 802-2 cladding surface temperature at an elevation of 0.46 m above fuel stack bottom (CLAD TMP 46-18002), from -0.5 to 2 s.

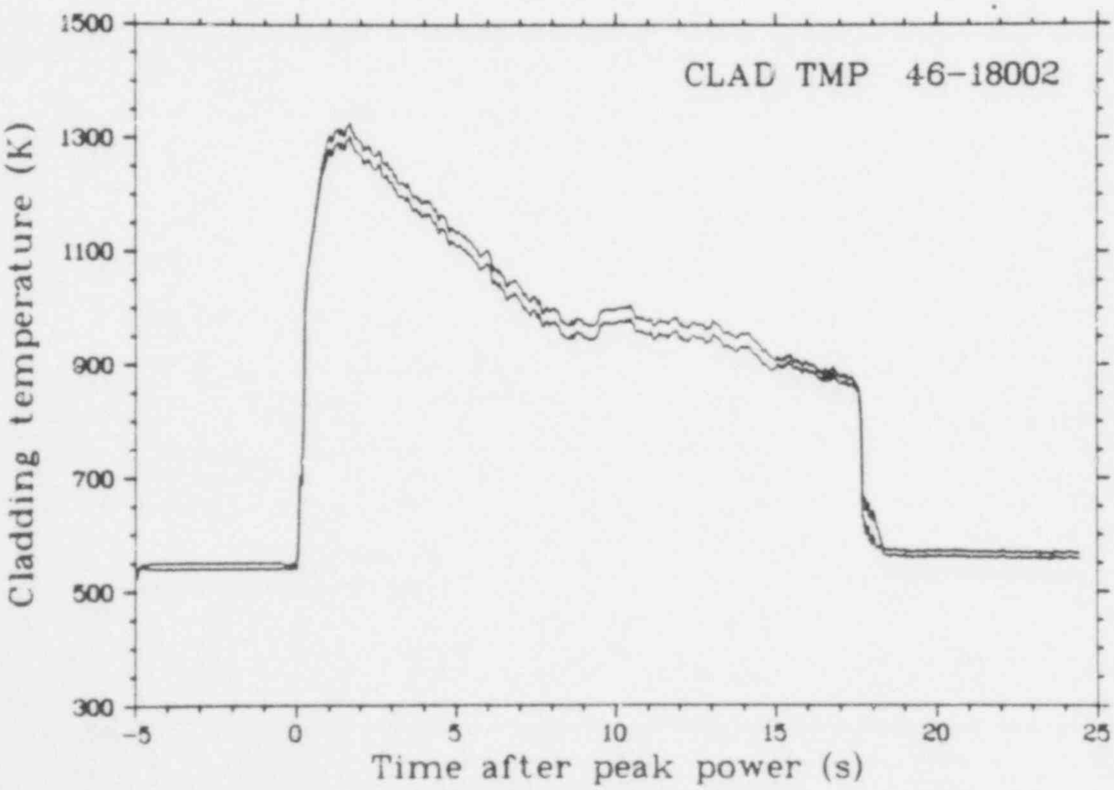

Fig. B-6 Uncertainty bands for the random variation component of the measurement uncertainty for the Rod 802-2 cladding surface temperature at an elevation of 0.46 m above fuel stack bottom (CLAD TMP 46-18002), from -5 to 25 s.

631 136

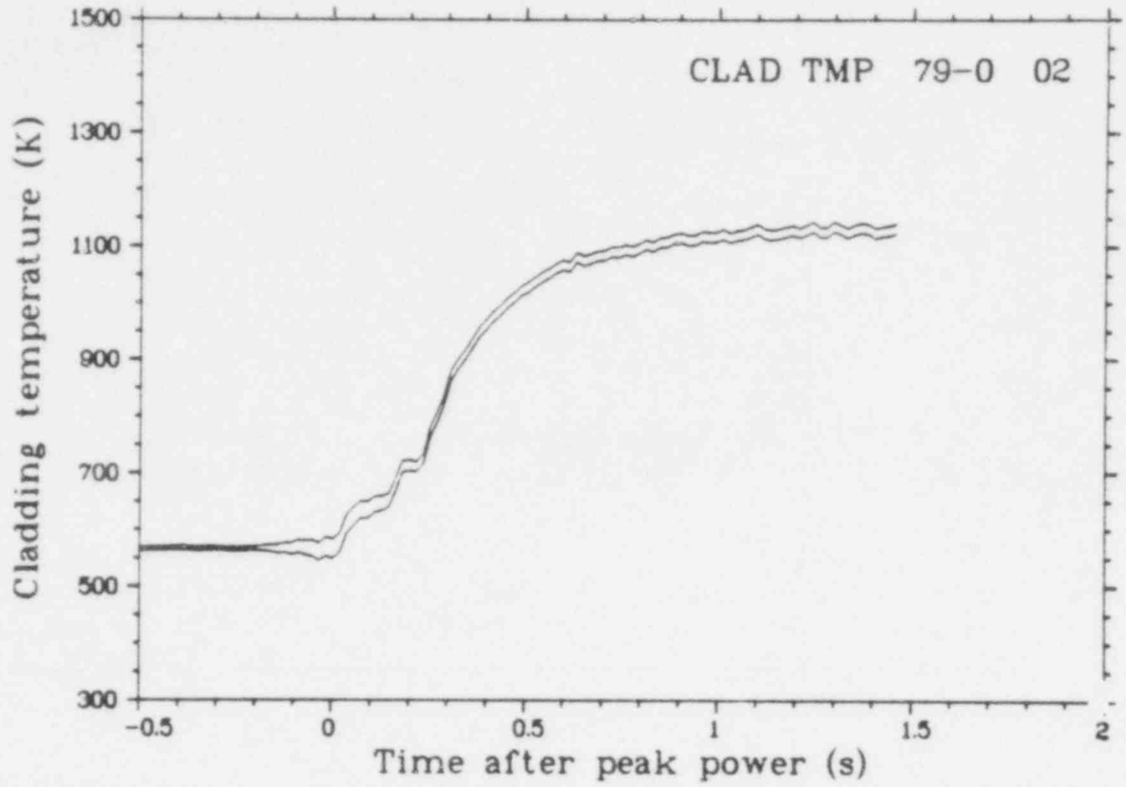

Fig. B-7 Uncertainty bands for the random variation component of the measurement uncertainty for the Rod 802-2 cladding surface temperature at an elevation of 0.79 m above fuel stack bottom (CLAD TMP 79-0 02), from -0.5 to 2 s.

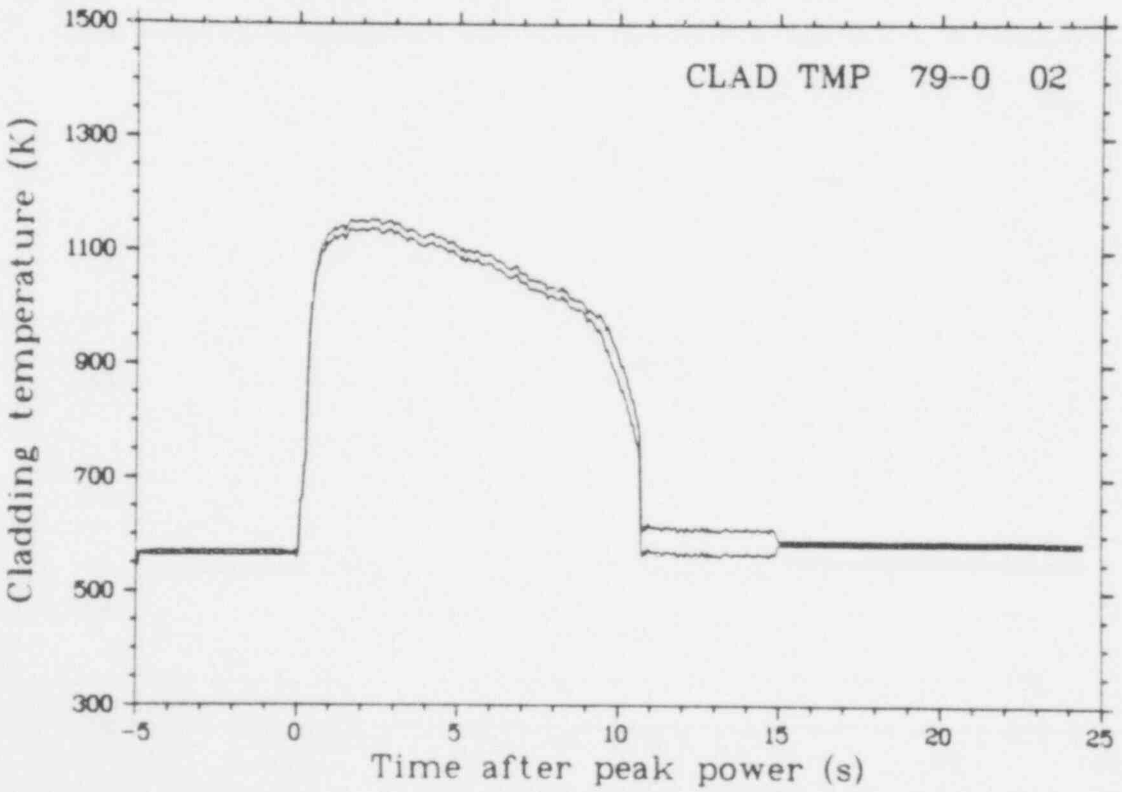

Fig. B-8 Uncertainty bands for the random variation component of the measurement uncertainty for the Rod 802-2 cladding surface temperature at an elevation of 0.79 m above fuel stack bottom (CLAD TMP 79-0 02), from -5 to 25 s.

631 137

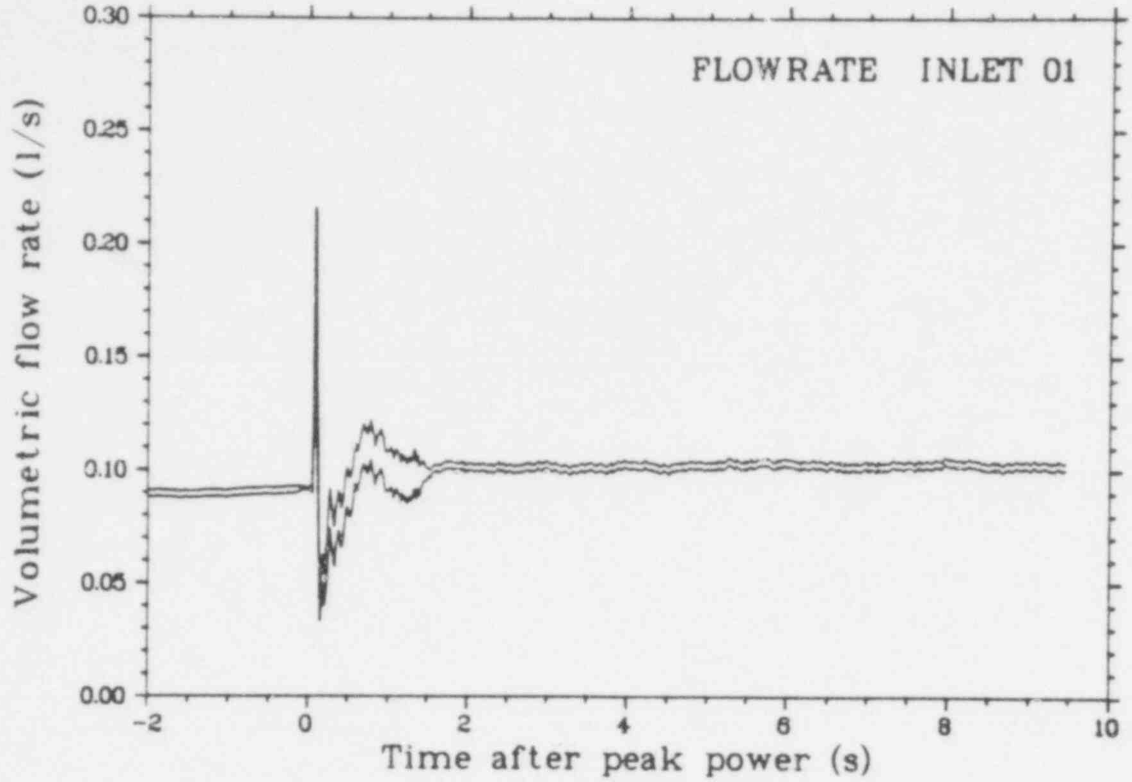

Fig. B-9 Uncertainty bands for the random variation component of the measurement uncertainty for the coolant flow rate at the Rod 802-1 shroud inlet (FLOWRATE INLET 01).

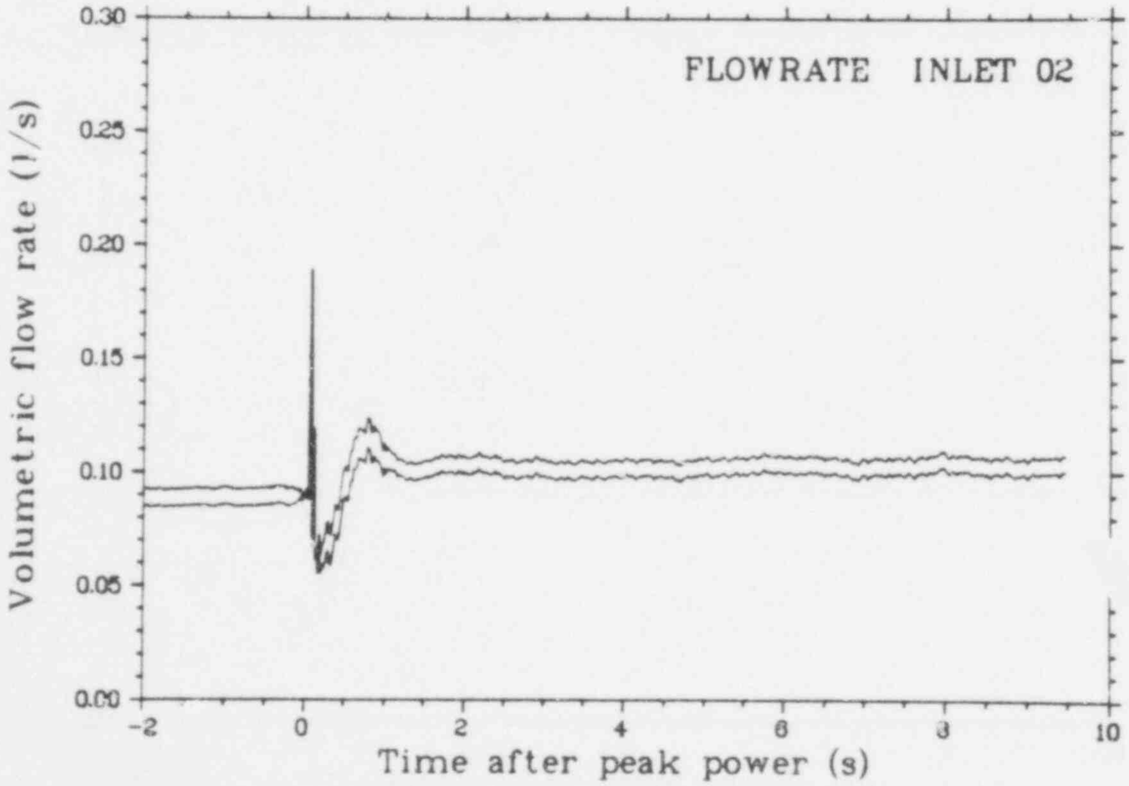

Fig. B-10 Uncertainty bands for the random variation component of the measurement uncertainty for the coolant flow rate at the Rod 802-2 shroud inlet (FLOWRATE INLET 02).

631 138

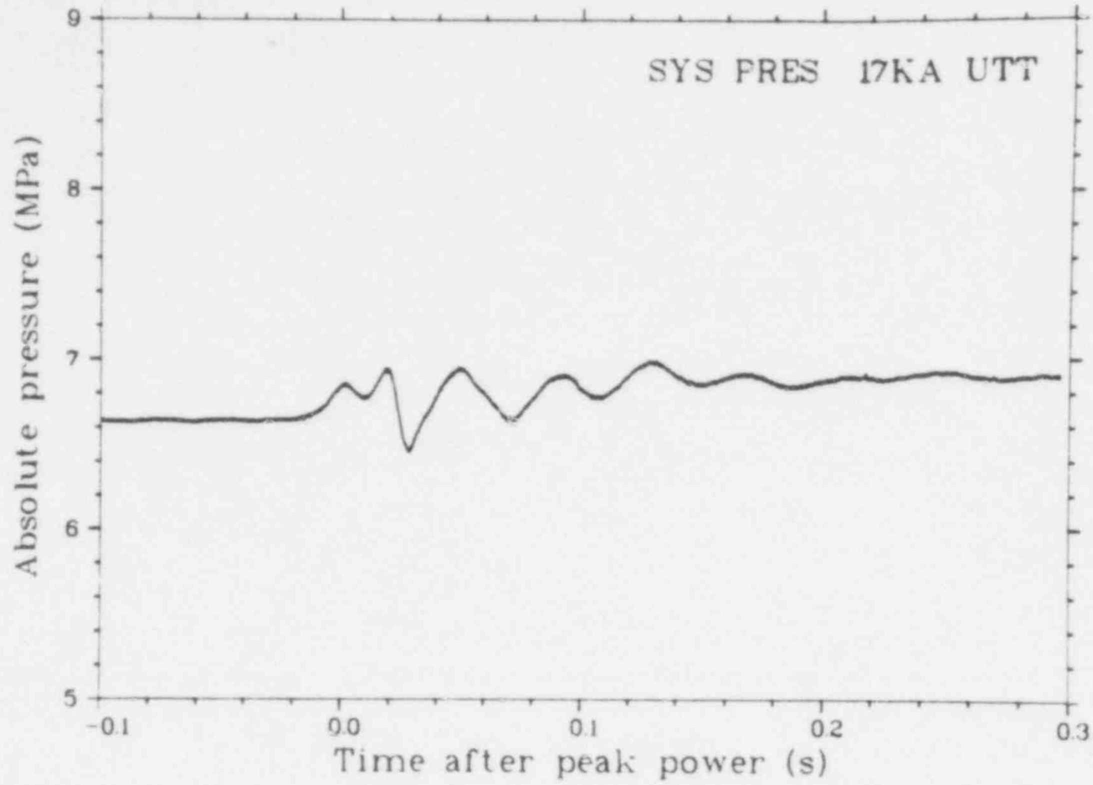

Fig. B-11 Uncertainty bands for the random variation component of the measurement uncertainty for the absolute system pressure in the upper test train (SYS PRES 17KA UTT), from -0.1 to 0.3 s.

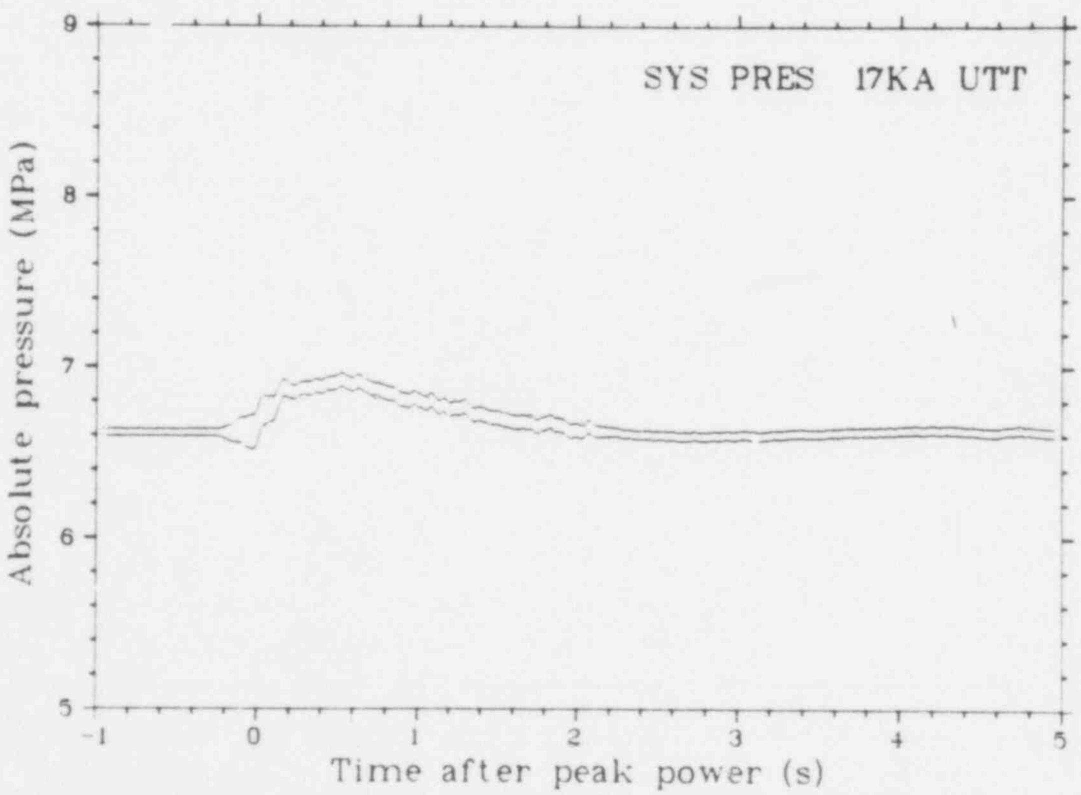

Fig. B-12 Uncertainty bands for the random variation component of the measurement uncertainty for the absolute system pressure in the upper test train (SYS PRES 17KA UTT), from -1 to 5 s.

631 139

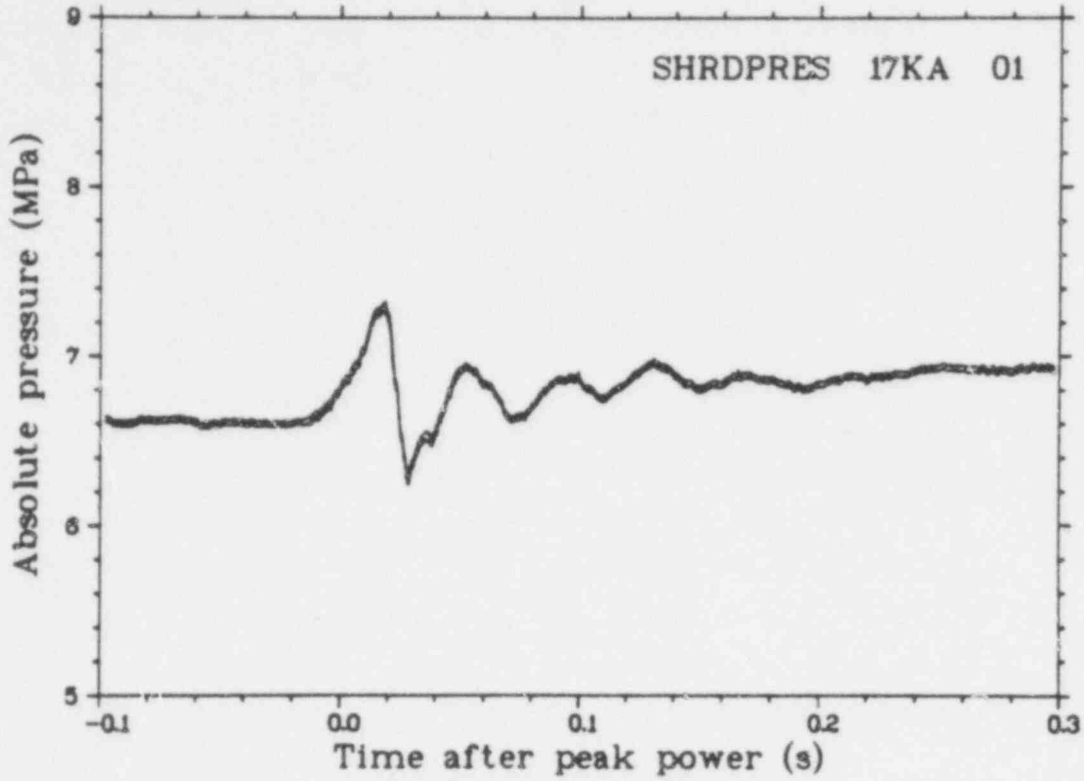

Fig. B-13 Uncertainty bands for the random variation component of the measurement uncertainty for the absolute pressure in the Rod 802-1 shroud (SHRD PRES 17KA 01), from -0.1 to 0.3 s.

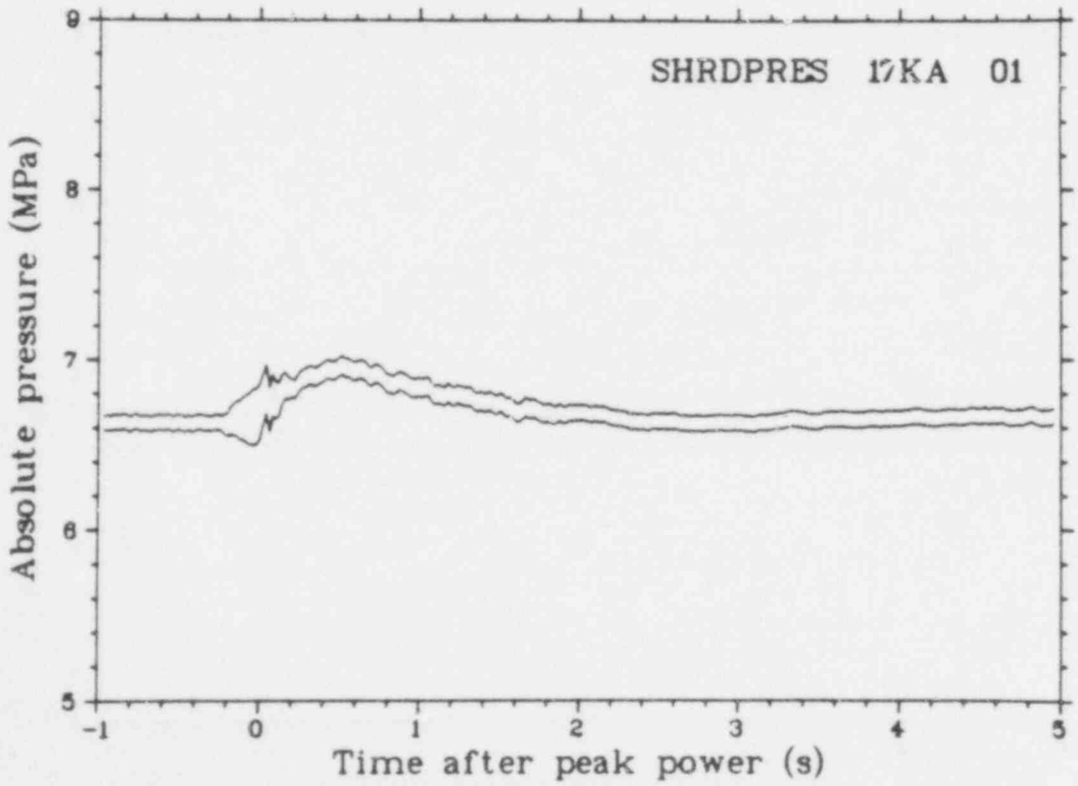

Fig. B-14 Uncertainty bands for the random variation component of the measurement uncertainty for the absolute pressure in the Rod 802-1 shroud (SHRD PRES 17KA 01), from -1 to 5 s.

631 140

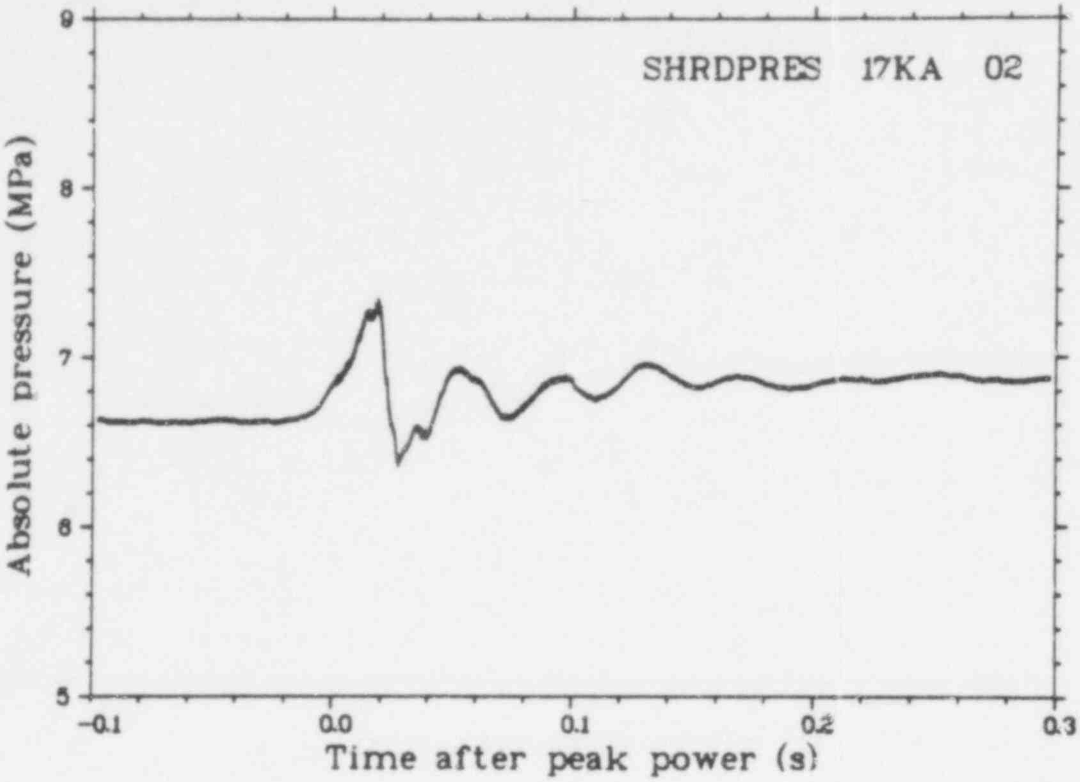

Fig. B-15 Uncertainty bands for the random variation component of the measurement uncertainty for the absolute pressure in the Rod 802-2 shroud (SHRD PRES 17KA 02), from -0.1 to 0.3 s.

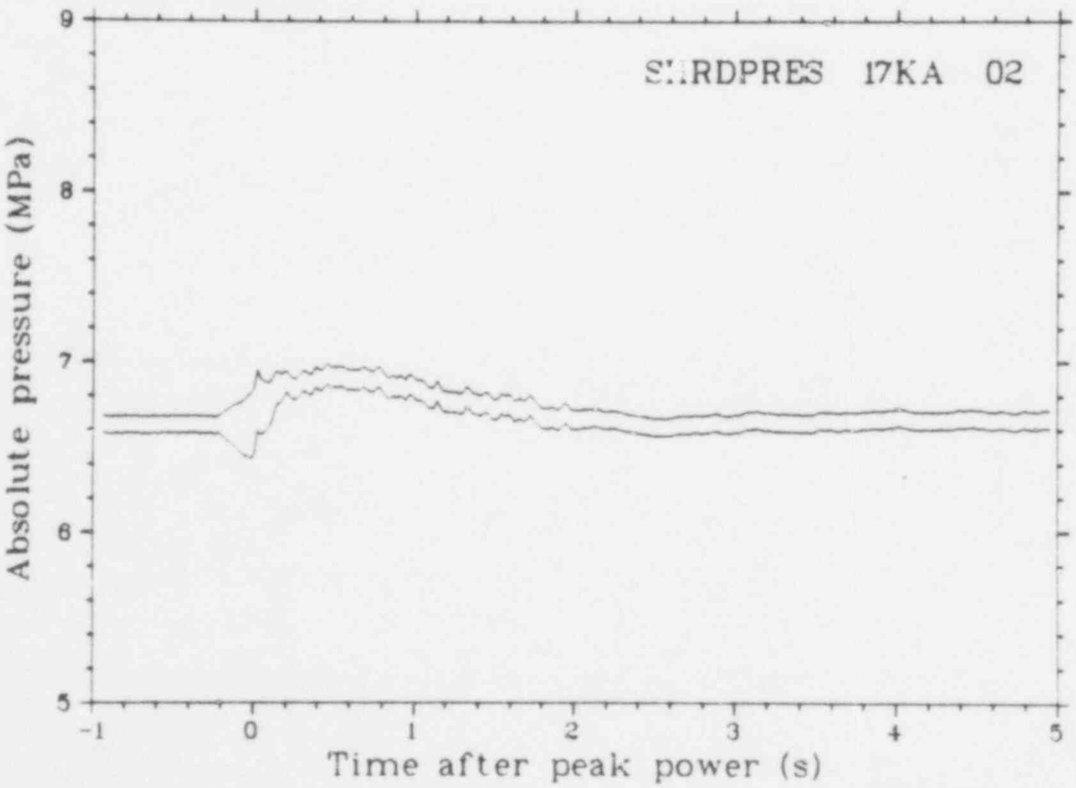

Fig. B-16 Uncertainty bands for the random variation component of the measurement uncertainty for the absolute pressure in the Rod 802-2 shroud (SHRD PRES 17KA 02), from -1 to 5 s.

631 141

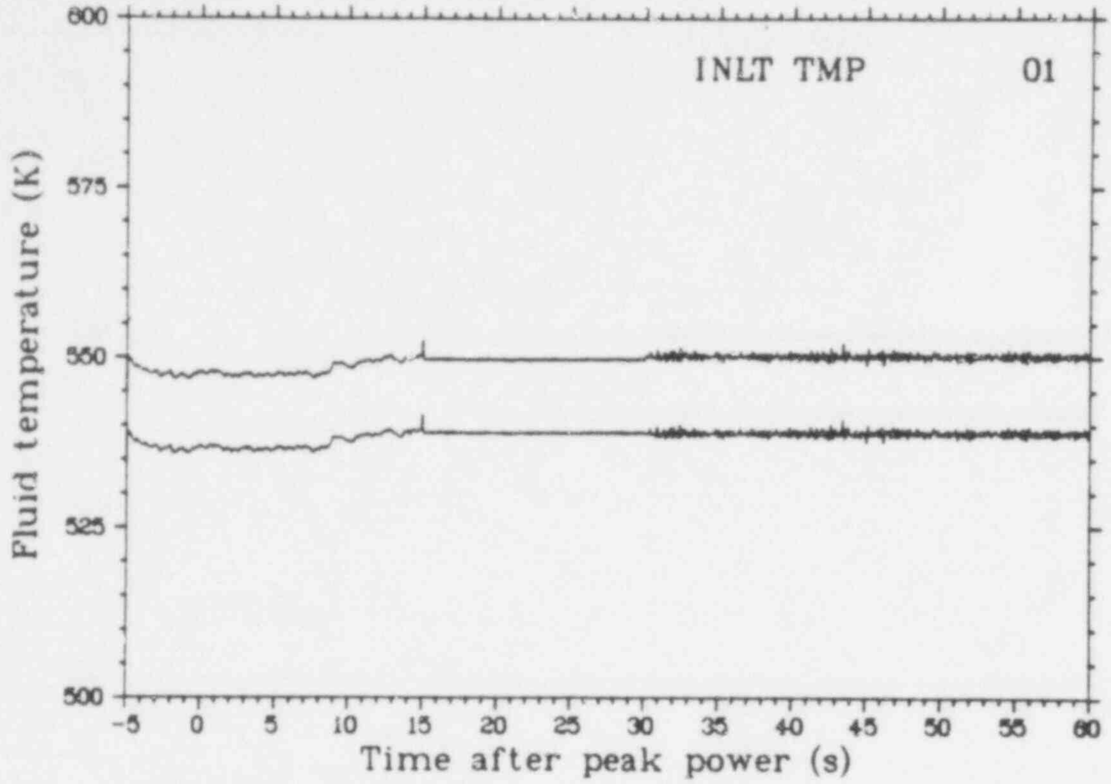

Fig. B-17 Uncertainty bands for the random variation component of the measurement uncertainty for the coolant temperature at the Rod 802-1 shroud inlet (INLT TMP 01).

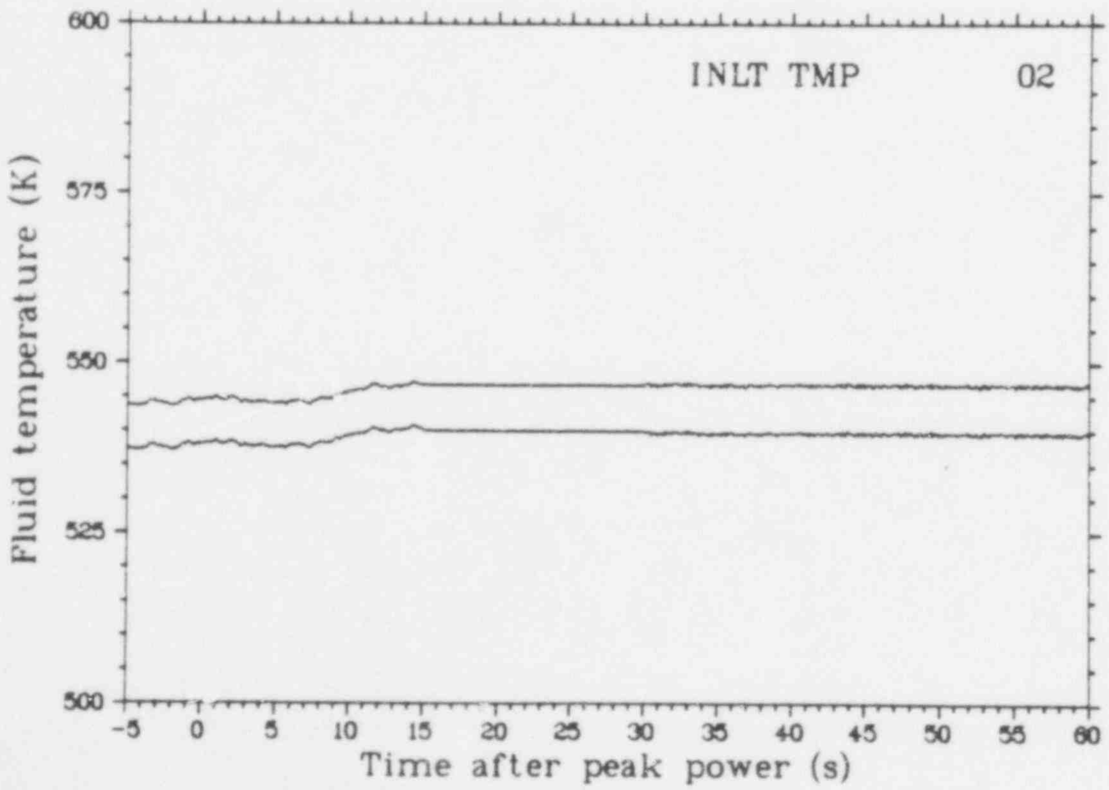

Fig. B-18 Uncertainty bands for the random variation component of the measurement uncertainty for the coolant temperature at the Rod 802-2 shroud inlet (INLT TMP 02).

631 142

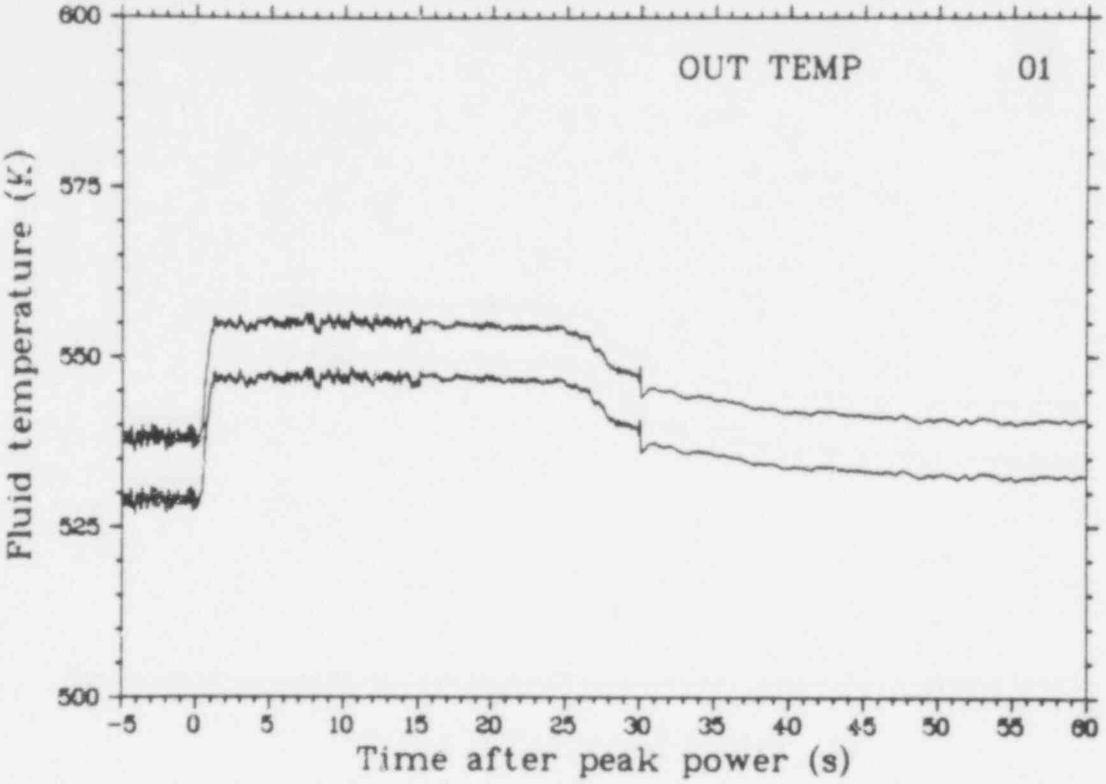

Fig. B-19 Uncertainty bands for the random variation component of the measurement uncertainty for the coolant temperature at the Rod 802-1 shroud outlet (OUT TEMP 01).

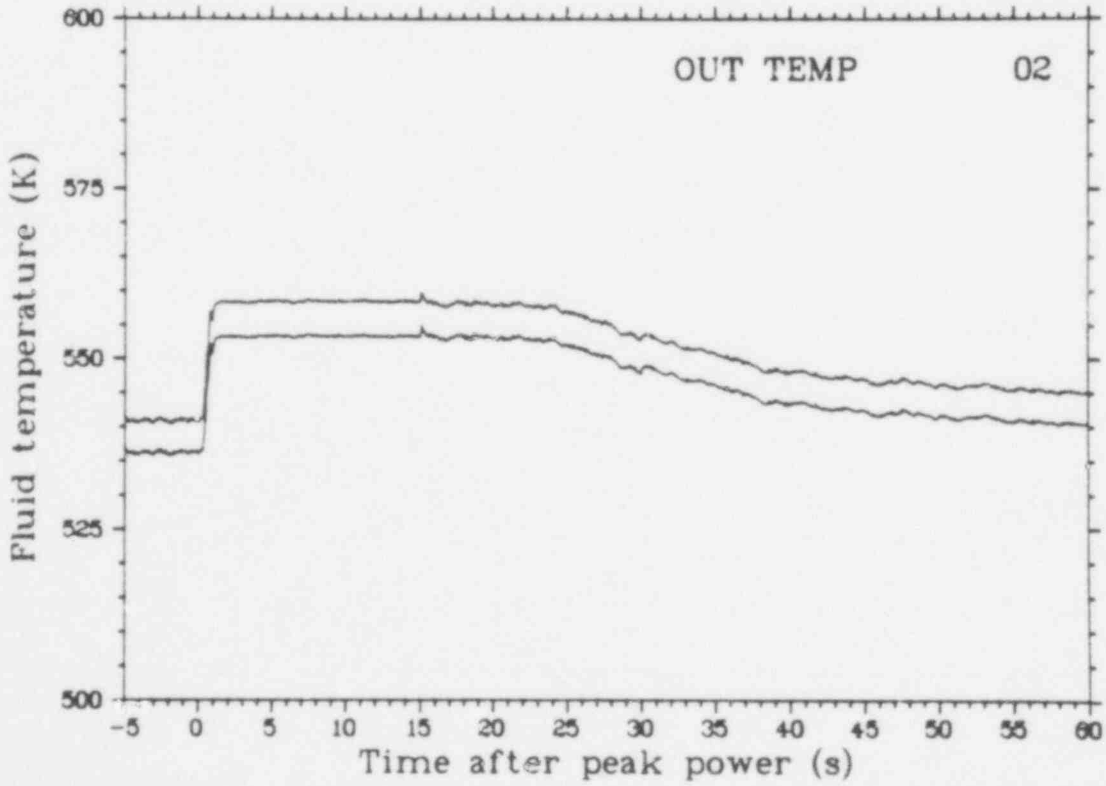

Fig. B-20 Uncertainty bands for the random variation component of the measurement uncertainty for the coolant temperature at the Rod 802-2 shroud outlet (OUT TEMP 02).

431 143

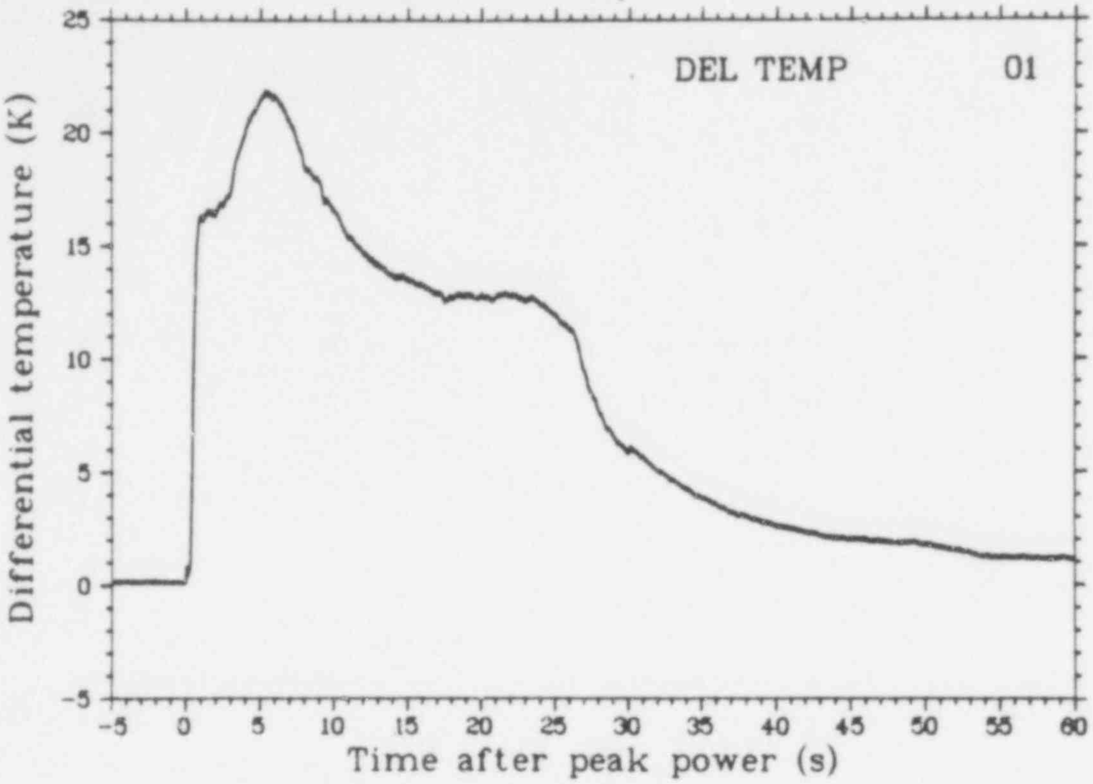

Fig. B-21 Uncertainty bands for the random variation component of the measurement uncertainty for the coolant temperature increase across the Rod 802-1 shroud (DEL TEMP 01).

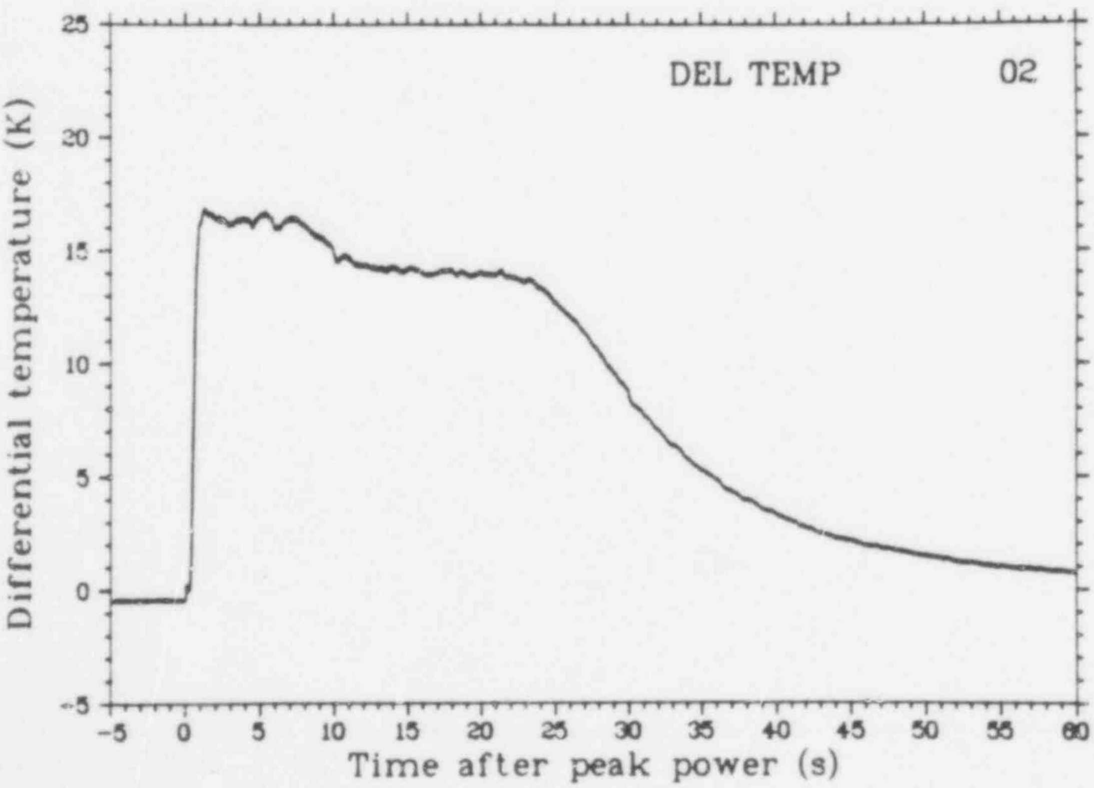

Fig. B-22 Uncertainty bands for the random variation component of the measurement uncertainty for the coolant temperature increase across the Rod 802-2 shroud (DEL TEMP 02).

REFERENCE

B-1. G. E. Box and G. M. Jenkins, *Time Series Analysis — Forecasting and Control*, San Francisco: Holden-Day Inc., 1976.